Blind Multiuser Detection for Time-Frequency Spread Multicarrier CDMA

by

Wilson Tam

B.A.Sc., University of British Columbia, Vancouver, Canada, 2005

A THESIS SUBMITTED IN PARTIAL FULFILLMENT OF

THE REQUIREMENTS FOR THE DEGREE OF

MASTER OF APPLIED SCIENCE

in

THE FACULTY OF GRADUATE STUDIES

(Electrical and Computer Engineering)

THE UNIVERSITY OF BRITISH COLUMBIA

October 2007

Abstract

Multicarrier transmission technology has shown tremendous potential in realizing high data rates for next generation broadband wireless communication systems. Multicarrier modulation schemes are robust to frequency selective fading which are inherent in broadband wireless channels. This thesis considers blind multiuser detection for the recently proposed time frequency spread multicarrier CDMA (TF-MC-CDMA) system in which the system uses both time and frequency domain spreading to achieve diversity in both time and frequency domains. The challenge for TF-MC-CDMA multiuser detection is to mitigate multiple access interference (MAI) in both the time and the frequency domain. The objective of this thesis is to develop and analyze the performance of blind multiuser detection algorithms for TF-MC-CDMA for three types of channel models: AWGN with MAI, slowly fading downlink Rayleigh multipath channels, and the slowly fading downlink multipath channels with Doppler shift induced intercarrier interference (ICI).

A new suboptimal decoupling technique for blind multiuser detection for TF-MC-CDMA in AWGN with MAI is proposed. It is found that the original TF-MC-CDMA blind multiuser detection problem can be suboptimally decoupled into two blind multiuser DS-CDMA problems. These two problems can be solved separately using blind DS-CDMA multiuser techniques. Our effort focused on using blind linear multiuser detectors in which we investigated into four types of blind detection methods: blind direct matrix inversion (DMI) method, blind CMOE RLS method, blind subspace

multiuser detection method using SVD and PASTd adaptive subspace tracking.

The suboptimal decoupling technique for blind multiuser detection for TF-MC-CDMA is extended to slowly fading downlink Rayleigh multipath channels known as type I detectors. Computer simulation results show that type I detectors do not work well in slowly fading multipath channels even though such a scheme provides very good performance in AWGN with MAI. In slowly fading channels, the orthogonality of the time domain signature sequences is preserved. We propose a type II detector which uses a cascade implementation with the time domain detection output acts as the input of the frequency domain detection. Computer simulations show that type II detectors provide much better performance than type I detectors.

Blind multiuser detection for TF-MC-CDMA is further extended for slowly fading Rayleigh multipath channels with Doppler shift induced ICI. In mobile channels, Doppler shifts combined with multipath effects create random subcarrier frequency shifts which in turn cause subcarrier frequency mismatch. Such mismatch leads to the loss of orthogonality among subcarriers thus creating ICI. Our analysis shows that Doppler shifts induced ICI has the effect of destroying the common-channel property in downlink channels. The downlink TF-MC-CDMA signal becomes a quasi-uplink signal because of user dependent subchannel gains.

The type II detector for slowly fading Rayleigh multipath channels is further extended to apply in such channels with Doppler shift induced ICI. It is shown through analysis and computer simulations that the proposed type II detectors implemented using CMOE RLS algorithm, blind subspace SVD algorithm, and the blind subspace PASTd adaptive subspace tracking algorithm, without modifications, provide robust performance in multipath channels with Doppler shift induced ICI.

Contents

List of Tables

List of Figures

List of Symbols

$\text{argmax}\{\cdot\}$	Argument maximizing the expression in the bracket
$\text{argmin}\{\cdot\}$	Argument minimizing the expression in the bracket
$\lvert\cdot\rvert$	Absolute value of a complex number
$*$	Convolution
$\ln x$	Natural logarithm of x
$\text{Re}\{\cdot\}$	Real part of a complex number
$\delta(\cdot)$	Dirac delta function
$\lVert\cdot\rVert$	Frobenius norm
$\text{sgn}\{\cdot\}$	Sign of a real number
$\text{E}\{\cdot\}$	Expectation
$[\cdot]^*$	Complex conjugate
$[\cdot]^T$	Matrix or vector transposition
$[\cdot]^H$	Matrix or vector Hermitian transposition
$\boldsymbol{I}_m$	Identity matrix with dimension $m \times m$

List of Abbreviations

1G	First Generation
2G	Second Generation
3G	Third Generation
4G	Fourth Generation
AMPS	Advanced Mobile Phone System
AWGN	Additive White Gaussian Noise
BER	Bit Error Rate
BPSK	Binary Phase Shift Keying
CDMA	Code Division Multiple Access
CMOE	Constrained Minimum Output Energy
DFT	Discrete Fourier Transform
DMI	Direct Matrix Inversion
DS-CDMA	Direct Sequence CDMA
EDGE	Enhanced Data Rates for GSM Evolution
EVD	Eigenvalue Decomposition

FDMA	Frequency Division Multiple Access
FFT	Fast Fourier Transform
FIR	Finite Impulse Response
GPRS	General Packet Radio Service
GSM	Global Systems for Mobile Communications
HSDPA	High Speed Downlink Packet Access
IDFT	Inverse Discrete Fourier Transform
IEEE	Institute of Electrical and Electronic Engineers
IFFT	Inverse Fast Fourier Transform
ISI	Inter-symbol Interference
ITU	International Telecommunication Union
LMMSE	Linear Minimum Mean Square Error
LTV	Linear Time Varying
MAI	Multiple Access Interference
MC-CDMA	Multicarrier CDMA
MC-DS-CDMA	Multicarrier Direct Sequence CDMA
MMS	Multimedia Messaging Service
MMSE	Minimum Mean Square Error
MOE	Minimum Output Energy

MUD	Multiuser Detection/Detector
OFDM	Orthogonal Frequency Divison Multiplexing
PASTd	Projection Approximation Subspace Tracking with deflation
RLS	Recursive Least Squares
RMS	Root Mean Square
SINR	Signal to Interference and Noise Ratio
SMS	Short Messaging Service
SNR	Signal to Noise Ratio
SVD	Singular Value Decomposition
TDL	Tapped Delay Line
TDMA	Time Division Multiple Access
TF	Time Frequency
TF-MC-CDMA	Time Frequency spread Multicarrier CDMA
UMTS	Universal Mobile Telecommunication System
WGN	White Gaussian Noise
WLAN	Wireless Local Area Network
WSSUS	Wide Sense Stationary Uncorrelated Scattering

Acknowledgements

First and foremost, I thank my parents for everything, without their support, this work would not have been possible. I would like to thank my supervisor Dr. Cyril Leung for his valuable guidance and criticisms. I would also like to thank my colleagues Jingjun Li and Derrick Wan who always extend their helping hands without hesitation. Finally, I would like to thank my thesis examination committee members Dr. Lutz Lampe and Dr. Shahriar Mirabbasi for their time and efforts.

WILSON TAM

THE UNIVERSITY OF BRITISH COLUMBIA

October 2007

To my parents.

Chapter 1

Introduction

1.1 Overview of Current Wireless Communication Systems

During the past two decades, wireless communications have been one of the fastest growing industries in the world. Much of the growth in the past 10 years can be attributed to the ever increasing popularity of the mobile cellular market. According to the GSM Association (GSMA), the 2 billionth mobile phone user was subscribed in June 2006 and it was estimated that new users are subscribing at a rate of 1000 per minute world wide. The demand for ubiquitous connectivity anywhere, anytime in the near future is certainly unquestioned.

The first wave of wireless revolution came with the introduction of the first generation (1G) analog systems such as AMPS which was built upon frequency division multiple access (FDMA). In 1G systems, voice service was the only service provided to subscribers. With the emergence of digital communication technology, evolution towards second generation digital systems such as GSM (2G), and later EDGE/GPRS(2.5G) provided subscribers with a wider variety of data communication services on top of the still dominant voice service which include limited internet

access and the popular short messaging service (SMS). Current third generation (3G) mobile communication systems are built upon code division multiple access (CDMA) using direct sequence spreading codes in the time domain and allow users to enjoy much higher data rates than ever before. CDMA systems are robust to narrow band interference and provide an efficient utilization of both time and frequency and thus are able to deliver enhanced voice services and sufficiently high data rates to support a broader range of services such as multimedia, streaming applications, multimedia messaging service (MMS) and internet surfing capability. Another distinct advantage of CDMA over traditional FDMA and TDMA is a cellular re-use factor of one [1]. Combined with soft capacity limits in CDMA based cellular networks (which offer a graceful degradation when the multiple access interference exceeds a tolerable level as new users are admitted into the system), this creates the possibility of intelligent soft hand-off procedures when mobile users roam across cell boundaries. Although the international standardization body for fourth generation (4G) has not yet released the official specifications for the next generation system requirements, it is anticipated that 4G systems will accommodate broadband services at data rates comparable to those in contemporary WLAN systems.

1.1.1 Limitations of DS-CDMA in Broadband Wireless Channels

Existing 3G standards using DS-CDMA as the access air interface are adequate in achieving high data rates as long as the channel is not severely frequency selective. When a channel is frequency selective, a RAKE receiver must be used. For RAKE receivers to perform well, they require very accurate channel information and channel timing information which are usually acquired through training sequences and/or the use of pilot symbols. Utilizing the RAKE receiver, however, does not eliminate the

problem of intersymbol interference (ISI) caused by the frequency selectivity of the channel. As a result, equalization techniques may be required to mitigate the ISI. The combination of the RAKE receiver, channel estimation and equalization significantly increases the complexity in the design of the receivers. 4G systems will very likely operate in broadband wireless channels and the severely frequency selective nature of the channel will pose difficult challenges in the design of DS-CDMA receivers of practical complexity. Due to these limitations of DS-CDMA, multicarrier based transmission multiple access schemes have emerge as potential candidates for next generation access air interfaces [2].

1.2 Multicarrier-based Transmission

The concept of transmitting information over multiple subcarriers in parallel substreams was first proposed by [3] in 1966. In 1971, it was shown in [4] that such transmission can be realized using the discrete Fourier transform (DFT). However, the implementation of such a transmission scheme at the time it was first proposed was beyond existing technology. A major advancement in signal processing technology came with the invention of the fast Fourier transform (FFT) which enabled efficient computation of the discrete Fourier transform (DFT). This made possible the practical implementation of multicarrier transmission. The first popular standardized multicarrier based system was based on orthogonal frequency division multiplexing (OFDM) used in current WLAN standards IEEE 802.11a and 802.11g. The concept of OFDM is to transmit at high data rates over parallel narrowband subchannels in which the corresponding subcarriers are orthogonal. The advantage of OFDM based multicarrier transmission is inherent in broadband wireless communication systems in which the channel is highly frequency selective. By dividing the available spectrum into narrowband subcarriers and appropriately choosing the subcarrier bandwidth,

each narrowband subchannel can be treated as frequency non-selective fading. The success of OFDM, particularly in WLAN systems, has evoked its possible application in broadband mobile communications [5] and solving the need for complex equalization in 3G DS-CDMA systems.

1.2.1 Multicarrier CDMA

Multicarrier CDMA (MC-CDMA), first proposed in [6, 7] is a multiple access scheme that is based on a combination of OFDM and DS-CDMA. The main idea of MC-CDMA is to use OFDM transmission while separating multiple access users using CDMA. Two popular implementations of MC-CDMA exist: the first one retains the name MC-CDMA, the other is known as MC-DS-CDMA. MC-CDMA spreads the user's signature sequence in the frequency domain by pre-multiplying a chip at each OFDM subcarrier branch. Therefore, the sequence of chips across all the subcarriers constitutes the user's frequency domain signature sequence. MC-DS-CDMA, on the other hand, spreads the original data sequence in time first using DS-CDMA and then transmitting the time domain spreaded data stream using OFDM transmission. A detailed comparison of the two multicarrier multiple access schemes is given in [8] and [9]. Both MC-CDMA and MC-DS-CDMA retain the robustness to frequency selective fading while uncompromising the benefits of using CDMA.

1.2.2 Time-Frequency Spread Multicarrier CDMA

Recently, a new multicarrier based multiple access scheme known as time frequency spread MC-CDMA (TF-MC-CDMA) was proposed by [10, 11] which combines MC-CDMA and MC-DS-CDMA. The main idea behind TF-MC-CDMA is to spread the data in both the time and frequency domains. There are many advantages to TF-MC-CDMA. Firstly, like MC-CDMA and MC-DS-CDMA, TF-MC-CDMA inherits

the benefits of OFDM based transmission and is robust to frequency selectivity in wireless channels. Secondly, the maximum user capacity for TF-MC-CDMA is given by the product of the spreading gain of the time domain spreading and the spreading gain of the frequency domain spreading. This allows the use of short codes in both the time and frequency domain to achieve the same maximum user capacity in MC-CDMA and DS-CDMA employing long codes and high chip rates. Through both time and frequency domain spreading, TF-MC-CDMA is able to benefit from time and frequency diversity gains. Thirdly, TF-MC-CDMA allows a very flexible means for resource allocation. Because TF-MC-CDMA systems are not fixed with solely time domain spreading or solely frequency domain spreading, its adaptability is very attractive in supporting a much wider range of services and data rates in broadband wireless systems [5, 12].

1.3 Challenges and Motivation

Multiple access interference (MAI) is a common problem in all CDMA based multiple access systems. Whether it is MC-CDMA, MC-DS-CDMA, DS-CDMA, or TF-MC-CDMA, the performance of the system depends on the severity of the MAI among the users. MAI results from the non-orthogonality of the user signals at the receiver. This lack of orthogonality can be due to either the use of non-orthogonal codes (i.e. M-sequences or Gold sequences), or the orthogonality of the codes is corrupted by the channel, or both. It was shown in [13] that multiuser detection techniques are quite effective in combating MAI; however, it is also known that multiuser detection methods almost always significantly increase the complexity of the receiver. Furthermore, [13] has shown that the complexity of the optimal multiuser detection method grows exponentially with the number of users, making it unattractive for practical implementation. Suboptimal, low complexity multiuser detection methods will be a

key aspect of receiver design in CDMA based systems.

1.3.1 Multiuser Detection in TF-MC-CDMA Systems

Since TF-MC-CDMA systems employ both time and frequency spreading, multiuser detection will very likely be used in both the time and the frequency domain because MAI can be present in both domains for reasons discussed previously. An optimal multiuser detection method (which minimizes the probability of symbol error) would be overly complex. Linear multiuser detection methods (a class of suboptimal multiuser detection methods) are attractive due to their simple implementation. The idea of linear multiuser detection is to compute a set of weights such that using these weights, the linearly weighted chip samples at the receiver produce an output that minimizes a certain criterion such as the MAI (the linear decorrelating detector) or the mean square error (the linear MMSE detector). For linear multiuser detection, the challenge is to devise methods that can efficiently compute those weights and at the same time gives acceptable performance.

1.3.2 Blind Signal Processing Techniques

Non-blind multiuser detection requires the knowledge of the signature waveforms of all users in the system as well as accurate channel information. In many applications, the receiver only knows its own signature waveform. This is particularly true in receivers used in mobile handsets. Furthermore, estimation of channel parameters usually requires training sequences and/or pilot symbols both of which represent overhead. These difficulties motivate the use of blind signal processing techniques in which [14] first applied to DS-CDMA multiuser detection problems. In TF-MC-CDMA, the blind multiuser detection problem is, based on only the received signal, the desired user's own time domain spreading signature and its frequency domain

signature, to mitigate MAI in the received signal and perform detection when the channel is unknown to the receiver.

1.4 Review of Related Works

The original multicarrier CDMA system was first proposed in [6, 7]. TF-MC-CDMA has been proposed more recently, as a means of achieving diversity gains in both the time and the frequency domain and also greater flexibility and efficiency in resource utilization. It was shown in [10] that TF-MC-CDMA outperformed single carrier systems using the RAKE receiver in frequency selective Rayleigh fading channels when system parameter values are properly matched to channel attributes such as coherence bandwidth and the delay spread. The uplink and downlink performances of TF-MC-CDMA systems in indoor and outdoor wireless channels were investigated in [15] and it was found that the system performance benefitted from both time and frequency diversity gains. The presence of MAI is a fundamental limitation in any CDMA based system and TF-MC-CDMA, unfortunately, suffers the same limitation. Multiuser detection methods enhance the performance of CDMA based systems by mitigating MAI. The complexity of multiuser detection methods ranges from the most complex optimal multiuser detectors to non-linear and linear detectors. The optimal multiuser detector and a few selection of non-linear and linear multiuser detectors for DS-CDMA systems were extensively investigated in [13]. Non-blind, linear multiuser receivers, namely the decorrelation detector and the MMSE detector, were studied for TF-MC-CDMA in AWGN channels in [16] and [17]; in particular, it was shown in [17] that the total supported users in the system can be grouped using the time domain spreading sequences with users in the same group sharing the same time domain signature sequence but have different frequency domain signature sequence. Such a scheme reduces the potentially large joint cross-correlation matrix

into two smaller cross-correlation matrix, one for the time domain and one for the frequency domain. Complexity reduction is achieved by applying separate time and frequency domain detection and the authors in [17] have shown that such method gives comparable performance to the joint time and frequency domain detection. However, the drawback of methods proposed in [17] is that it requires knowledge of all users' time and frequency domain signature sequences as well as accurate knowledge of the noise power.

When the desired user only knows its own time and frequency domain signature sequences, blind multiuser detectors must be used. This assumption is generally appropriate for receivers used in mobile handsets. Linear blind multiuser receivers are especially attractive due to their low complexity compared to the optimal multiuser detector. The constrained minimum output energy detector (CMOE) for DS-CDMA was investigated in [14] and [18] which demonstrated all linear blind detectors can be represented in a canonical form and such form facilitated adaptive implementations which was investigated in [19]. It was shown in [20] that the linear blind multiuser detector for DS-CDMA can be equivalently formulated using the subspace decomposition by decomposing the data correlation matrix into a signal eigen-subspace and a noise eigen-subspace. It was further shown in [20] that both the blind decorrelating detector and the blind MMSE detector can be computed through subspace decomposition. Many recent works, such as that of [21] and [22], have applied the blind subspace methods to MC-CDMA and MC-DS-CDMA systems. Subspace methods have shown considerable promise because the framework allows for adaptive implementation using existing subspace tracking algorithms [20, 23, 24] and blind joint channel estimation [22, 25].

Subcarrier frequency offsets in mobile channels due to Doppler shifts causes inter-carrier interference (ICI) in systems using OFDM based transmission [26]. It is shown

in [27] that using a time domain signal analysis, the ICI in MC-CDMA can be modeled as weighted frequency domain sampling. The effect of Doppler induced ICI in mobile fading channels has been investigated for pure OFDM systems in [28] and [26]. The main result is that ICI creates leakage of energy from one subcarrier to another when subcarriers are no longer orthogonal due to the random offsets caused by the Doppler shifts in the channel. In multipath fading channels, each path arriving at the receiver experiences a different Doppler frequency shift as a result of the random angle of arrival. Therefore for TF-MC-CDMA, it is in general that due to multipath propagation and user mobility, the orthogonality of the subcarriers are corrupted as a result of ICI and at the same time, the orthogonality (if orthongonal codes are used) of the frequency domain spreading sequences are lost due to the combination of both multipath fading and ICI. Past research focus has been on mitigating solely the ICI problem in OFDM systems; this is achieved through ICI cancellation and suppression techniques [29–31] all of which adds to the complexity of the receiver. In most downlink applications, the orthogonality of the spreading sequences is critical for high speed data transfer such as HSDPA for 3G mobile systems. For TF-MC-CDMA to perform well, the receiver must be able to overcome the two major impairments, MAI and ICI.

1.5 Thesis Contributions

The objective of this thesis is to propose blind multiuser detection methods for TF-MC-CDMA in three different propagation environments: (1) the AWGN channel, (2) the downlink multipath Rayleigh fading channel and (3) the mobile Rayleigh fading channel with Doppler shift induced ICI. The main contributions of the thesis are summarized as follows:

- An improved time and frequency domain signature sequence allocation scheme

is proposed. This scheme clarifies the time signature grouping scheme in [17] by minimizing the number of users within a time domain signature group (and also the number of users sharing the same frequency domain signature sequence). Our proposed scheme ensures that all time domain groups have a minimal number of users sharing the same time domain signature sequences and thereby keeping the number of interfering signals in the time and frequency domain to a minimal.

- A new suboptimal decoupling approach to blind linear multiuser detection for TF-MC-CDMA is proposed. The original linear blind multiuser detection problem for TF-MC-CDMA can be suboptimally decoupled into two DS-CDMA multiuser detection problems. This allows for separate blind detection for the time and frequency domain multiuser detection with each of them being equivalent to a blind multiuser DS-CDMA detection problem. Using the decoupling strategy, the linear blind multiuser detector for each of the time and frequency domain problem can be solved using existing linear blind multiuser detection algorithms for DS-CDMA:
  - Direct matrix inversion (DMI) method
  - Constrained minimum output energy (CMOE) recursive least squares (RLS) method
  - Blind subspace method using singular value decomposition (SVD)
  - Blind subspace method using PASTd adaptive subspace tracking

  The performance of each method in AWGN channel is investigated where non-orthogonal spreading sequences are used. Performance in moderate, moderate heavy, and full system capacity loads were investigated for each implementation method.

- The decoupling method for TF-MC-CDMA blind linear multiuser detection is extended to detection in slowly fading Rayleigh multipath channel on the downlink. This is known as the type I blind detector. It is shown that the CMOE RLS, blind subspace multiuser detection using SVD and adaptive subspace tracking using PASTd are all applicable to type I implementation. The only added complexity comes from the joint blind channel estimation. Using computer simulations, the performance for type I detector using CMOE RLS, blind subspace detection using SVD and adaptive subspace tracking using PASTd algorithm are investigated. A TF-MC-CDMA type II blind detector is also proposed for the same channel model. In contrast to type I detector which maintains the same parallel architecture as for the AWGN case, the type II detector uses a cascade implementation in which the output of the time domain detector is fed into the frequency domain detector. Since the time domain signatures remain orthogonal in slowly fading channels, the type II detector is able to reduce the number of interferers for the frequency domain detection stage by matched filtering out users that does not share the same time domain signature. The performance of the blind CMOE RLS algorithm, blind subspace detection using SVD, and adaptive subspace tracking using PASTd are investigated using computer simulations for the type II implementation. Simulation results showed that type II blind detectors provide better performance than type I blind detectors.

- We further extend TF-MC-CDMA blind multiuser detection to slowly fading mobile Rayleigh multipath downlink channel with Doppler shift induced ICI. Our work contributes to the modeling and analysis of Doppler shift induced ICI in TF-MC-CDMA and showed that the random Doppler induced ICI in a mobile channel has the effect of destroying the common multiuser-channel property

of the downlink channel. As a result, the original TF-MC-CDMA downlink blind multiuser detection problem becomes a quasi-uplink multiuser detection problem where the channel now becomes user dependent. We extended the type II blind multiuser detection methods for slowly fading Rayleigh multipath downlink channel (without ICI) to the one with Doppler induced ICI. It is shown that the original method developed for the downlink channel without ICI still provides very good performance. Computer simulation results confirm that the blind type II receiver, implemented using the blind CMOE RLS, blind subspace using SVD and blind subspace using adaptive subspace tracking with PASTd give robust performance in mobile channels with Doppler induced ICI.

1.6 Thesis Outline

The roadmap for the rest of the thesis is as follows: Chapter 2 presents the TF-MC-CDMA transmission system model as well as the channel models used in the thesis. Chapter 3 discusses blind multiuser detection algorithms for TF-MC-CDMA signal in AWGN channels when non-orthogonal spreading sequences are used. Chapter 4 extends the TF-MC-CDMA blind multiuser detection methods proposed in Chapter 3 to slowly fading Rayleigh multipath channels. Chapter 5 further extends the work of Chapter 4 to blind multiuser detection in mobile Rayleigh multipath channels with Doppler shift induced ICI. Finally, conclusions and future research directions are discussed in Chapter 6.

Chapter 2

Time Frequency Spread Multicarrier Spread Spectrum System Model

2.1 Introduction

In this chapter, the TF-MC-CDMA system and channel models are described. The chapter is divided into three sections; in Section 2.2, the transmitter model and modulation for the TF-MC-CDMA system are described and the motivation for the time frequency spread spectrum system is discussed. The model is the basis for the discussions of receiver designs in the remaining chapters. Section 2.3 describes the additive white Gaussian noise (AWGN) channel with multiple access interference (MAI) and the synchronous downlink multipath Rayleigh fading channel that is used to assess TF-MC-CDMA system performance in the remaining chapters. For the downlink Rayleigh multipath fading channel model, four sub-models, namely, frequency non-selective slowly fading, frequency non-selective fast fading, frequency-selective slow fading, and frequency-selective fast fading channels are discussed. Section 2.4,

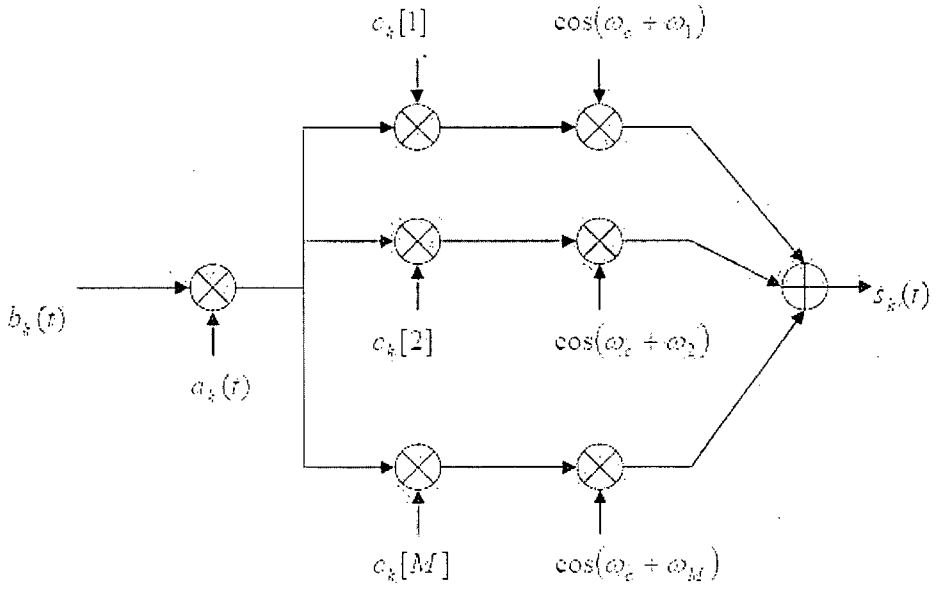

Figure 2.1: TF-MC-CDMA transmitter model

discusses the demodulation process for TF-MC-CDMA signals. A summary of the chapter is provided in Section 2.5.

2.2 Transmitter Model

The transmission model considered for the TF spread MC-CDMA system follows that in [17]. The transmitter can be thought of as K users transmitting simultaneously and synchronously. The block diagram for the k^{th} user is shown in Fig. 2.1. It is assumed that a bit stream, $d_k[i] \in \{0, 1\}$, from a binary symmetric source (BSS) is to be sent for the k^{th} user, $k \in \{1, 2, ..., K\}$. The bit stream is then modulated using binary phase shift keying (BPSK) into $b_k[i] \in \{-1, +1\}$. The BPSK modulated sequence is passed through a linear time invariant (LTI) filter with a rectangular pulse shape impulse response of duration T_b resulting in an output waveform given by 2.1.

$$b_k(t) = \sum_{i=0}^{\infty} b_k[i] P_{T_b}(t - iT_b) \tag{2.1}$$

The signal $b_k(t)$ is then mixed with a direct sequence (DS) time domain (TD) code $a_k(t)$ given by 2.2 with spreading gain N and chip duration T_c,

$$a_k(t) = \sum_{j=0}^{N-1} a_k[j] P_{T_c}(t - jT_c) \tag{2.2}$$

where $NT_c = T_b$ and $\begin{bmatrix} a_k[0] & \dots & a_k[N-1] \end{bmatrix}^T = \mathbf{a}_k$ is the k^{th} user time domain chip sequence. The DS time domain spread signal is replicated over M branches onto M subcarriers of frequency ω_m, $\{\omega_m; m = 1, 2, ..., M\}$. In branch m, $a_k(t)b_k(t)$ is pre-multiplied by a frequency domain chip sequence $c_k[m]$ of duration T_c. We further assume that the set of subcarrier frequencies satisfy the orthogonality condition over the interval T_c given by

$$\int_0^{T_c} \exp(j(\omega_m t + \phi_m)) \exp(-j(\omega_l t + \phi_l)) dt = 0, \quad m \neq l \tag{2.3}$$

and

$$\int_0^{T_c} \exp(j(\omega_m t + \phi_m)) \exp(-j(\omega_l t + \phi_l)) dt \neq 0, \quad m = l \tag{2.4}$$

Hence, together with the carrier frequency ω_c, the transmitted signal $s_k(t)$ for the k^{th} user is given by the sum of the outputs of all M subcarrier branches, i.e.

$$s_k(t) = \sqrt{\frac{2P}{M}} \sum_{m=1}^{M} b_k(t) a_k(t) c_k[m] \cos\{(\omega_c + \omega_m) t\} \tag{2.5}$$

where P is the energy of $s_k(t)$, i.e.

$$P = \int_0^{T_c} s_k(t) s_k^*(t) dt \tag{2.6}$$

The overall transmitted passband signal is

$$\begin{aligned} s(t) &= \sum_{k=1}^{K} s_k(t) \\ &= \sqrt{\frac{2P}{M}} \sum_{k=1}^{K} \sum_{m=1}^{M} b_k(t) a_k(t) c_k[m] \cos\{(\omega_c + \omega_m) t\} \end{aligned} \tag{2.7}$$

2.2.1 Equivalent Complex Baseband Signal

It is known from [32] and [33] that a transmitted passband signal can be written in the form

$$s(t) = \sqrt{2}\mathrm{Re}\left\{s_{LP}(t)\exp\left(j\omega_c t\right)\right\} \tag{2.8}$$

where $s_{LP}(t)$ is the equivalent lowpass complex baseband signal of $s(t)$. Equation 2.7 can be re-written as

$$s(t) = \sqrt{2}\mathrm{Re}\left\{\sqrt{\frac{P}{M}}\sum_{k=1}^{K}\sum_{m=1}^{M} b_k(t)a_k(t)c_k[m]\exp\left\{j\omega_m t\right\}\exp\left\{j\omega_c t\right\}\right\} \tag{2.9}$$

A comparison of 2.8 and 2.9 shows that

$$\begin{aligned} s_{LP}(t) &= \sqrt{\frac{P}{M}}\sum_{k=1}^{K}\sum_{m=1}^{M} b_k(t)a_k(t)c_k[m]\exp\left(j\omega_m t\right) \\ &= \sqrt{\frac{P}{M}}\sum_{k=1}^{K} b_k(t)a_k(t)\left\{\sum_{m=1}^{M} c_k[m]\exp\left(j\omega_m t\right)\right\} \end{aligned} \tag{2.10}$$

The term in the curly braces in 2.10 can be realized and implemented using the IDFT [4] when the subcarrier frequency set $\{\omega_m\}_{m=1}^{M}$ is chosen to have minimum subcarrier frequency separation and satisfy the orthogonality condition given by 2.3 and 2.4.

To find the minimum possible subcarrier frequency separation, the orthogonality condition given in 2.3 can be re-written as

$$\int_0^{T_c} \exp(j(\omega_m - \omega_l)t)\exp(j(\phi_m - \phi_l))dt = 0, \quad m \neq l \tag{2.11}$$

Equation 2.11 holds if and only if

$$(\omega_m - \omega_l)\frac{T_c}{2} = n\pi, \quad n \text{ is any nonzero integer} \tag{2.12}$$

The minimum subcarrier frequency separation is obtained for $n = 1$ and is equal to $\frac{2\pi}{T_c}$. If minimum subcarrier frequency spacing is used, the subcarrier frequencies are

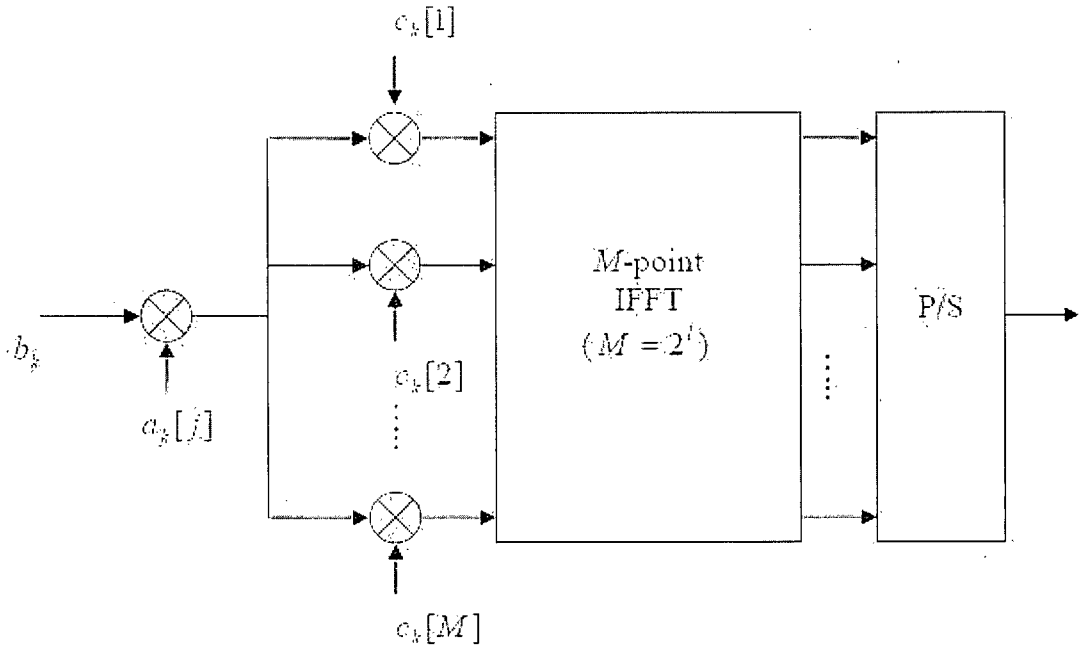

Figure 2.2: TF-MC-CDMA baseband transmitter implementation using IDFT/IFFT

then given by

$$\omega_m = \omega_0 + \frac{2\pi m}{T_c}, \quad m = 0, 1, ..., M-1 \tag{2.13}$$

where ω_0 is an arbitrary frequency offset. For $\omega_0 = 0$, the complex baseband signal $s_{LP}(t)$ can be written as

$$s_{LP}(t) = \sqrt{\frac{P}{M}} \sum_{k=1}^{K} b_k(t) a_k(t) \left\{ \sum_{m=0}^{M-1} c_k[m] \exp\left(j \frac{2\pi m}{T_c} t \right) \right\} \tag{2.14}$$

It is shown in [34] that the signal $s_{LP}(t)$ can be reconstructed from samples taken at a rate of $\frac{M}{T_c}$ samples per second, i.e.

$$s_{LP}[n] = s_{LP}\left(\frac{nT_c}{M}\right) = \sqrt{\frac{P}{M}} \sum_{k=1}^{K} b_k a_k[j] \left\{ \sum_{m=0}^{M-1} c_k[m] \exp\left(j \frac{2\pi mn}{M} \right) \right\} \tag{2.15}$$

The term inside the curly braces in 2.15 is an M-point IDFT. Using this fact, the TF-MC-CDMA modulation can be efficiently implemented using IFFT if M is chosen to be a power of 2. This is shown in Fig. 2.2.

2.2.2 Allocation of Spreading Sequences

In TF-MC-CDMA, each user is allocated a pair of signature sequences, one for the time domain spreading (TDS) and the other for the frequency domain spreading (FDS). As long as no two users share the same TDS and FDS signature sequence pair, the system is able to support up to $N \times M$ users, where N and M are the TDS and FDS spreading gains respectively. In [17], a scheme is proposed that allocates TDS and FDS sequence pairs by grouping the K users in the system into N groups with each group being represented by one of the N TDS sequences in the set $\{\mathbf{a}_1, \mathbf{a}_2, ..., \mathbf{a}_N\}$, where $\mathbf{a}_k = \begin{bmatrix} a_k[1] & \dots & a_k[N] \end{bmatrix}^T$, and with each group supporting at most $\chi = \lfloor \frac{K}{N} \rfloor$ users. The users within a group are then separated by the χ FDS signatures chosen from the set $\{\mathbf{c}_1, \mathbf{c}_2, ..., \mathbf{c}_M\}$ where $\mathbf{c}_k = \begin{bmatrix} c_k[1] & \dots & c_k[M] \end{bmatrix}^T$ is the vector that contains the FDS of the k^{th} user. However, [17] did not specify how to choose the TDS and FDS signature sequence pairs to minimize MAI in the system. To achieve minimization of MAI, it is desirable to minimize the number of users sharing the same TDS signature sequence and the number of users sharing the same FDS signature sequence. This motivates us to propose a simple, systematic way of allocating the time and frequency signature sequences that achieves this result. The TDS and FDS signature sequence pairs can be viewed in an arranged two dimensional array, the TF sequence matrix, as shown in Fig. 2.3. Using the TF sequence matrix, each user is assigned a pair of TDS/FDS sequences according to the following rule.

In the first case, suppose the number of available TDS sequence N is equal to the number of available FDS sequence M. Therefore, the TF sequence matrix is a square matrix of size N by N (or M by M). Then,

1. The pairs along the main diagonal of the TF-sequence matrix are assigned first sequentially going from left to right.

2. Once the main diagonal pairs are used up, this means that the last main diagonal

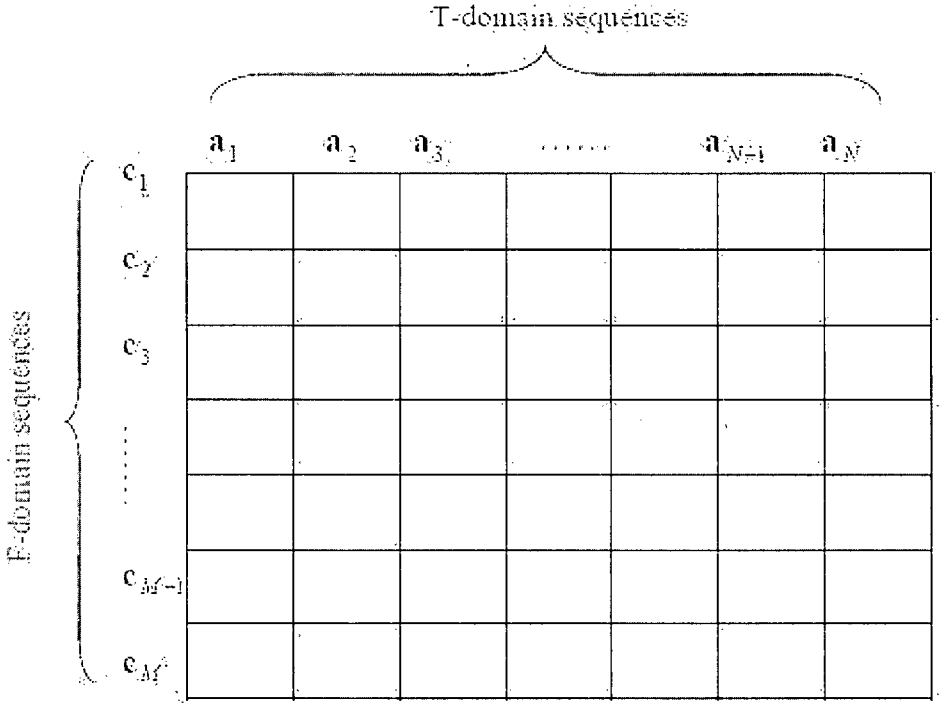

Figure 2.3: TF spreading sequence matrix

pair belonging to the last column has just been assigned. The next pair is selected from the first column. From the first column, let $R[i-1]$ be the row number of the last signature sequence pair assigned from the first column. Then, the row number of the next pair assigned is computed as $((R[i-1]+N) \mod M)+1$.

3. The following pair to be assigned will come from the next column to the right of the column number of the last assigned pair. If the last column is reached, the next column will be again the first column. We again use the row number of the last pair assigned from the current column of consideration to compute the row number of the next pair assigned using the same method as the previous step.

4. This process is continued until all pairs have been used up

For the case when the number of available TDS sequence N is not equal to the number of available FDS sequence M, without loss of generality, suppose that $N < M$, and hence a long rectangular TF sequence matrix with N columns and M rows(this is because we can always switch TDS and FDS labels), then

1. The pairs along the main diagonal of the TF-sequence matrix are assigned first sequentially going from left to right.

2. Once the main diagonal pairs are used up, this means that the last main diagonal pair belonging to the last column has just been assigned. The next pair is selected from the first column. From the first column, let $R[i-1]$ be the row number of the last signature sequence pair assigned from the first column. Then, the row number of the next pair assigned is computed as $(R[i-1]+N)$ mod M. Therefore, the next assigned pair is located on column 1 and row $(R[i-1]+N) \mod M$. Note that the modulo operation gives row numbers going from $0, ..., M-1$. Since the row number in the TF-sequence matrix goes from $1, ..., M$, this means that a computed 0^{th} row actually corresponds to the M^{th} row.

3. The following pair to be assigned will come from the next column to the right of the column number of the last assigned pair. If the last column is reached, the next column will be again the first column. We again use the row number of the last pair assigned from the current column of consideration to compute the row number of the next pair assigned using the same method as the previous step.

4. This is continued until all pairs in the TF-sequence matrix are assigned.

It was shown in [16, 17] that if the n^{th} time group (i.e. the group of users with the same time domain signature sequence) contains χ_n users, then, the passband transmitted signal in 2.7 can be equivalently re-written as

$$s(t) = \sqrt{\frac{2P}{M}} \sum_{n=1}^{N} \sum_{\kappa=1}^{\chi_n} \sum_{m=1}^{M} b_{n\kappa}(t) a_n(t) c_\kappa[m] \cos\left\{(\omega_c + \omega_m)\, t\right\} \tag{2.16}$$

The equivalent complex baseband signal can also be re-written as

$$s_{LP}(t) = \sqrt{\frac{P}{M}} \sum_{n=1}^{N} \sum_{\kappa=1}^{\chi_n} \sum_{m=1}^{M} b_{n\kappa}(t) a_n(t) c_\kappa[m] \exp\left(j\omega_m t\right) \tag{2.17}$$

2.3 Channel Models

In this section, the channel models to be used for the performance analysis of TF-MC-CDMA are reviewed. In particular, two channel models are presented: (1) the AWGN channel and (2) the downlink multipath Rayleigh fading channel. For the latter, four types of fading are considered (based on different channel characteristics) from the wide sense stationary uncorrelated scattering (WSSUS) channel model.

2.3.1 AWGN Channel

The non-fading channel for TF-MC-CDMA is modeled as

$$r(t) = s(t) + n(t) \tag{2.18}$$

where $n(t)$ is a WGN process with double sided power spectral density equal to $\frac{N_0}{2}$ and $r(t)$ is the received signal. When non-orthogonal spreading sequences are used for the TD and FD, the severity of the MAI is determined by the pairwise cross correlations of the TDS sequences $\{\rho_{ij}; i, j = 1, 2, ..., K\}$, and also the pairwise cross correlation of the frequency-domain spreading sequences $\{\beta_{ij}; i, j = 1, 2, ..., K\}$, where

$$\begin{aligned} \rho_{ij} &= \tfrac{1}{N} \sum_{n=1}^{N} a_i[n] a_j[n] \\ \beta_{ij} &= \tfrac{1}{M} \sum_{m=0}^{M-1} c_i[m] c_j[m] \end{aligned} \tag{2.19}$$

In [16] and [17], the authors investigated the performance of non-blind TF-MC-CDMA multiuser detection using this channel model and M-sequences was used for both the TDS and FDS signature sequences.

2.3.2 Downlink Multipath Rayleigh Fading Channel

The multipath Rayleigh fading channel is modeled as a tapped-delay line linear time varying (LTV) filter [35, 36]. This model is motivated by the fact that copies of the original signal arrive at the receiver with different delays and complex attenuations. Following the analysis given in [33] and [1], the statistical properties of the multipath Rayleigh fading channel can be described by the autocorrelation function $R_{hh}(t, t', \tau, \tau')$ of the LTV channel impulse response $h(t, \tau)$, where t is the time variable and τ is the delay variable,

$$R_{hh}(t, t', \tau, \tau') \equiv E\left\{h^*(t, \tau)h(t', \tau')\right\} \tag{2.20}$$

The wide sense stationary (WSS) assumption states that the autocorrelation function depends only on the difference of the variables t and t' , i.e.

$$R_{hh}(t, t + \Delta t, \tau, \tau') = R_{hh}(\Delta t, \tau, \tau') \tag{2.21}$$

where $\Delta t = |t - t'|$.

In the frequency domain (i.e. the Fourier transform of the t variable), WSS means that contributions from different Doppler frequencies of the channel are uncorrelated. For Gaussian process, WSS directly implies strict sense stationarity which is equivalent to stating that the statistics of the channel does not change with time. The uncorrelated scattering (US) assumption states that the statistics of the different delays are uncorrelated, i.e.

$$R_{hh}(t, t', \tau, \tau') = P_{hh}(t, t', \tau)\delta(\tau - \tau') \tag{2.22}$$

where $P_{hh}(t, t', \tau)$ is called the delay cross power spectral density function. Equivalently, in a multipath fading channel, the US assumption states that paths with different delays are uncorrelated and that any path does not provide any information on another path.

The tapped delay line (TDL) model is a popular model because it satisfies the assumptions of the WSSUS channel [1]. Using the TDL channel model, the continuous time LTV channel impulse response of a multipath fading channel with L resolvable propagation paths is given by

$$h(t, \tau) = \sum_{l=0}^{L-1} g_l(t)\delta(\tau - \tau_l) \tag{2.23}$$

where $g_l(t)$, τ_l represent the complex path gains and the delay of the l^{th} path. The time correlation of the complex path gains of the l^{th} path is given by their corresponding Doppler spectrum. To use the TDL model in computer simulation when doing analysis, the path delays must be converted or rounded to an integer multiple of the sampling time. Hence, in discrete computer simulation with sampling time T_s, the tapped delay line model channel response is

$$h(t, \tau) = \sum_{l=0}^{L'-1} g_l(t)\delta(\tau - lT_s) \tag{2.24}$$

where L' is the length of the channel impulse response in units of T_s.

The Doppler spectrum in Rayleigh fading is obtained as following the derivation given in [1]. Suppose the mobile station is moving at speed v and the l^{th} path arrives in an incident angle θ, then it experiences a Doppler shift given by

$$\upsilon = \frac{f_c v}{c}\cos(\theta) = f_d \cos(\theta) \tag{2.25}$$

where f_d denotes the maximum Doppler shift and is equal to $\frac{f_c v}{c}$. It is further assumed that the arrival incident angle is uniformly distributed, i.e.

$$p_\theta(\theta) = \frac{1}{2\pi}, \quad \theta \in (-\pi, +\pi] \tag{2.26}$$

Using 2.25 and 2.26 and doing a transformation of variables yields the probability density function for the Doppler shift ν

$$p_v(v) = \frac{1}{\pi} \frac{1}{f_d \left|\sin\left(\theta\right)\right|} = \frac{1}{\pi f_d \sqrt{1 - \left(\frac{v}{f_d}\right)^2}} \tag{2.27}$$

Assuming that an ideal isotropic antenna is used and received power is uniformly distributed over all incident angles, hence the Doppler power spectral density, or the Doppler spectrum is given by

$$\Phi_D(v) = \frac{\sigma_h^2}{\pi f_d \sqrt{1 - \left(\frac{v}{f_d}\right)^2}} \tag{2.28}$$

where σ_h^2 is the mean received power. The autocorrelation function is obtained by taking the inverse Fourier transform of the Doppler power spectral density,

$$\phi_{hh}(\Delta t) = \sigma_h^2 J_0(2\pi f_d \Delta t) \tag{2.29}$$

In Rayleigh fading, the gain on the path l, g_l, is assumed to be zero mean complex Gaussian with variance σ_h^2. Using this assumption, the envelope or the amplitude magnitude has Rayleigh distribution given by the PDF

$$\begin{aligned} p_r(r) &= \tfrac{2r}{\sigma_h^2} \exp\left(-\tfrac{r^2}{\sigma_h^2}\right) \\ r &= \sqrt{g_l g_l^*} \end{aligned} \tag{2.30}$$

From the above discussion on Rayleigh multipath fading channel, four types of fading can be distinguished. The root mean square (RMS) delay spread measures the time dispersive nature of the channel. This is can be computed directly from the power delay profile. In practice, the delay of the first arrival path is set to zero and the delay of all other paths that arrives at the receiver later are all measured relative to the first path. The RMS delay spread is given by

$$\tau_{rms} = \sqrt{\frac{\sum_{l=1}^{L} \sigma_h^2[l](\tau_l^2 - \tau_l)}{\sum_{l=1}^{L} \sigma_h^2[l]}} \tag{2.31}$$

where $\sigma_h^2[l]$ is the mean received power of path l and τ_l is the delay of path l. One can also define the coherence bandwidth B_C being proportional to the inverse of the RMS delay spread

$$B_C \approx \frac{1}{\tau_{rms}} \tag{2.32}$$

Then, with respect to the symbol period T_s (and system bandwidth $B_s = \frac{1}{T_s}$), two types of fading are differentiated. If $T_s >> \tau_{rms}$ or equivalently $B_s << B_C$, then the channel is a flat fading channel or a frequency non-selective channel. If $T_s << \tau_{rms}$ or equivalently $B_s >> B_c$, then the channel is a frequency selective channel. A flat fading channel is non-dispersive and only scales the transmitted signal by a complex gain. A frequency selective channel is dispersive and this dispersion induces intersymbol interference (ISI)

The Doppler spread or Doppler bandwidth B_D is defined as the range of frequencies over which the Doppler spectrum is non-zero. In Rayleigh fading, the Doppler bandwidth is approximately equal to the maximum Doppler shift

$$B_D \approx f_d = \frac{v f_c}{c} \tag{2.33}$$

The coherence time T_C can be defined as being proportional to the inverse of the Doppler bandwidth

$$T_C \approx \frac{1}{B_D} \tag{2.34}$$

With respect to the symbol period, one can differentiate two other types of fading. If $T_s << T_C$ or equivalently $B_s >> B_D$, then the channel is a slowly fading channel. If $T_s >> T_C$ or equivalently $B_s << B_D$, then the channel is a fast fading channel. In a slowly fading channel, the channel does not change much or can be assumed static over a symbol period or several symbol periods. In fast fading, the channel changes within a symbol period. Table 2.1 summarizes the four types of fading model.

CHANNEL TYPE	CONDITIONS
frequency non-selective, slowly fading	$T_s >> \tau_{rms}$, $B_s << B_C$ $T_s << T_C$, $B_s >> B_D$
frequency selective, slowly fading	$T_s << \tau_{rms}$, $B_s >> B_C$ $T_s << T_C$, $B_s >> B_D$
frequency non-selective, fast fading	$T_s >> \tau_{rms}$, $B_s << B_C$ $T_s >> T_C$, $B_s << B_D$
frequency selective, fast fading	$T_s << \tau_{rms}$, $B_s >> B_C$ $T_s >> T_C$, $B_s << B_D$

Table 2.1: Summary of channel fading models in mobile wireless channels

2.3.3 Cyclic Prefix Insertion and Removal of Block ISI

In using OFDM based transmission, implementation using the IDFT and DFT modulation and demodulation requires the insertion of cyclic prefix. This is crucial to the performance in frequency selective channels for any system that uses OFDM based transmission including TF-MC-CDMA. Without loss of generality, let us assume our channel is frequency selective and that the equivalent discrete time channel (after sampling our signal) has L taps, then it can be written as a discrete time varying finite impulse response (FIR) filter

$$h[k,n] = \sum_{l=0}^{L-1} g_l[k]\delta[n-l] \tag{2.35}$$

Then, the received OFDM block consisting of M transmitted symbols then will experience block ISI with the previous OFDM block with L overlapping symbols. The problem with block ISI is that the output, which is obtained by linear convolution with the channel impulse response, has a different value than the circular convolution between the signal and the channel impulse response. In OFDM implementation using IDFT and DFT, the circular convolution operation in the time domain is equivalent to multiplication operation in the frequency domain [37, 38]. Ideally, we would like to have the circular convolution operation have the same output as the true linear convolution. To avoid block ISI and have circular convolution and linear convolution

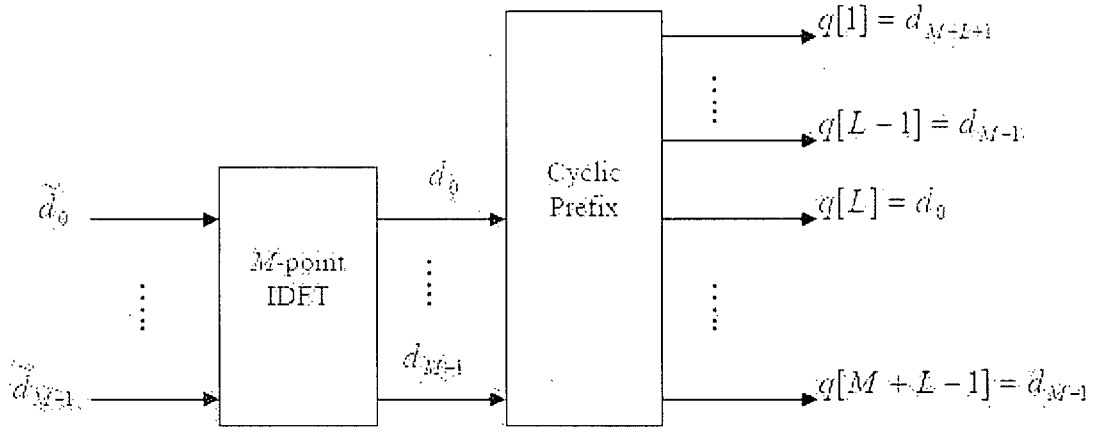

Figure 2.4: Cyclic Prefix Insertion

to produce the same output, a prefix is inserted consisting of the $L-1$ cyclically rotated symbols to our original OFDM data block as shown in Fig. 2.4.

Note that we can also achieve the same result by zero padding instead of adding cyclic prefix. By using the cyclic prefix, we can write the output as the circular convolution of the input signal and the channel impulse response. Denoting $\mathbf{d}$ as our original OFDM data block, $\mathbf{h} = \begin{bmatrix} g_0 & \dots & g_{L-1} \end{bmatrix}^T$ as the channel impulse response, then we have

$$\begin{aligned} \mathbf{y} &= \mathbf{d} * \mathbf{h} \\ DFT_M\{\mathbf{y}\} &= DFT_M\{\mathbf{d} * \mathbf{h}\} = DFT_M\{\mathbf{d}\} \circ DFT_M\{\mathbf{h}\} \end{aligned} \tag{2.36}$$

where $\circ$ denotes element by element multiplication and DFT_M denotes the M-point DFT. From the above, one can define an equivalent frequency domain transfer function $\mathbf{H}$ of the channel impulse response $\mathbf{h}$

$$\mathbf{H} = DFT_M\{\mathbf{h}\} = \sum_{l=0}^{M} g_l \exp\left(\frac{-j2\pi ml}{M}\right) = \sum_{l=0}^{L-1} g_l \exp\left(\frac{-j2\pi ml}{M}\right), \quad M > L \tag{2.37}$$

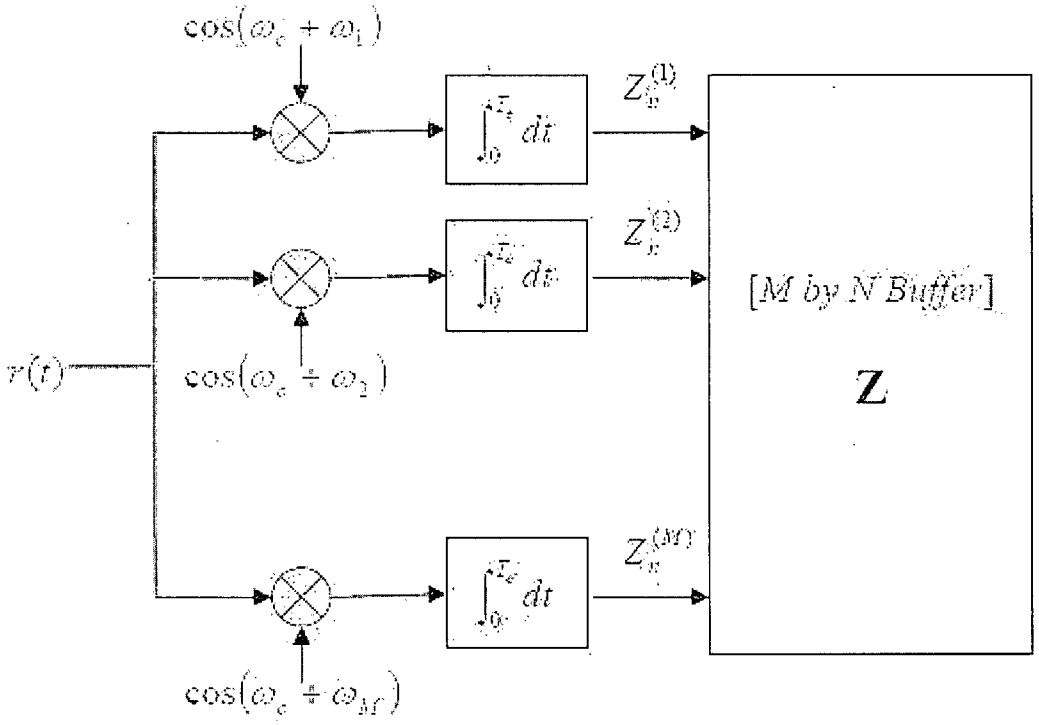

Figure 2.5: Passband Demodulator

2.4 TF-MC-CDMA Demodulation

In this section, the demodulator used for demodulating TF-spread MC-CDMA signal is discussed. The purpose of the demodulator is to extract the set of sufficient statistics from the observation data with no loss of information. The set of sufficient statistics at the output will be used for detection processing. In particular, we will discuss two equivalent demodulation process: (1) Bandpass model demodulation and (2) complex baseband model demodulation.

2.4.1 Passband Model Demodulation

The system block diagram of the demodulator is shown in Fig. 2.5. From the demodulator system block diagram, the received signal (signal plus noise) coming from the

demodulator output at the n^{th} time domain chip of the l^{th} subcarrier is given by

$$Z_n^{(l)} = \int_{(n-1)T_c}^{nT_c} r(t) P_{T_c}(t - nT_c) \cos(\omega_l t) dt \tag{2.38}$$

The noise component, specifically, of the output of the n^{th} time domain chip epoch of the l^{th} subcarrier is given by

$$N_n^{(l)} = \int_{(n-1)T_c}^{nT_c} n(t) P_{T_c}(t - nT_c) \cos(\omega_l t) dt \tag{2.39}$$

The statistical properties of the noise term $N_n^{(l)}$ are straight forward to derive using the AWGN properties of the noise process $n(t)$.

$$\begin{aligned} E\left\{N_n^{(l)}\right\} &= E\left\{\int_{(n-1)T_c}^{nT_c} n(t) P_{T_c}(t - nT_c) \cos(\omega_l t) dt\right\} \\ &= \int_{(n-1)T_c}^{nT_c} E\{n(t)\} P_{T_c}(t - nT_c) \cos(\omega_l t) dt \\ &= 0 \end{aligned} \tag{2.40}$$

Furthermore, we have

$$\begin{aligned} E\left\{N_n^{(l)} N_j^{(m)}\right\} &= \int_{(n-1)T_c}^{nT_c} \int_{(j-1)T_c}^{jT_c} E\left\{n(t)n(\tau)\right\} P_{T_c}(t - nT_c) P_{T_c}(\tau - jT_c) \times \\ &\times \cos(\omega_l t) \cos(\omega_m \tau) dt d\tau \\ &= \int_{(n-1)T_c}^{nT_c} \int_{(j-1)T_c}^{jT_c} \frac{N_0}{2} \delta(t - \tau) P_{T_c}(t - nT_c) P_{T_c}(\tau - jT_c) \times \\ &\times \cos(\omega_l t) \cos(\omega_m \tau) dt d\tau \\ &= \int_{(n-1)T_c}^{nT_c} \int_{(j-1)T_c}^{jT_c} \frac{N_0}{2} \delta(t - \tau) \delta_{nj} \delta_{ml} P_{T_c}(t - nT_c) P_{T_c}(\tau - jT_c) \times \\ &\times \cos(\omega_l t) \cos(\omega_m \tau) dt d\tau \\ &= \frac{N_0}{2} \delta_{nj} \delta_{ml} \int_{(n-1)T_c}^{nT_c} \cos^2(\omega_l t) dt \\ &= \frac{N_0}{2} \frac{T_c}{2} \delta_{nj} \delta_{ml} \end{aligned} \tag{2.41}$$

Hence, at the output of the demodulator, we accumulate N time domain chips from each of M carriers for a total of MN buffered chips per transmitted symbol.

2.4.2 Equivalent Complex Baseband Model Demodulation

The demodulation for the equivalent baseband model implemented using IDFT modulation is accomplished using the inverse operation - the DFT. Applying the M point IDFT to the sampled received signal given in 2.15,

$$DFT_M\left\{s_{LP}[n]\right\} = \frac{1}{\sqrt{M}}\sum_{n=0}^{M-1} s_{LP}[n]\exp\left(\frac{-j2\pi m'n}{M}\right) \tag{2.42}$$

Expanding and applying the orthogonality principle yields

$$\begin{aligned} DFT_M\left\{s_{LP}[n]\right\} &= \frac{1}{\sqrt{M}}\sum_{n=0}^{M-1}\left(\sqrt{\frac{P}{M}}\sum_{k=1}^{K} b_k a_{kj}\left\{\sum_{m=0}^{M-1} c_k[m]\exp\left(j\frac{2\pi mn}{M}\right)\right\}\right)\times \\ &\quad \times \exp\left(\frac{-j2\pi m'n}{M}\right) \\ &= \frac{\sqrt{P}}{M}\sum_{k=1}^{K}\sum_{m=0}^{M-1} b_k a_{kj} c_k[m]\sum_{n=0}^{M-1}\exp\left(\frac{j2\pi\left(m-m'\right)n}{M}\right) \\ &= \frac{\sqrt{P}}{M}\sum_{k=1}^{K}\sum_{m=0}^{M-1} b_k a_{kj} c_k[m] M\delta_{mm'} \\ &= \sqrt{P}\sum_{k=1}^{K} b_k a_{kj} c_k[m'] \end{aligned} \tag{2.43}$$

The sampled complex lowpass noise process is given by

$$\begin{aligned} W[m] &= DFT_M\left\{w\left[\frac{nT_c}{M}\right]\right\} = DFT_M\left\{w[n]\right\} \\ &= \frac{1}{\sqrt{M}}\sum_{n=0}^{M-1} w[n]\exp\left(\frac{-j2\pi mn}{M}\right) \end{aligned} \tag{2.44}$$

The statistical properties of the complex baseband sampled noise process are

$$\begin{aligned} E\left\{W[m]\right\} &= \sum_{n=0}^{M-1} E\left\{w[n]\right\}\exp\left(\frac{-j2\pi mn}{M}\right) \\ &= 0 \end{aligned} \tag{2.45}$$

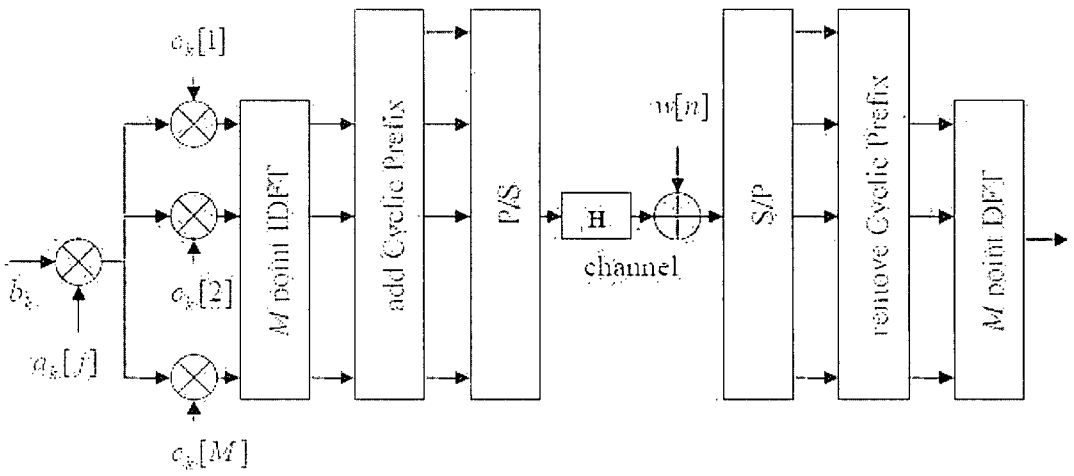

Figure 2.6: Complex Baseband Modulator and Demodulator

$$E\{W[m]W[l]\} = \frac{1}{M}\sum_{n=0}^{M-1}\sum_{n'=0}^{M-1} E\{w[n]w[n']\}\exp\left(\frac{-j2\pi mn}{M}\right)\exp\left(\frac{-j2\pi n'l}{M}\right)$$
$$= N_0\delta_{ml} \tag{2.46}$$

Fig. 2.6 summarizes the complex baseband modulation and demodulation.

2.5 Summary

In this chapter, the main principles of TF-MC-CDMA transmission and modulation are presented. The unique feature of TF-MC-CDMA is the realization of using two signature sequences for multiple access: one in the time domain (DS-CDMA), and the other in the frequency domain (MC-CDMA). We have also provided an efficient TDS and FDS sequence pair allocation scheme that minimizes the number of interferers in the each time domain group (and also for each frequency domain group). Furthermore, the characteristics and assumptions of the commonly used multipath fading channel model are reviewed. Finally, the demodulation for TF-MC-CDMA is

presented.

Chapter 3

Blind Multiuser Detection for a TF-MC-CDMA Signal in AWGN

3.1 Introduction

In this chapter, blind multiuser detection methods for TF-MC-CDMA systems in AWGN are described. The results of this chapter build on the work in [16, 17] which uses separate time and frequency linear multiuser detection by using the decorrelation detector and the MMSE detector when the receiver has perfect knowledge of the signature sequences of all users in the system as well as the noise power of the channel. Furthermore, the decorrelation detector and the MMSE detector considered are implemented using matrix inversion. It is shown in [17] that by using a two stage detection scheme, one for the time-domain spreading and the other for the frequency domain spreading, the size of the matrix to be inverted in order to compute the multiuser detector weights can be reduced. The motivation for the work in this chapter is to extend the two stage non-blind linear multiuser detection proposed by [17] to a fully blind approach. To make a valid comparison between the our results and those in [16, 17], the work presented in this chapter retains the same transmission

and channel model (AWGN) as those in [16, 17], but our work focuses on blind signal processing techniques which do not require the receiver knowledge of the signature sequences of other users or the noise power. Furthermore, we also investigate into more computationally appealing adaptive multiuser detection methods.

The roadmap for this chapter is as follows: Section 3.2 describes the linear multiuser detection problem formulation for TF-MC-CDMA. Section 3.3 discusses the algorithms for TF-MC-CDMA blind multiuser detection. Section 3.4 provides a discussion of the performance measures and evaluations for blind multiuser detection methods for TF-MC-CDMA. Section 3.5 presents computer simulation results of the blind multiuser detection algorithms presented in this chapter. Finally, a summary of the chapter is provided in Section 3.6.

3.2 Linear Multiuser Detection for TF-MC-CDMA

The purpose of using multiuser detection in TF-MC-CDMA is to mitigate the MAI in both the TD and FD and hence provide a better performance than that of conventional single user matched filter detection. It was shown in [17] that the exact bit error rate performance of the TF-MC-CDMA single user matched filter detector in AWGN channel is given by

$$\Pr\{\hat{b}_1 \neq b_1\} = \frac{1}{2^{K-1}} \sum_{b_2 \in \{-1,+1\}} \cdots \sum_{b_K \in \{-1,+1\}} Q\left(\sqrt{\frac{2E_b}{N_0}}\left[1 - \sum_{k=2}^{K} b_k \rho_{1k} \beta_{1k}\right]\right) \quad (3.1)$$

where, without loss of generality, it is assumed that the desired user is user 1. It is shown by computer simulation in [16] and [17] that the non-zero cross correlation $\{\rho_{1k}\}_{k=2}^{K}$ and $\{\beta_{1k}\}_{k=2}^{K}$ of the time and frequency domain signature sequences of the desired user and the other users cause the matched filter receiver performance to have a relatively high bit error rate (BER) floor.

Proceeding from the passband demodulated signal given by 2.38, the discrete

signal output of the n^{th} sampled time chip from the m^{th} subcarrier stream of the TF-MC-CDMA passband demodulator in AWGN channel is given by

$$Z_n^{(m)} = S_n^{(m)} + N_n^{(m)}, \quad n = 1, ..., N; m = 1, ..., M \tag{3.2}$$

where

$$S_n^{(m)} = \sqrt{\frac{2P}{M}} \frac{T_c}{2} \sum_{k=1}^{K} b_k a_k[n] c_k[m] \tag{3.3}$$

and it was shown in 2.40 and 2.41 that $N_n^{(m)}$ is a zero-mean Gaussian random variable with covariance $\frac{N_0}{2}\frac{T_c}{2}\delta_{nj}\delta_{ml}$. After demodulation, the observation data for one information symbol is collected in the N by M matrix $\mathbf{Z}$ where the elements of $\mathbf{Z}$ are given by

$$z_{nm} = Z_n^{(m)}, \quad n = 1, ..., N; m = 1, ..., M \tag{3.4}$$

Based only on the observation data and the knowledge of user 1's TD and FD signature sequence pair, our goal is to compute two sets of multiuser detection coefficients (one for the TD, one for the FD) such that the mean square error (MSE) is minimized. Mathematically, this is stated as

$$(\mathbf{w}_t^*, \mathbf{w}_f^*) = \underset{\mathbf{w}_t \in \mathbb{C}^{N\times 1}, \mathbf{w}_f \in \mathbb{C}^{M\times 1}}{\arg\min} E\left\{ \left\| Ab_1 - \left(\mathbf{w}_t^H \mathbf{Z}\right)^* \mathbf{w}_f \right\|^2 \right\} \tag{3.5}$$

where $A = \sqrt{\frac{2P}{M}}\frac{T_c}{2}$ is the energy of user one (other users also have the same energy).

The optimal linear MMSE detector for TF-MC-CDMA is given by the solution to the optimization problem given in 3.5.

3.3 Adaptive Blind Multiuser Detection for TF-MC-CDMA

In order to find a solution for 3.5, one must simultaneously solve for the time domain and frequency domain detector coefficients. This is generally a computationally com-

plex problem. This motivates us to propose an intuitive albeit suboptimal approach by decoupling the joint optimization problem into two separate optimization problems, one for the blind TD MUD and one for the blind FD MUD. To do this, we first note that if one considers one particular subcarrier stream m, then this corresponds to m^{th} column of the observation matrix $\mathbf{Z}$, $\mathbf{z}^{(m)}$

$$\mathbf{z}^{(m)} = \begin{bmatrix} S_1^{(m)} \\ S_2^{(m)} \\ \vdots \\ S_N^{(m)} \end{bmatrix} + \begin{bmatrix} N_1^{(m)} \\ N_2^{(m)} \\ \vdots \\ N_N^{(m)} \end{bmatrix} = \mathbf{s}^{(m)} + \mathbf{n}^{(m)} \tag{3.6}$$

Substituting 3.3 into 3.6 yields

$$\mathbf{z}^{(m)} = \sum_{k=1}^{K} \sqrt{\frac{2P}{M}} \frac{T_c}{2} \left(b_k c_k[m]\right) \mathbf{a}_k + \mathbf{n}^{(m)} \tag{3.7}$$

where $\mathbf{a}_k = [\ a_k[1] \quad \ldots \quad a_k[N]]^T$ is the time domain spreading chip sequence of user k and $\mathbf{n}^{(l)}$ is a zero mean Gaussian random vector with covariance $\frac{N_0}{2}\frac{T_c}{2}\mathbf{I}_{N\times N}$. It might be noted that 3.7 is equivalent to a multiuser signal model in DS-CDMA in AWGN channel. The synchronous DS-CDMA signal model has the form [13, 39] $\mathbf{r}[i] = \sum_{k=1}^{K} A_k B_k[i]\mathbf{s}_k + \mathbf{w}[i]$ where A_k, $B_k[i]$, $\mathbf{s}_k$ are the received amplitude, the i^{th} transmitted symbol and signature sequence of the k^{th} user respectively and $\mathbf{w}[i]$ is a zero mean complex Gaussian random vector. If one denotes $b_k c_k[m]$ as B_k, then 3.7 can be interpreted as a DS-CDMA multiuser signal.

Similarly, considering the n^{th} time chip epoch, one would get the n^{th} row of the matrix $\mathbf{Z}$ and get the equations of the same form as 3.6

$$\mathbf{z}_n^T = \begin{bmatrix} S_n^{(1)} \\ S_n^{(2)} \\ \vdots \\ S_n^{(M)} \end{bmatrix} + \begin{bmatrix} N_n^{(1)} \\ N_n^{(2)} \\ \vdots \\ N_n^{(M)} \end{bmatrix} = \mathbf{s}_n^T + \mathbf{n}_n^T \tag{3.8}$$

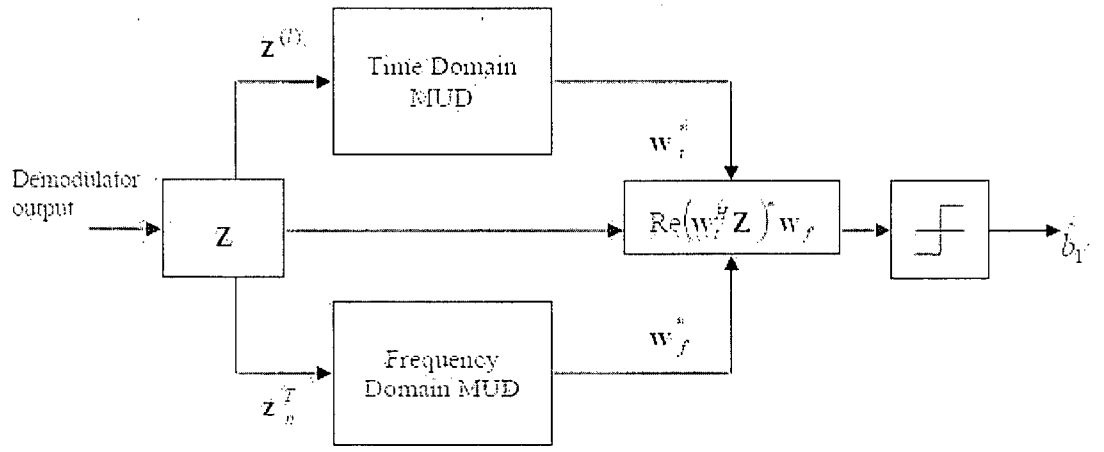

Figure 3.1: TF-MC-CDMA Multiuser Detector Architecture

Again, combining with 3.3 we obtain

$$\mathbf{z}_n^T = \sum_{k=1}^{K} \sqrt{\frac{2P}{M}} \frac{T_c}{2} \left(b_k a_k[n]\right) \mathbf{c}_k + \mathbf{n}_n^T \tag{3.9}$$

where $\mathbf{n}_n^T$ is a zero mean Gaussian random vector with covariance $\frac{N_0}{2}\frac{T_c}{2}\mathbf{I}_{M\times M}$. Denoting $b_k a_k[n]$ as B_k, then 3.9 can also be interpreted as a DS-CDMA multiuser signal. This result is significant because the joint TF-MC-CDMA blind multiuser detection problem is now split into two separate DS-CDMA blind MMSE multiuser detection problem and they can be simultaneously processed in parallel. Furthermore, because blind linear MMSE multisuer detection in DS-CDMA has been extensively studied, many techniques developed in past literatures can be applied. From 3.5 and 3.7, the optimization problem in 3.5 is decoupled into two DS-CDMA blind LMMSE multiuser detection problems, namely

$$\begin{aligned} \mathbf{w}_t^* &= \underset{\mathbf{w}_t \in \mathbb{C}^{N\times 1}}{\operatorname{argmin}} \; E\left\{ \left\| A\left(b_k c_k[m]\right) - \mathbf{w}_t^H \mathbf{z}^{(m)} \right\|^2 \right\} \\ \mathbf{w}_f^* &= \underset{\mathbf{w}_f \in \mathbb{C}^{M\times 1}}{\operatorname{argmin}} \; E\left\{ \left\| A\left(b_k a_k[n]\right) - \mathbf{w}_f^H \mathbf{z}_n^T \right\|^2 \right\} \end{aligned} \tag{3.10}$$

The block diagram for a detector for the decoupled problem is shown in Fig. 3.1. In Fig. 3.1, the slicer (the right most block in the diagram) threshold is set to zero.

It should be noted here that the decoupled DS-CDMA optimization problems in 3.10 can be modified, by considering both the received signal and its complex conjugate, to the Widely Linear (WL) formulation which was shown in [40] to improve contemporary linear MMSE processing. However, in this thesis, although we only limit the analysis to linear MMSE processing, the application of the WL MMSE processing to the decoupling technique presented here is straight forward. Three different methods are now considered for solving the decoupled blind linear MMSE multiuser detection problem: direct matrix inversion (DMI), recursive least squares (RLS) and the blind subspace detection.

3.3.1 Direct Matrix Inversion (DMI) Method

The direct matrix inversion method (DMI) for blind detection of DS-CDMA multiuser signals was discussed in [39]. The direct matrix inversion method involves computing the inverse of the data correlation matrix of the received signal. Using the analysis of the DMI method for DS-CDMA blind detection in [39], 3.10 can be re-written as 3.11 by expanding

$$\begin{aligned}\mathbf{w}_t^* &= \underset{\mathbf{w}_t \in \mathbb{C}^{N\times 1}}{\operatorname{argmin}} \left[\mathbf{w}_t^H E\left\{\mathbf{z}^{(m)}\left(\mathbf{z}^{(m)}\right)^H\right\}\mathbf{w}_t - 2\mathbf{w}_t^H \mathrm{Re}\left\{A^* E\left\{\mathbf{z}^{(m)}\left(b_k c_k[m]\right)\right\}\right\}\right] \\ \mathbf{w}_f^* &= \underset{\mathbf{w}_f \in \mathbb{C}^{M\times 1}}{\operatorname{argmin}} \left[\mathbf{w}_f^H E\left\{\mathbf{z}_n^T\left(\mathbf{z}_n^T\right)^H\right\}\mathbf{w}_f - 2\mathbf{w}_f^H \mathrm{Re}\left\{A^* E\left\{\mathbf{z}_n^T\left(b_k a_k[n]\right)\right\}\right\}\right]\end{aligned} \tag{3.11}$$

Setting the derivatives with respect to $\mathbf{w}_t$ and $\mathbf{w}_f$ in 3.11 to zero yields

$$\begin{aligned}2\mathbf{C}_t\mathbf{w}_t^* - 2|A|^2\mathbf{a}_k &= \mathbf{0} \\ 2\mathbf{C}_f\mathbf{w}_f^* - 2|A|^2\mathbf{c}_k &= \mathbf{0}\end{aligned} \tag{3.12}$$

since

$$\begin{aligned}E\left\{\mathbf{z}^{(m)}\left(b_k c_k[m]\right)\right\} &= A\mathbf{a}_k \\ E\left\{\mathbf{z}_n^T\left(b_k a_k[n]\right)\right\} &= A\mathbf{c}_k\end{aligned} \tag{3.13}$$

Defining

$$\begin{aligned} \mathbf{C}_t &\equiv E\left\{\mathbf{z}^{(m)}\left(\mathbf{z}^{(m)}\right)^H\right\} \\ \mathbf{C}_f &\equiv E\left\{\mathbf{z}_n^T\left(\mathbf{z}_n^T\right)^H\right\} \end{aligned} \tag{3.14}$$

the detector coefficients for user one are then given by

$$\begin{aligned} \mathbf{w}_t^* &= |A|^2 \mathbf{C}_t^{-1}\mathbf{a}_1 \\ \mathbf{w}_f^* &= |A|^2 \mathbf{C}_f^{-1}\mathbf{c}_k \end{aligned} \tag{3.15}$$

The matrices $\mathbf{C}_t$ and $\mathbf{C}_f$ can be estimated through their corresponding sample correlations from the received signal either through block sampling averaging or adaptively/recursively updated using a forgetting factor as in

$$\begin{aligned} \hat{\mathbf{C}}_t[p,m] &= \lambda\hat{\mathbf{C}}_t[p,m-1] + (\mathbf{z}^{(m)}[p])(\mathbf{z}^{(m)}[p])^H \\ \hat{\mathbf{C}}_f[p,n] &= \lambda\hat{\mathbf{C}}_f[p,n-1] + (\mathbf{z}_n[p]^T)(\mathbf{z}_n[p]^T)^H \end{aligned} \tag{3.16}$$

where λ is the forgetting factor, $\hat{\mathbf{C}}_t[p,m]$ is the update of the time domain sample correlation matrix for the m^{th} subcarrier stream, $\{m : m = 1, 2, ..., M\}$, during the p^{th} transmitted bit, $\{p : p = 0, 1, 2, ...\}$, and $\hat{\mathbf{C}}_f[p,n]$ is the update of the frequency domain sample correlation matrix for the n^{th} time chip epoch, $\{n : n = 1, 2, ..., N\}$ during the p^{th} transmitted bit. It can be noted that $\hat{\mathbf{C}}_t[p,0]$ is equivalent to $\hat{\mathbf{C}}_t[p-1,M]$ and similarly $\hat{\mathbf{C}}_f[p,0]$ is equivalent to $\hat{\mathbf{C}}_f[p-1,N]$.

Note that the received power A only affects $\mathbf{w}_t^*$ and $\mathbf{w}_f^*$ through positive scaling. The decision of the estimated information bit is unaffected because using BPSK, the decision is computed as $\hat{b}_1[p] = \text{sgn}\left(\text{Re}\left\{\left(\mathbf{w}_t^{*H}\mathbf{Z}\right)^*\mathbf{w}_f^*\right\}\right)$ and is unaffected by positive scaling of the parameters $\mathbf{w}_t^*$ and $\mathbf{w}_f^*$. Therefore, estimation of the received power is not needed for detection. Furthermore, the detector coefficients need not be computed every symbol time. In practice, for non-fading channels, the sample correlation matrices for both the time and frequency domain reaches convergence after a relatively few data symbols and re-computing the detector coefficients from the

// Blind TF-MC-CDMA DMI Receiver in AWGN
In the p^{th} symbol, input matrix $\mathbf{Z}[p]$
for$(m = 1, 2, ..., M)$
update $\hat{\mathbf{C}}_t[p, m] = \lambda \hat{\mathbf{C}}_t[p, m-1] + (\mathbf{z}^{(m)}[p])(\mathbf{z}^{(m)}[p])^H$
end for
for$(n = 1, 2, ..., N)$
update $\hat{\mathbf{C}}_f[p, n] = \lambda \hat{\mathbf{C}}_f[p, n-1] + (\mathbf{z}_n[p]^T)(\mathbf{z}_n[p]^T)^H$
end for
Compute Detectors
$\mathbf{w}_t^* = \hat{\mathbf{C}}_t^{-1}\mathbf{a}_1$
$\mathbf{w}_f^* = \hat{\mathbf{C}}_f^{-1}\mathbf{c}_1$
Perform detection
$\hat{b}_1[p] = \text{sgn}\left(\text{Re}\left\{\left(\mathbf{w}_t^{*H}\mathbf{Z}\right)^* \mathbf{w}_f^*\right\}\right)$

Table 3.1: Blind TF-MC-CDMA DMI Receiver Algorithm

updates of the sample correlation matrices further beyond that point does little change to the performance of the detector. For fading channels, periodic re-computation of the detector coefficients are necessary due to the time varying nature of the channel. The period between update would depend on the coherence time of the fading channel. The DMI algorithm is summarized in Table 3.1.

3.3.2 CMOE Recursive Least Squares (RLS) Method

The main drawback of the DMI method is the need for inverting the sample correlation matrices $\hat{\mathbf{C}}_t$ and $\hat{\mathbf{C}}_f$. To avoid computing matrix inversions, the method of recursive least squares (RLS) can be used. The RLS method is based on solving constrained minimum output energy (MOE)/CMOE detector for blind multiuser detection in DS-CDMA first proposed in [14]. It is shown in [13] that the DS-CDMA CMOE detector and the blind linear MMSE detector optimization problems give solutions that differ only by a positive scaling constant. Therefore, minimizing the MOE is equivalent to minimizing the MSE. It is later shown in [18] that the CMOE detector can be generalized to problems that have more than one user signature code constraint.

Using the analysis given in [39], the CMOE alternative representation of the TF-MC-CDMA MMSE decoupled optimization problem in 3.10 is given by

$$\begin{aligned}\mathbf{w}_t^* &= \underset{\mathbf{w}_t \in \mathbb{C}^{N\times 1}}{\operatorname{argmin}}\ E\left\{\left\|\mathbf{w}_t^H \mathbf{z}^{(m)}\right\|^2\right\}, \quad \mathbf{w}_t^H \mathbf{a}_1 = 1 \\ \mathbf{w}_f^* &= \underset{\mathbf{w}_f \in \mathbb{C}^{M\times 1}}{\operatorname{argmin}}\ E\left\{\left\|\mathbf{w}_f^H \mathbf{z}_n^T\right\|^2\right\}, \quad \mathbf{w}_f^H \mathbf{c}_1 = 1\end{aligned} \tag{3.17}$$

Based on the CMOE constrained optimization problem above, the RLS algorithm computes the detector weights according to the minimization of the sum of exponentially weighted mean-square output with a forgetting factor [39]

$$\begin{aligned}\mathbf{w}_t^* &= \underset{\mathbf{w}_t \in \mathbb{C}^{N\times 1}}{\operatorname{argmin}} \sum_{m=0}^{l[p]} \lambda^{l[p]-i} \left\|\mathbf{w}_t^H \mathbf{z}^{(m)}\right\|^2, \quad \mathbf{w}_t^H \mathbf{a}_1 = 1 \\ \mathbf{w}_f^* &= \underset{\mathbf{w}_f \in \mathbb{C}^{N\times 1}}{\operatorname{argmin}} \sum_{n=0}^{j[p]} \lambda^{j[p]-i} \left\|\mathbf{w}_f^H \mathbf{z}_n^T\right\|^2, \quad \mathbf{w}_f^H \mathbf{c}_1 = 1\end{aligned} \tag{3.18}$$

The first summation in 3.18 states that the sum is over all subcarrier stream going from the zeroth subcarrier stream from the zeroth transmitted symbol to the l^{th} subcarrier stream of the p^{th} symbol. Similarly, the second summation in 4.15 states that the sum is over all time chips going from the zeroth time chip from the zeroth transmitted symbol to the j^{th} chip of the p^{th} symbol.

The solution to the optimization problem in 3.18 (up to a real positive scaling constant) has a similar form to the DMI method

$$\begin{aligned}\mathbf{w}_t^* &= \mathbf{C}_t^{-1}\mathbf{a}_1 \\ \mathbf{w}_f^* &= \mathbf{C}_f^{-1}\mathbf{c}_1\end{aligned} \tag{3.19}$$

where again,

$$\begin{aligned}\mathbf{C}_t[p,m] &= \lambda \mathbf{C}_t[p,m-1] + \mathbf{z}^{(m)}\mathbf{z}^{(m)H} \\ \mathbf{C}_f[p,n] &= \lambda \mathbf{C}_f[p,n-1] + \mathbf{z}_n^T(\mathbf{z}_n^T)^H\end{aligned} \tag{3.20}$$

To compute the detector, the RLS algorithm avoids computing the inverse of the correlation directly by using the matrix inversion lemma [39] to recursively estimate

// Blind TF-MC-CDMA CMOE RLS Receiver in AWGN

Initialization:

$\mathbf{\Phi}_t[0,0] = \mathbf{I}_{N\times N},\ \mathbf{\Phi}_f[0,0] = \mathbf{I}_{M\times M}$

In the p^{th} symbol, input matrix $\mathbf{Z}[p]$

for$(m = 1, 2, ..., M)$

Compute Kalman Gain:

$\mathbf{k}_t[p,m] = \frac{\lambda^{-1}\mathbf{\Phi}_t[p,m-1]\mathbf{z}^{(m)}[p]}{1+\lambda^{-1}\mathbf{z}^{(m)}[p]^H\mathbf{\Phi}_t[p,m-1]\mathbf{z}^{(m)}[p]}$

Compute Update:

$\mathbf{\Phi}_t[p,m] = \lambda^{-1}\left(\mathbf{\Phi}_f[p,m-1] - \mathbf{k}_f\left(\mathbf{z}^{(m)}[p]\right)^H\mathbf{\Phi}_t[p,m-1]\right)$

end for

for$(n = 1, 2, ..., N)$

Compute Kalman Gain:

$\mathbf{k}_f[p,n] = \frac{\lambda^{-1}\mathbf{\Phi}_f[p,n-1]\mathbf{z}_n[p]^T}{1+\lambda^{-1}(\mathbf{z}_n[p]^T)^H\mathbf{\Phi}_f[p,n-1]\mathbf{z}_n[p]^T}$

Compute Update:

$\mathbf{\Phi}_f[p,n] = \lambda^{-1}\left(\mathbf{\Phi}_f[p,n-1] - \mathbf{k}_f\left(\mathbf{z}_n[p]^T\right)^H\mathbf{\Phi}_f[p,n-1]\right)$

end for

Compute Detectors

$\mathbf{w}_t^* = \mathbf{\Phi}_t\mathbf{a}_1$

$\mathbf{w}_f^* = \mathbf{\Phi}_f\mathbf{c}_1$

Perform detection

$\hat{b}_1[p] = \mathrm{sgn}\left(\mathrm{Re}\left\{\left(\mathbf{w}_t^{*H}\mathbf{Z}\right)^*\mathbf{w}_f^*\right\}\right)$

Table 3.2: Blind CMOE RLS Receiver Algorithm

the matrix inverse. Letting $\mathbf{\Phi}_t[j] \approx \mathbf{C}_t[j]^{-1}$ and $\mathbf{\Phi}_f[j] \approx \mathbf{C}_f[j]^{-1}$, the matrix inversion lemma gives

$$\begin{aligned}\mathbf{\Phi}_t[j] &= \lambda^{-1}\mathbf{\Phi}_t[j-1] - \frac{\lambda^{-2}\mathbf{\Phi}_t[j-1]\mathbf{z}^{(m)}\mathbf{z}^{(m)H}\mathbf{\Phi}_t[j-1]}{1+\lambda^{-1}\mathbf{z}^{(m)H}\mathbf{\Phi}_t[j-1]\mathbf{z}^{(m)}} \\ \mathbf{\Phi}_f[j] &= \lambda^{-1}\mathbf{\Phi}_f[j-1] - \frac{\lambda^{-2}\mathbf{\Phi}_f[j-1]\mathbf{z}_n^T(\mathbf{z}_n^T)^H\mathbf{\Phi}_f[j-1]}{1+\lambda^{-1}(\mathbf{z}_n^T)^H\mathbf{\Phi}_f[j-1]\mathbf{z}_n^T}\end{aligned} \tag{3.21}$$

where j is the iteration index.

The RLS algorithm has a much faster convergence than the least mean squares (LMS) method using gradient descent method and is therefore less sensitive to the choice of initial values [39]. The TF-MC-CDMA blind MOE RLS multiuser detection algorithm is summarized in Table 3.2.

3.3.3 Blind Subspace-Based Method

The method of subspace blind multiuser detection for DS-CDMA was first proposed in [20]. The idea is to decompose the autocorrelation matrix into a signal subspace and a noise subspace through eigendecomposition. To see this, we consider the decoupled multiuser detection problem for the time domain (the exact analysis holds for the frequency domain multiuser detection problem)

$$\mathbf{C}_t \equiv E\left\{\mathbf{z}^{(l)}\left(\mathbf{z}^{(l)}\right)^H\right\} = \mathbf{S}_t\left|\mathbf{A}\right|^2\mathbf{S}_t^H + \sigma_t^2\mathbf{I}_{N\times N} \tag{3.22}$$

where

$$\begin{aligned}\mathbf{S}_t &= [\mathbf{a}_1|\mathbf{a}_2|...|\mathbf{a}_{U_t}]\\ \sigma_t^2 &= \tfrac{N_0}{2}\tfrac{T_c}{2}\\ |\mathbf{A}|^2 &= diag(A_1^2,...,A_{U_t}^2)\end{aligned} \tag{3.23}$$

and U_t represents the number of linearly independent TDS signature sequence used in the system, and A_i represents the superposition of the amplitudes of all users that uses the TDS signature i, $i = 1,...,U_t$. It is assumed that the spreading signature sequences in the time and frequency domain form linearly independent sets. This is usually not a problem in practical applications because the transmitter and receiver can be coordinated to use sequence sets that are linearly independent. On average, the effect of the channel does not affect the linear independence of the sequence sets. Assuming this condition is satisfied, then the eigendecomposition of the autocorrelation matrix can be written as

$$\begin{aligned}\mathbf{C}_t &= \mathbf{U}_s^{(t)}\mathbf{\Lambda}_s^{(t)}\mathbf{U}_s^{(t)H} + \sigma_t^2\mathbf{U}_n^{(t)}\mathbf{U}_n^{(t)H}\\ \mathbf{\Lambda}_s^{(t)} &= diag\left(\lambda_1^{(t)},...,\lambda_{U_t}^{(t)}\right)\end{aligned} \tag{3.24}$$

where $\left\{\lambda_i^{(t)}\right\}_{i=1}^{U_t}$ are the U_t largest eigenvalues of $\mathbf{C}_t$ in descending order, the N by U_t matrix $\mathbf{U}_s^{(t)}$ contains the corresponding U_t eigenvectors as its columns and the N by $N - U_t$ $\mathbf{U}_n^{(t)}$ contains the $N - U_t$ eigenvectors corresponding to the eigenvalue σ_t^2.

The blind LMMSE detector is obtained by substituting the subspace decomposition of $\mathbf{C}_t$ into 3.19, i.e.

$$\begin{aligned}\mathbf{w}_t^* &= \mathbf{C}_t^{-1}\mathbf{a}_1 = (\mathbf{U}_s^{(t)}\mathbf{\Lambda}_s^{(t)}\mathbf{U}_s^{(t)H} + \sigma_t^2\mathbf{U}_n^{(t)}\mathbf{U}_n^{(t)H})^{-1}\mathbf{a}_1 \\ &= \mathbf{U}_s^{(t)}(\mathbf{\Lambda}_s^{(t)})^{-1}\mathbf{U}_s^{(t)H}\mathbf{a}_1 + \tfrac{1}{\sigma_t^2}\mathbf{U}_n^{(t)}\mathbf{U}_n^{(t)H}\mathbf{a}_1 \\ &= \mathbf{U}_s^{(t)}(\mathbf{\Lambda}_s^{(t)})\mathbf{U}_s^{(t)H}\mathbf{a}_1\end{aligned} \tag{3.25}$$

where the last equality holds since the eigenvectors contained in the matrix $\mathbf{U}_s^{(t)}$ span the signal subspace which means that the vector $\mathbf{a}_1$ can be expressed as a linearly combination of the eigenvectors in the matrix $\mathbf{U}_s^{(t)}$ and therefore

$$(\mathbf{U}_n^{(t)})^H\mathbf{a}_1 = \mathbf{0} \tag{3.26}$$

Using a similar analysis for the FD case in the decoupled multiuser detection problem yields

$$\mathbf{w}_f^* = \mathbf{U}_s^{(f)}(\mathbf{\Lambda}_s^{(f)})^{-1}\mathbf{U}_s^{(f)H}\mathbf{c}_1 \tag{3.27}$$

Hence, the blind LMMSE detector for both the FD and TD detection can be computed once $\mathbf{U}_s^{(t)}$, $\mathbf{\Lambda}_s^{(t)}$, $\mathbf{U}_s^{(f)}$, and $\mathbf{\Lambda}_s^{(f)}$ are estimated. Two methods are shown in [20] and [39] to estimate the subspace parameters, namely, singular value decomposition and adaptive subspace tracking using PASTd algorithm.

Singular Value Decomposition

The subspace parameters can be tracked by applying the singular value decomposition of the sample data matrix, or equivalently, the eigenvalue decomposition of the sample correlation matrix. The sample correlation matrix can be obtained through block sampling averaging or recursively updating using an exponentially weighted window with a forgetting factor as in 3.20. As in the DMI method, the subspace parameters need not be computed every symbol duration. In practice, for non-fading channels, the sample correlation matrices for both the time and frequency domain

// Blind TF-MC-CDMA Subspace (SVD) Receiver in AWGN

In the pth symbol, input matrix $\mathbf{Z}[p]$

for$(m = 1, 2, ..., M)$

Compute Update:

$\hat{\mathbf{C}}_t[p, m] = \lambda \hat{\mathbf{C}}_t[p, m-1] + (\mathbf{z}^{(m)}[p])(\mathbf{z}^{(m)}[p])^H$

end for

for$(n = 1, 2, ..., N)$

Compute Update:

$\hat{\mathbf{C}}_f[p, n] = \lambda \hat{\mathbf{C}}_f[p, n-1] + (\mathbf{z}_n[p]^T)(\mathbf{z}_n[p]^T)^H$

end for

Apply Eigenvalue decomposition to $\hat{\mathbf{C}}_t$ and $\hat{\mathbf{C}}_f$
to get eigenvectors and eigenvalues:

$\left\{\hat{\mathbf{u}}_j^{(t)}\right\}_{j=1}^{U_t}, \left\{\hat{\mathbf{u}}_j^{(f)}\right\}_{j=1}^{U_f}, \left\{\hat{\lambda}_j^{(t)}\right\}_{j=1}^{U_t}, \left\{\hat{\lambda}_j^{(f)}\right\}_{j=1}^{U_f}$

Compute Detectors

$\mathbf{w}_t^* = \hat{\mathbf{U}}_s^{(t)}(\hat{\mathbf{\Lambda}}_s^{(t)})^{-1}\hat{\mathbf{U}}_s^{(t)H}\mathbf{a}_1$

$\mathbf{w}_f^* = \hat{\mathbf{U}}_s^{(f)}(\hat{\mathbf{\Lambda}}_s^{(f)})^{-1}\hat{\mathbf{U}}_s^{(f)H}\mathbf{c}_1$

Perform detection

$\hat{b}_1[p] = \text{sgn}\left(\text{Re}\left\{\left(\mathbf{w}_t^{*H}\mathbf{Z}\right)^* \mathbf{w}_f^*\right\}\right)$

Table 3.3: Blind Subspace SVD Receiver Algorithm

reaches convergence after a relatively few data symbols and re-computing the subspace matrices and detector coefficients from the updated sample correlation matrices further beyond that point does little improvement to the performance of the detector. For fading channels, periodic re-computation of the detector coefficients are necessary due to the time varying nature of the channel. The period between update would depend on the coherence time of the fading channel. The TF-MC-CDMA blind subspace algorithm using SVD is summarized in Table 3.3.

Adaptive Subspace Tracking Using PASTd

A computationally more attractive algorithm for estimating the subspace parameters is adaptive subspace tracking. In addition to its computational advantage, it is adaptable to changes in channel conditions even when the channel is time varying and thus more robust in practical applications. The PASTd algorithm was first pro-

posed by [22] and first applied to DS-CDMA systems by Wang [30]. The concept of adaptive subspace tracking can be summarized as follows [22] [24]. We consider the optimization problem of the scalar function

$$J(\mathbf{W}) = E\left\{\left\|\mathbf{r}[i] - \mathbf{W}\mathbf{W}^H\mathbf{r}[i]\right\|^2\right\} \tag{3.28}$$

where $\mathbf{r}[i]$ is a noisy observation vector with correlation matrix given by $\mathbf{C}_r = E\left\{\mathbf{r}[i]\mathbf{r}[i]^H\right\}$ and $\mathbf{W} \in C^{N\times q}, q < N$. There are two important properties of this optimization problem:

1. $\mathbf{W}$ is a stationary point (the point where the gradient is zero) of $J(\mathbf{W})$ if and only if $\mathbf{W}$ can be factored as $\mathbf{W} = \mathbf{U}_r\mathbf{Q}$ where $\mathbf{U}_r$ is a N by q matrix that contains any q distinct eigenvectors of $\mathbf{C}_r$, and $\mathbf{Q}$ is any q by q unitary matrix.

2. All stationary points of $J(\mathbf{W})$ are saddle points only except the case when $\mathbf{U}_r$ contains the q dominant eigenvectors (corresponding to the q largest eigenvalues) of $\mathbf{C}_r$. In that case, $J(\mathbf{W})$ attains the global minimum.

Here, we are interested in the case when $q = 1$. Then the solution to the optimization problem is simply given by the eigenvector corresponding to the largest eigenvalue. However, in practice, we only have access to the observation samples $\mathbf{r}[i]$ and not $\mathbf{C}_r$; hence, we modify the original optimization problem into the exponential weighted sum with a forgetting factor γ

$$J(\mathbf{W}) = \sum_{n=0}^{i} \gamma^{i-n} \left\|\mathbf{r}[n] - \mathbf{W}[i]\mathbf{W}[i]^H\mathbf{r}[n]\right\|^2 \tag{3.29}$$

The PASTd algorithm has two main components: (1) Projection approximation and (2) deflation. The projection approximation is

$$\mathbf{W}[i]^H\mathbf{r}[n] \approx \mathbf{W}[n-1]^H\mathbf{r}[n] = \mathbf{y}[n], \quad n = 1, 2, ...i \tag{3.30}$$

Then, applying the approximation, (3-29) becomes

$$J(\mathbf{W}) \approx \tilde{J}(\mathbf{W}) = \sum_{n=0}^{i} \gamma^{i-n} \left\|\mathbf{r}[n] - \mathbf{W}[i]\mathbf{y}[n]\right\|^2 \tag{3.31}$$

The RLS algorithm can once again be applied to solve for $\mathbf{W}[i]$, which, by property (2) above, is an approximation to the eigenvector of $\mathbf{C}_r$ corresponding to the largest eigenvalue. The deflation technique can now be applied. Once an estimate of the dominant eigenvector is obtained, the projection of the current observation vector $\mathbf{r}[i]$ onto it can be removed using a Gram-Schmidt like procedure and the problem is now "deflated" or dimensionally reduced. Thus, if we repeat the same procedure (i.e. applying the RLS algorithm again and solving for $\mathbf{W}[i]$), we would get an estimate of the next dominant eigenvector. Once we have the estimates of the eigenvectors and eigenvalues, the blind subspace LMMSE detector can be computed. The algorithm is summarized in Table 3.4.

3.4 Performance Measure

The most commonly used performance measure for a multiuser detector is the bit error rate (BER). In TF-MC-CDMA, parameters such as the TDS factor and FDS factor also play a significant role in determining the overall system performance and efficiency in resource utilization. Another measure for blind multiuser detectors is the output signal to interference plus noise ratio (SINR). This is computed as the ratio of the desired signal to the sum of the total interference plus ambient noise. For TF-MC-CDMA linear multiuser detectors, the output SINR is defined as

$$SINR(\mathbf{w}_t, \mathbf{w}_f) = \frac{E\left\{(\mathbf{w}_t^H \mathbf{Z}[p])^* \mathbf{w}_f | b_1[\mathrm{p}]\right\}^2}{E\left\{Var\left((\mathbf{w}_t^H \mathbf{Z}[p])^* \mathbf{w}_f | b_1[\mathrm{p}]\right)\right\}} \tag{3.32}$$

From the output SINR information, we can evaluate the convergence speed for multiuser detection algorithms. Also important measures are how BER performance and the output SINR changes with the number of users in the system. To summarize, bit error rate performance evaluated with multiuser capacity, output SINR, resource utilization efficiency and rate of convergence are important in designing multiuser

// Blind TF-MC-CDMA Subspace (PASTd) Receiver in AWGN

In the p^{th} symbol, input matrix $\mathbf{Z}[p]$ and previous estimates $\left\{\hat{\lambda}_k^{(t)}, \hat{\mathbf{u}}_k^{(t)}\right\}_{k=1}^{U_t}$, $\left\{\hat{\lambda}_k^{(f)}, \hat{\mathbf{u}}_k^{(f)}\right\}_{k=1}^{U_f}$

for$(m = 1, 2, ..., M)$

  Input $\mathbf{z}^{(m)}[p]$

  Set $\mathbf{x}_1^{(t)} = \mathbf{z}^{(m)}[p]$

  for$(k = 1, 2, ..., U_t)$

    Projection Approximation: $y_k^{(t)} = \hat{\mathbf{u}}_k^{(t)}[p, m-1]^H \mathbf{x}_k^{(t)}$

    Eigenvalue Update: $\hat{\lambda}_k^{(t)}[p, m] = \gamma \hat{\lambda}_k^{(t)}[p, m-1] + \left|y_k^{(t)}\right|^2$

    Eigenvector Update:

$$\hat{\mathbf{u}}_k^{(t)}[p, m] = \hat{\mathbf{u}}_k^{(t)}[p, m-1] + \left(\frac{y_k^{(t)*}}{\hat{\lambda}_k^{(t)}[p,m]}\right)\left(\mathbf{x}_k^{(t)} - \hat{\mathbf{u}}_k^{(t)}[p, m-1] y_k^{(t)}\right)$$

    Deflation: $\mathbf{x}_{k+1}^{(t)} = \mathbf{x}_k^{(t)} - \hat{\mathbf{u}}_k^{(t)}[p, m] y_k^{(t)}$

  end for

end for

for$(n = 1, 2, ..., N)$

  Input $\mathbf{z}_n[p]^T$

  Set $\mathbf{x}_1^{(f)} = \mathbf{z}_n[p]^T$

  for$(k = 1, 2, ..., K)$

    Projection Approximation: $y_k^{(f)} = \hat{\mathbf{u}}_k^{(f)}[p, n-1]^H \mathbf{x}_k^{(f)}$

    Eigenvalue Update: $\hat{\lambda}_k^{(f)}[p, n] = \gamma \hat{\lambda}_k^{(f)}[p, n-1] + \left|y_k^{(f)}\right|^2$

    Eigenvector Update:

$$\hat{\mathbf{u}}_k^{(f)}[p, n] = \hat{\mathbf{u}}_k^{(f)}[p, n-1] + \left(\frac{y_k^{(f)*}}{\hat{\lambda}_k^{(f)}[p,n]}\right)\left(\mathbf{x}_k^{(f)} - \hat{\mathbf{u}}_k^{(f)}[p, n-1] y_k^{(f)}\right)$$

    Deflation: $\mathbf{x}_{k+1}^{(f)} = \mathbf{x}_k^{(f)} - \hat{\mathbf{u}}_k^{(f)}[p, n] y_k^{(f)}$

  end for

end for

Compute Detectors

$$\mathbf{w}_t^* = \hat{\mathbf{U}}_s^{(t)} (\hat{\mathbf{\Lambda}}_s^{(t)})^{-1} \hat{\mathbf{U}}_s^{(t)H} \mathbf{a}_1$$

$$\mathbf{w}_f^* = \hat{\mathbf{U}}_s^{(f)} (\hat{\mathbf{\Lambda}}_s^{(f)})^{-1} \hat{\mathbf{U}}_s^{(f)H} \mathbf{c}_1$$

Perform detection

$$\hat{b}_1[p] = \text{sgn}\left(\text{Re}\left\{\left(\mathbf{w}_t^{*H} \mathbf{Z}\right)^* \mathbf{w}_f^*\right\}\right)$$

Table 3.4: Blind Subspace PASTd Receiver Algorithm

receivers.

3.4.1 Receiver Complexity

In this section, we briefly discuss the complexity of the blind receivers for TF-MC-CDMA in AWGN proposed in this chapter. The DMI receiver requires two matrix inversions: one for the time domain and one for the frequency domain. The size of the sample correlation matrices are N by N and M by M for the time and frequency domain respectively. Using normal Gaussian elimination to find the matrix inverse, the complexity is $O(N^3+M^3)$. The CMOE RLS algorithm has a complexity of $O(N^2)$ per update for the time domain detector and $O(M^2)$ per update for the frequency domain detector. However, in our algorithm, there are M updates per symbol for the TD detector and N updates per symbol for the FD detector. Therefore, the total complexity for the CMOE RLS algorithm is $O(NM^2 + MN^2)$. The subspace SVD involves computing the singular value decomposition on the received data, or equivalently the eigendecomposition of the sample correlation matrices for both the time and frequency domain. The worst case complexity for eigendecomposition for the time domain is $O(N^3)$ and for the frequency domain is $O(M^3)$. Therefore, the total complexity for the blind subspace SVD method is $O(M^3 + N^3)$. The adaptive subspace tracking algorithm using PASTd has a complexity of $O(\hat{N}N)$ per update for the time domain where $\hat{N}$ denotes the number of time domain signature/groups used. Therefore, the maximum complexity occurs when $\hat{N} = N$ (when all available time domain sequences are used) and the complexity will be $O(N^2)$ per update for the time domain. For the frequency domain, the complexity is $O(\chi_n M)$ where χ_n denotes the number of users within the n^{th} time domain group or using the n^{th} time domain signature sequence. Under a fully loaded system, the adaptive subspace tracking multiuser detection using PASTd is then $O(N^2 + M^2)$ per update. Suppose

Multiuser Detector	Complexity
DMI	$O(N^3 + M^3)$
CMOE RLS	$O(NM^2 + MN^2)$
Subspace SVD	$O(N^3 + M^3)$
Subspace PASTd	$O(MU_tN + N\chi_nM)$

Table 3.5: Summary of TF-MC-CDMA Blind Multiuser detection complexity for AWGN channel

TD spreading gain	7
FD spreading gain	15
Number of subcarriers	15
TDS sequence type	M-sequences
FDS sequence type	M-sequences

Table 3.6: Simulation parameters

the number of TDS sequence used is U_t and χ_n denotes the number of users within the n^{th} TD group, then the total complexity for the blind subspace PASTd algorithm is $O(MU_tN + N\chi_nM)$ per symbol. The complexity of the algorithms are summarized in Table 3.5.

3.5 Simulation Results

Computer simulations were carried out to illustrate the performances of the four types of blind detectors for TF-MC-CDMA discussed in this chapter: the DMI method, the MOE RLS method, the subspace SVD method, and the adaptive subspace tracking PASTd method. The parameter values chosen are listed in Table 3.6.

The number of users used in the simulation reflect three levels of loading in a typical TF-MC-CDMA system:

- Case 1: 49 users - moderate load
- Case 2: 77 users - moderate heavy load

- Case 3: 105 users - full load

Figures 3.2, 3.3 and 3.4 show the BER performance for each case. Not surprisingly, the DMI method gives the best BER performance. The subspace method using SVD can achieve almost the same BER as the DMI method. The adaptive subspace tracking algorithm using PASTd has a slightly degraded performance; the degradation increases slightly with loading and at a target BER of 10^{-3}, the penalty is approximately 1dB for 105 users. It can be seen that the adaptive subspace tracking outperforms the CMOE RLS receiver with comparable complexity. The difference or gap between the performance of the CMOE RLS receiver and other blind multiuser receiver considered, namely the DMI, blind subspace SVD, and the blind subspace PASTd detector, increases with system loading. In a fully loaded system with 105 users, the difference in performance between the adaptive subspace tracking receiver and the CMOE RLS is more than 6dB at a target BER of 10^{-4}. Nonetheless, comparing with the matched filter detector, the CMOE RLS blind multiuser receiver remains a much better alternative.

The output SINR curves as a function of the number of data smaples are shown in Fig. 3.5, 3.6 and 3.7 and agree with the BER performance results. The DMI and the subspace SVD methods have almost identical output SINR curves. The output SINR of the adaptive subspace tracking receiver using PASTd is approximately 1dB less than that of the DMI and subspace SVD receiver for the 49 and 77 user case and slightly greater than 1dB less for the 105 (full capacity) users case. The output SINR curves also show the convergence rate of the proposed receivers. It can be seen that the CMOE RLS converges the fastest, the output SINR reaches stabilizes after approximately 60 data samples. The convergence of the DMI and subspace SVD are similar; they reach convergence after approximately 200 samples. The adaptive subspace tracking using PASTd has the slowest convergence. The result shown for

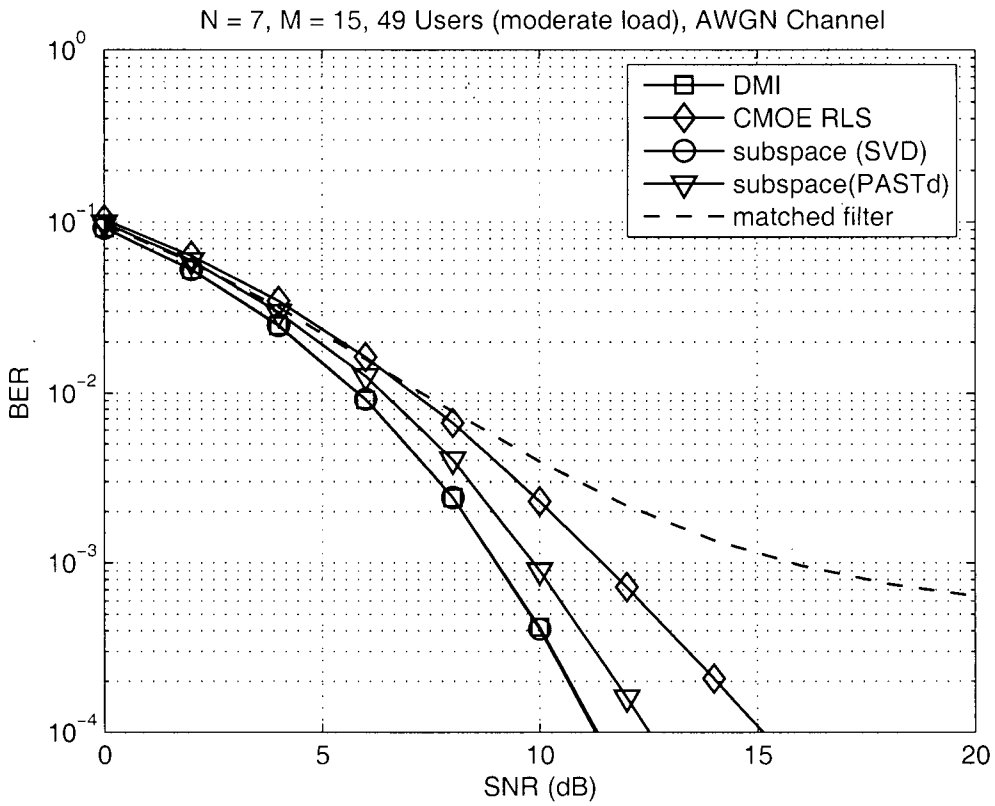

Figure 3.2: BER Performance with 49 Users

the PASTd tracking has been accelerated by using doing an SVD decomposition on the first 50 data samples. Even with the acceleration, the PASTd tracking algorithm has the slowest rate of convergence.

Finally, Fig. 3.8 and 3.9 shows the BER and output SINR as a function of the number of users in the system. In Fig. 3.8, it can be seen that the BER performance deteriorates fairly quickly going from 5 users to about 45 users. Beyond 50 users, the BER degradation stabilizes to a steady increase. Fig. 3.9 shows similar results that the system output SINR degrades fairly quickly from 5 users to 45 users and then stabilizes to a steady degradation as the number of users in the system increases.

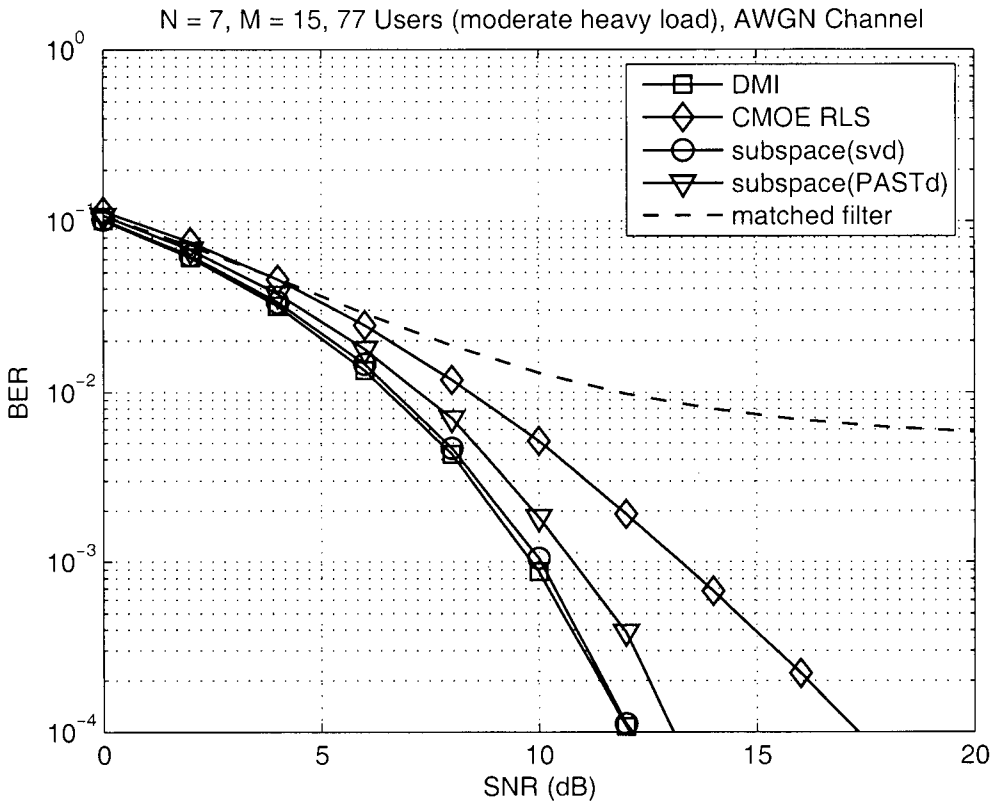

Figure 3.3: BER Performance with 77 Users

3.6 Summary

In this chapter, the blind multiuser detection problem for TF-MC-CDMA in AWGN was investigated. It was shown that the blind LMMSE detector for TF-MC-CDMA can be suboptimally decoupled into two DS-CDMA blind multiuser detection problems, one for the frequency domain, and one for the time domain. Three methods for solving the decoupled multiuser detection problem, namely the DMI method, CMOE RLS method, and the subspace method were studied. For the subspace multiuser detection method, two implementations were considered: the singular value decomposition method and the adaptive subspace tracking method using the PASTd algorithm. Finally, simulation BER curves for the different multiuser detectors studied were presented and discussed.

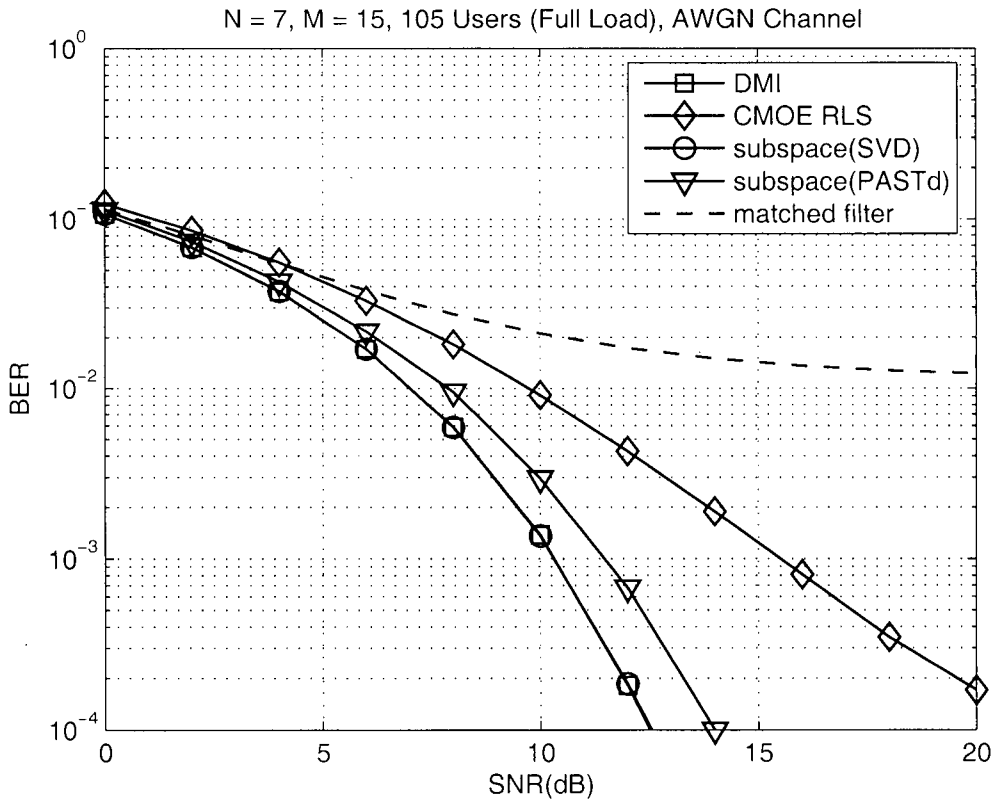

Figure 3.4: BER Performance with 105 Users

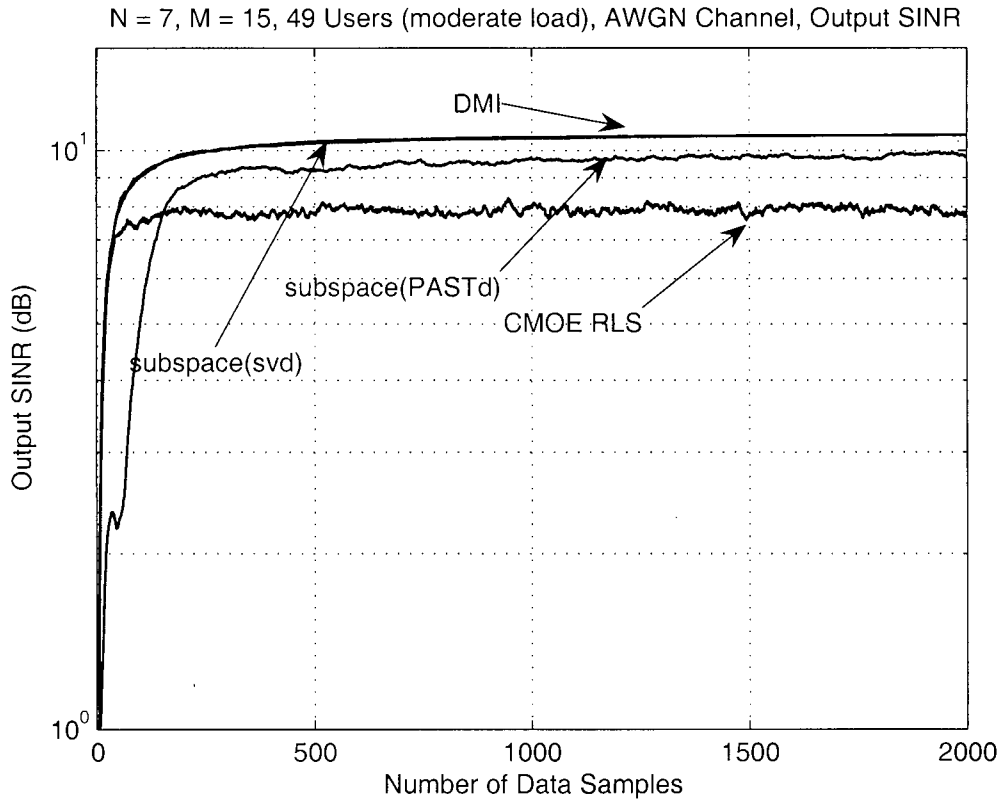

Figure 3.5: Output SINR with 49 Users at SNR 10dB

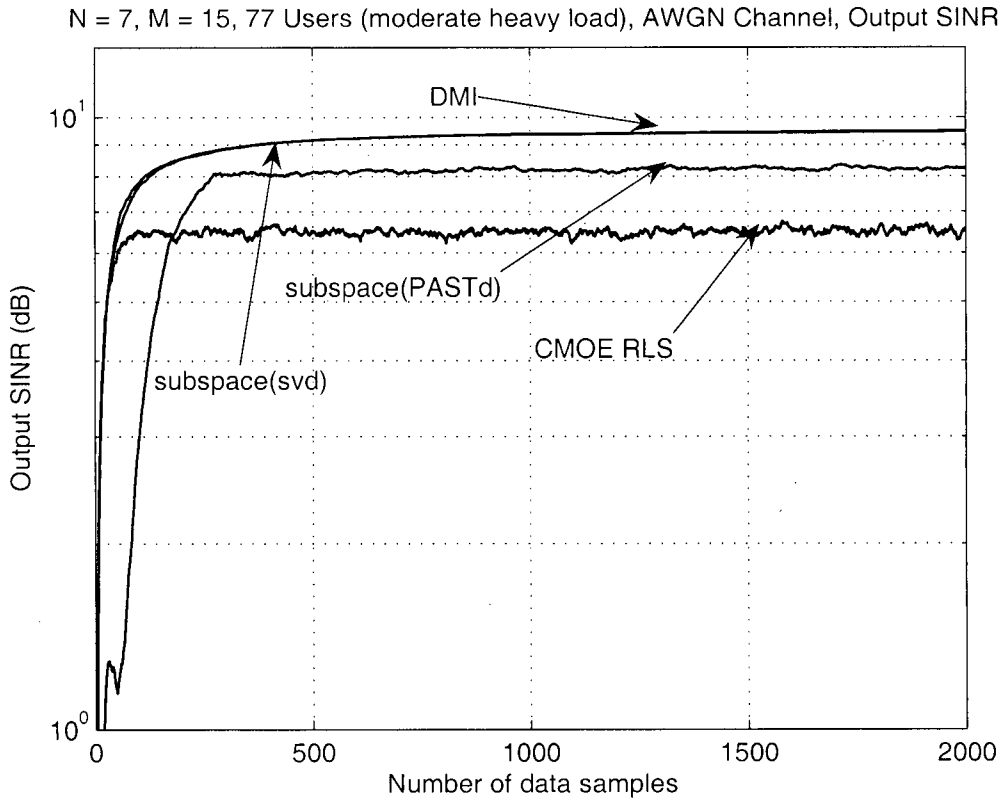

Figure 3.6: Output SINR with 77 Users at SNR 10dB

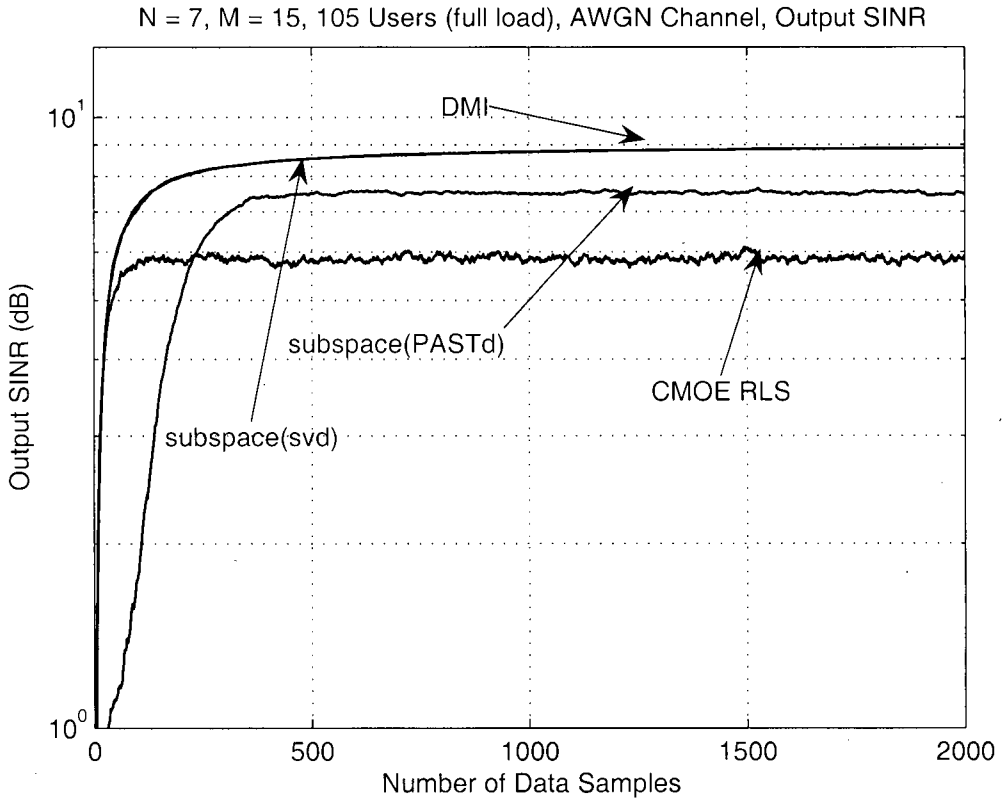

Figure 3.7: Output SINR with 105 Users at SNR 10dB

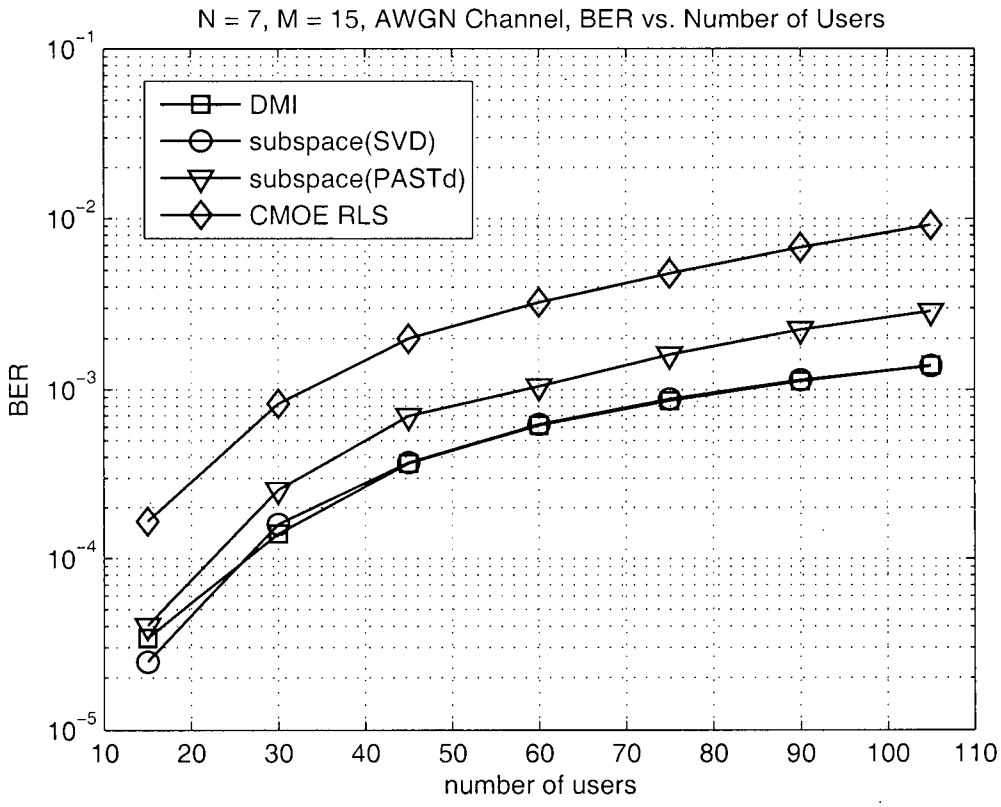

Figure 3.8: BER performance plotted against the number of users at SNR 10dB

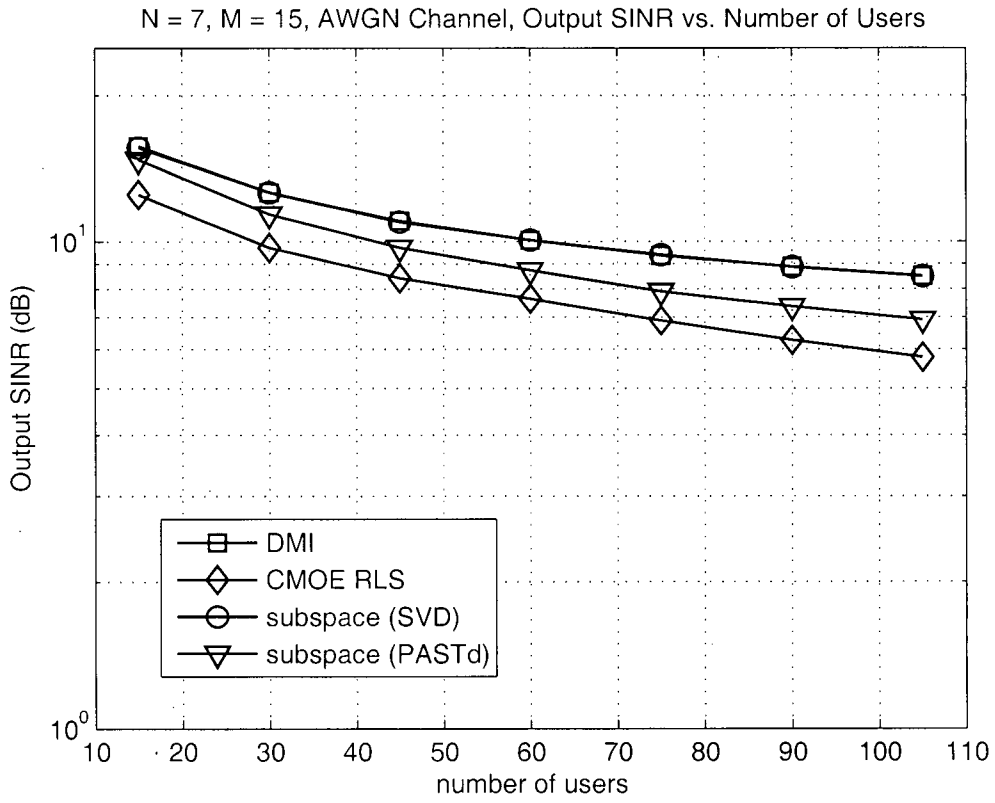

Figure 3.9: Output SINR plotted against the number of users at SNR 10dB

Chapter 4

TF-MC-CDMA Blind Multiuser Detection in Slowly Fading Rayleigh Multipath Channel

4.1 Introduction

The distinct advantage of using multicarrier based transmission is to combat frequency selective fading by transmitting in multiple subcarrier streams such that each stream experiences frequency non-selective fading. In this chapter, the channel is assumed to be varying slowly with respect to overall transmission rate. Rayleigh fading multipath channels are common in urban mobile communications where line of sight signals are often not available and all received energies are from reflected and scattered signals. In this chapter, blind linear multiuser detection algorithms are proposed for TF-MC-CDMA system in downlink multipath fading channels. In particular, the focus is on the design of low complexity receiver algorithms suitable for implementation in mobile handsets. In most realistic situations, the mobile receiver may only know its own signature sequence and does not know the channel without

using training sequences or pilot symbols. In this chapter, we discuss blind multiuser detectors for TF-MC-CDMA where the receiver has no knowledge of the channel information and has only knowledge of its own TD and FD signature sequences.

This chapter is organized as follows: Section 4.2 reviews the signal model in downlink slowly fading Rayleigh multipath channels in a TF-MC-CDMA system. Section 4.3 presents the TF-MC-CDMA blind multiuser detection problem in slowly fading Rayleigh multipath channels. Section 4.4 discusses the blind multiuser detection algorithms. Section 4.5 reviews performance measures. Section 4.6 provides computer simulation results. Finally, section 4.7 concludes with a summary of the chapter.

4.2 Linear Multiuser Detection for TF-MC-CDMA in Frequency Selective Fading Channels

An important motivation for using multicarrier based transmission is to maintain a robust system performance in frequency selective channels. This is achieved through transmission in multiple narrowband subcarriers such that each subcarrier stream experiences frequency non-selective or flat fading. TF-MC-CDMA systems inherit this characteristic that is also present in MC-CDMA, OFDM and MC-DS-CDMA systems. A TF-MC-CDMA signal in frequency selective downlink fading channel model with L paths represented by a tapped-delay line time varying channel impulse response $h(t,\tau)$ is considered

$$h(t,\tau) = \sum_{l=1}^{L} g_l(t)\delta\left(\tau - lT_c\right) \tag{4.1}$$

where $g_l(t)$ is the time varying complex gain of path l and T_c is the chip duration. Referring to the analysis in Section 2.3.3, the sampled received signal can be written in terms of the discrete time convolution of the transmitted signal and the discrete

time channel response given by

$$r_{LP}[n,k] = s_{LP}[n] * h[k,n] + w[n] \tag{4.2}$$

where $s_{LP}[n]$ is given by 2.15, $w[n]$ is a complex WGN random variable with variance N_0, and $h[k,n]$ is the equivalent discrete time channel impulse response of $h(t,\tau)$ given by 2.35. The discrete time demodulated equivalent baseband signal is given by the DFT of 4.2

$$DFT_M\left\{r_{LP}[n,k]\right\} = DFT_M\left\{s_{LP}[n] * h[n,k]\right\} + DFT_M\left\{w[n]\right\} \tag{4.3}$$

Without using multicarrier modulation, the received signal would experience ISI as a result of the frequency selectivity of the channel. However, in multicarrier modulation, the use of IFFT/FFT implementation and the insertion of a cyclic prefix (as discussed in Section 2.3.3) eliminates the ISI between OFDM blocks. The insertion of a cyclic prefix (longer than the delay spread of the channel) enables the FFT demodulation process to be equivalent to a circular convolution between the signal and the channel in the time domain [37, 38]. Hence in the frequency domain, under the circular convolution theorem, the DFT of the transmitted signal and the DFT of the discrete time channel response multiplies. At the FFT demodulator output, each subcarrier stream is a flat faded signal. The complex channel gain for each subcarrier stream is obtained by computing the DFT of the discrete channel impulse response. Using this fact, along with 2.37, 2.42, and 2.43, the demodulated downlink TF-MC-CDMA signal in a frequency selective channel can be expressed as

$$Z_n[m] = \sqrt{P}\sum_{k=1}^{K} b_k a_k[n] c_k[m] H[m] + W_n[m], \quad m = 1, 2, ..., M \tag{4.4}$$

or equivalently

$$Z_n[m] = H[m]S_n[m] + W_n[m], \quad m = 1, 2, ..., M \tag{4.5}$$

where $H[m] = \sum_{l=0}^{L-1} g_l \exp\left(\frac{-j2\pi ml}{M}\right)$.

Based on only the knowledge of the desired user's TD and FD signature sequences, we propose blind linear MMSE multiuser detector that performs blind detection for the TF-MC-CDMA signal and jointly estimate the channel.

4.3 Blind Multiuser Detection in Slowly Fading Channels

The decoupling method proposed in Chapter 3 for blind linear multiuser detection for TF-MC-CDMA signal in AWGN can also be applied in the case for the slowly fading Rayleigh multipath channel. Similarly to the blind multiuser detection problem for the AWGN channel with MAI case, the full discrete time TF-MC-CDMA demodulated signal naturally decouples into one which involves only the TD spreading and one that only involves the FD spreading.

The m^{th} column of $\mathbf{Z}$ gives the TD multiuser detection problem

$$\mathbf{z}[m] = \sqrt{P}H[m]\sum_{k=1}^{K}\left(b_k c_k[m]\right)\mathbf{a}_k + \mathbf{W}[m], \quad m = 1, 2, ..., M \tag{4.6}$$

The n^{th} row of $\mathbf{Z}$ gives the FD multiuser detection problem

$$\mathbf{z}_n^T = \sqrt{P}\sum_{k=1}^{K}\left(b_k a_k[n]\right)\tilde{\mathbf{c}}_k + \mathbf{W}_n^T, \quad n = 1, 2, ..., N \tag{4.7}$$

where

$$\begin{aligned}
\tilde{\mathbf{c}}_k &= diag(\mathbf{c}_k)\mathbf{H} \\
\mathbf{H} &= \begin{bmatrix} H[1] & H[2] & \dots & H[M] \end{bmatrix}^T \\
diag(\mathbf{c}_k) &= \begin{bmatrix} c_k[1] & & \\ & \ddots & \\ & & c_k[M] \end{bmatrix}
\end{aligned} \tag{4.8}$$

It can be noted here that, more compactly written, the channel impulse response $\mathbf{g}$ and its DFT $\mathbf{H}$ is related by $\mathbf{H} = \mathbf{F}_{M\times L}\mathbf{g}$ where $\mathbf{F}_{M\times L}$ is the M by L Fourier matrix.

Matched filtering can be applied for the TD multiuser detection if orthogonal codes are used. Examining 4.6, the orthogonality of the TD signature sequences is preserved when the channel is fading slowly with respect to the symbol duration. On the downlink, the channel is synchronous in nature and thus warrants the use of orthogonal signature sequences. Two types of detection, type I and type II detection, are proposed and their performance are investigated. Our proposed type I detector uses separate "parallel" time and frequency domain processing through decoupling where the output of the TD MUD does not feed into the FD MUD or vice versa. The proposed type II detector uses a cascade implementation where the output of the TD processing is input into the FD processing. In the next two subsections, type I and type II detection are discussed.

4.3.1 Type I Receiver

The implementation of our proposed type I receiver uses the decoupled TD and FD processing introduced in Chapter 3 with the exception that the matched filter can be applied to the TD detection since orthogonality is preserved in the time domain for slowly fading channels. Therefore, for the TD detection, matched filtering is applied with the desired user's TDS sequence. Fig. 4.1 shows the system block diagram of the type I receiver. The frequency domain MUD is computed through the observation data given by the rows of the observation matrix $\mathbf{Z}$ in 4.7. The blind LMMSE for type I FD MUD solves the optimization problem

$$\begin{aligned} \mathbf{w}_f^* &= \underset{\mathbf{w}_f \in \mathbb{C}^{M\times 1}}{\operatorname{argmin}} \; E\left\{ \left\| \sqrt{P}\left(b_k a_k[n]\right) - \mathbf{w}_f^H \mathbf{z}_n^T \right\|^2 \right\} \\ \mathbf{z}_n^T &= \sqrt{P} \sum_{k=1}^{K} \left(b_k a_k[n]\right) \tilde{\mathbf{c}}_k + \mathbf{n}_n^T \end{aligned} \tag{4.9}$$

Re-examining 4.9, if one let $B_k = b_k a_k[n]$ and realizing that $\tilde{\mathbf{c}}_k = diag(\mathbf{c}_k)\mathbf{H}$ is the effective FD signature, then 4.9 is equivalent to the blind LMMSE multiuser

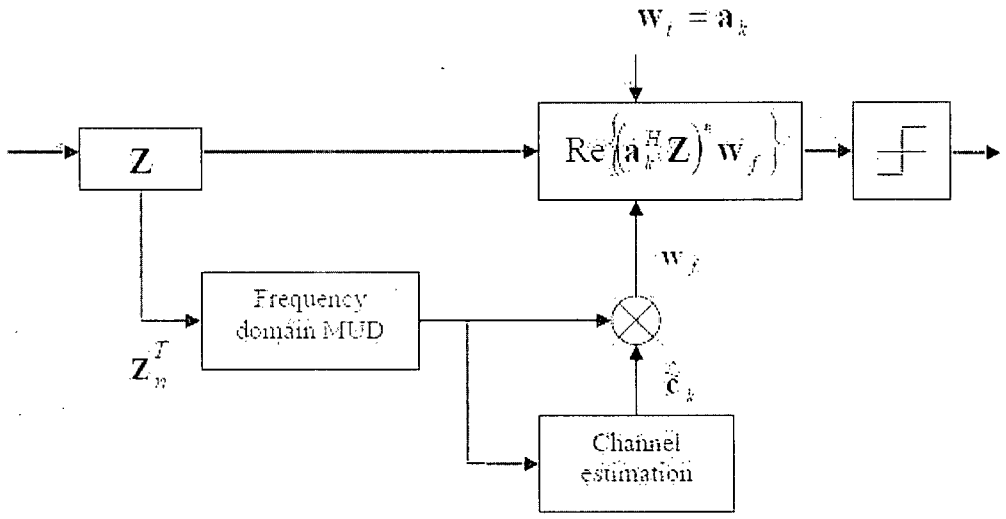

Figure 4.1: Type I detector architecture

optimization problem for MC-CDMA in a slowly fading frequency selective channel. The MC-CDMA multiuser signal model was investigated in [22, 25, 41, 42].

4.3.2 Type II Receiver

The implementation of the type II receiver uses a cascade architecture in which the TD matched filtering is first applied and then the output is input into the FD multiuser detector. Matched filtering of the desired user's time domain signature is applied at the first stage. The motivation for processing the TD detector using the matched filter first is to filter out interferers from other time groups (interferers that does not have the same TD signature as the desired user). Fig. 4.2 shows the system block diagram of the type II receiver. The type II receiver implementation takes advantage of the preserved orthogonality of the TD signature sequences to reduce the number of interferers for the FD detection. Reversing the process where the FD detection is computed first does not achieve the same result. The reason is that matched filtering can not be applied to the FD detection because orthogonality of the FDS is lost due

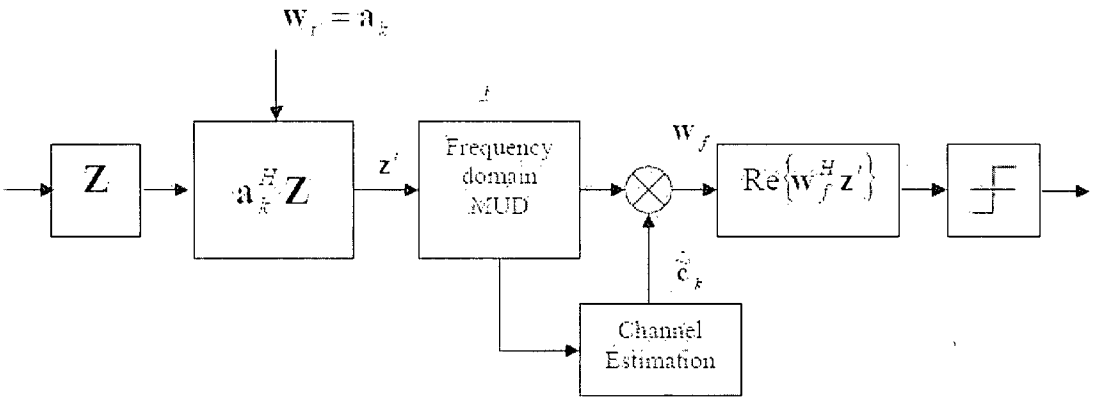

Figure 4.2: Type II detector architecture

to the effect of the channel. As a result, it is not possible to filter out interferers that have different FDS than the desired user. The equivalent multiuser signal model using TD signature grouping given in Section 2.2.3 is useful in the analysis of type II receivers. At the output of the demodulator, the elements of the N by M observation matrix $\mathbf{Z}$ using the TD signature grouping can be written as

$$Z_n[m] = \sqrt{P}\sum_{j=1}^{N}\sum_{\kappa=1}^{\chi_j} b_{j\kappa}a_n[j]c_\kappa[m]H[m] + W_n[m], \quad n = 1, ..., N \quad m = 1, ..., M \tag{4.10}$$

In vector notation, 4.10 is rewritten as

$$\mathbf{z}[m] = \sqrt{P}\sum_{j=1}^{N}\sum_{\kappa=1}^{\chi_j} b_{j\kappa}c_\kappa[m]H[m]\mathbf{a}_j + \mathbf{W}[m] \tag{4.11}$$

The inner product of 4.11 with user 1's TD signature sequence yields

$$\begin{aligned}\mathbf{a}_1^H\mathbf{z}[m] = z'[m] &= \sqrt{P}\sum_{j=1}^{N}\sum_{\kappa=1}^{\chi_j} b_{j\kappa}c_\kappa[m]H[m]\mathbf{a}_1^H\mathbf{a}_j + \mathbf{a}_1^H\mathbf{W}[m] \\ &= \sqrt{P}\sum_{\kappa=1}^{\chi_1} H[m]\left(b_{1\kappa}c_\kappa[m]\right) + w'[m], \quad m = 1, ..., M\end{aligned} \tag{4.12}$$

Equation 4.12 is simplified further in vector form to get

$$\mathbf{z}' = \begin{bmatrix} z'[1] \\ \vdots \\ z'[M] \end{bmatrix} = \sqrt{P}\sum_{\kappa=1}^{\chi_1} b_{1\kappa}\tilde{\mathbf{c}}_\kappa + \mathbf{w}' \tag{4.13}$$

where $b_{1\kappa}$ denotes the transmitted symbol of the user with TD signature sequence 1 and FD signature sequence κ. We assume our desired user has TD signature sequence number 1 and FD signature sequence number 1. The blind LMMSE detector optimization problem for the type II FD stage detection is thus given by

$$\mathbf{w}_f^* = \underset{\mathbf{w}_f \in \mathbb{C}^{M\times 1}}{\operatorname{argmin}} \; E\left\{ \left\| \sqrt{P}\,(b_{11}) - \mathbf{w}_f^H \mathbf{z}' \right\|^2 \right\} \tag{4.14}$$

Comparing with 4.9, the FD blind LMMSE multiuser detection problem given by 4.14 has the same form and is equivalent to blind multiuser detection for MC-CDMA multiuser signal in slowly fading frequency selective channel. Applying matched filtering for the FD MUD is inappropriate in this case because the orthogonality of the frequency domain spreading sequences is lost due to the effect of the channel. Therefore, blind multiuser detection techniques must be used for the FD processing. However, the CMOE RLS and blind subspace methods used for solving the decoupled TF-MC-CDMA multiuser detection problem in AWGN in Chapter 3 can be applied to the FD processing for both type I and type II detectors but with added complexity as a result of the need for joint blind channel estimation that must be performed in order to obtain the blind LMMSE detector for the FD multiuser detector.

The type I and type II FD multiuser detection problem have identical forms comparing 4.9, 4.13 and 4.14. If the system has K active users and $K < M$, then it is possible that all users have different FD signature sequence because for spreading sequences of length M, there can be at most M linearly independent sequences. Therefore, for $K < M$, the type I FD detector is required to suppress $K-1$ interfering FD signature sequences. However, for the type II FD detector, it is only required to suppress $\chi_1 - 1$ interfering FD signature sequences where χ_1 is the number of users sharing the same TD signature sequence as the desired user. By construction and definition of χ_1, $\chi_1 \leq K$.

If $K > M$, then there will be some users that share the same FD signature se-

quence and this means that all M linearly independent FD signature sequences are used in the system. Therefore, for the type I FD detector, it is required to suppress $M-1$ interfering FD signature sequences. However, for the type II FD detector, it is again only required to suppress $\chi_1 - 1$ interfering FD signature sequences. Furthermore, it is easy to see that $\chi_1 \leq M$.

To summarize, since the type I and type II detector FD MUD problem differ only in the number of users, we can then solve both problems using the same methods assuming the FD MUD problem has U-users (for type I, $U = M$; and for type II $U = \chi_1$ if $K > M$ and $U = K$ for type I and $U = \chi_1$ for type II if $K < M$). To solve the FD MUD problem, two methods used in Chapter 3 are revisited and applied to the TD MUD problem, namely, the CMOE RLS method and the subspace blind detection method.

4.3.3 CMOE RLS Blind Detection

From our analysis in the previous section, we have shown that the TF-MC-CDMA FD blind linear MMSE MUD problem for both type I and type II (differing only in the number of interfering FD signature sequences) is equivalent to blind linear MMSE MUD for MC-CDMA signal. It was shown in [22] that the CMOE RLS algorithm can be applied to MC-CDMA signal. We apply the CMOE RLS algorithm to the FD MUD of our proposed type I and type II detectors for TF-MC-CDMA signal and investigate its performance in slowly fading Rayleigh multipath channel.

Using the CMOE RLS blind detection algorithm, we seek a solution for the blind LMMSE multiuser detection problem given by 4.14. Using the CMOE criterion formulation, the same CMOE RLS optimization problem is arrived as presented in Section 3.3.2 with a slight modification in the constraint where the constraint is now on the effective FD signature sequence of the desired user instead of the original FD

signature sequence. The type I detector frequency domain CMOE RLS MUD problem is given by

$$\mathbf{w}_f^* = \underset{\mathbf{w}_f \in \mathbb{C}^{M\times 1}}{\operatorname{argmin}} \sum_{n=0}^{j[p]} \lambda^{j[p]-n} \left\| \mathbf{w}_f^H \mathbf{z}_n^T \right\|^2, \quad \mathbf{w}_f^H \tilde{\mathbf{c}}_1 = 1 \tag{4.15}$$

where $\tilde{\mathbf{c}}_1 = diag(\mathbf{c}_1)\mathbf{H}$ is the effective signature waveform and $j[p]$ denotes the j^{th} time chip of the p^{th} transmitted symbol. The summation in 4.15 states that the sum is over all time chips going from the zeroth time chip from the zeroth transmitted symbol to the j^{th} chip of the p^{th} symbol.

The solution to the CMOE RLS optimization problem is given by 3.19, i.e.

$$\mathbf{w}_f^* = \left(\tilde{\mathbf{c}}_1^H \mathbf{C}_f^{-1} \tilde{\mathbf{c}}_1\right)^{-1} \mathbf{C}_f^{-1} \tilde{\mathbf{c}}_1 \tag{4.16}$$

where the data correlation matrix is given by the recursive updates from the columns of $\mathbf{Z}$, namely

$$\mathbf{C}_f[p,n] = \lambda \mathbf{C}_f[p,n-1] + \mathbf{z}_n^T (\mathbf{z}_n^T)^H, \quad n = 1, ..., N \tag{4.17}$$

Recall that $\mathbf{C}_f[p,0]$ is equivalent to $\mathbf{C}_f[p-1,N]$.

The type II CMOE RLS MUD problem is given by

$$\mathbf{w}_f^* = \underset{\mathbf{w}_f \in C^{M\times 1}}{\operatorname{argmin}} \sum_{i=0}^{p} \lambda^{p-i} \left\| \mathbf{w}_f^H \mathbf{z}'[i] \right\|^2, \quad \mathbf{w}_f^H \tilde{\mathbf{c}}_1 = 1 \tag{4.18}$$

The solution of 4.18 is also given by 4.16 where now the data correlation matrix is given by the recursive updates from the output of the TD matched filter.

$$\mathbf{C}_f[p] = \sum_{i=0}^{p} \lambda^{p-i} \mathbf{z}'[i]\mathbf{z}'[i]^H = \lambda \mathbf{C}_f[p-1] + \mathbf{z}'[p]\mathbf{z}'[p]^H \tag{4.19}$$

Applying the CMOE RLS algorithm presented in Chapter 3 for the TF-MC-CDMA signal in AWGN, the inverse of the correlation matrix is approximated using the matrix inversion lemma and is given by

$$\mathbf{\Phi}_f[j] = \lambda^{-1}\mathbf{\Phi}_f[j-1] - \frac{\lambda^{-2}\mathbf{\Phi}_f[j-1]\mathbf{q}\mathbf{q}^H\mathbf{\Phi}_f[j-1]}{1+\lambda^{-1}\mathbf{q}^H\mathbf{\Phi}_f[j-1]\mathbf{q}} \tag{4.20}$$

where j denotes the iteration index and $\mathbf{q} = \mathbf{z}_n^T$ for type I detection and $\mathbf{q} = \mathbf{z}'$ for type II detection.

To complete the solution, it is necessary to solve for the effective FD signature $\tilde{\mathbf{c}}_1 = diag(\mathbf{c}_1)\mathbf{H}$. Since the user only knows its own FDS signature and not the channel, the channel must be jointly estimated in order to perform the detection. Once the channel parameters are estimated, the FD blind multiuser detector is given 4.16 for both type I and type II detectors.

Blind Channel Estimation

For the blind channel estimation for the FD MUD detector using the CMOE RLS algorithm, we make use the analysis for MC-CDMA blind channel estimation given in [22]. From the CMOE solution given in equation (4-16), the type I detector minimum output energy (MOE) is given by

$$MOE_I(\mathbf{w}_f^*) = E\left\{\left|\mathbf{w}_f^{*H}\mathbf{z}_n^T\right|^2\right\} \tag{4.21}$$

Similarly, the MOE for type II is given by

$$MOE_{II}(\mathbf{w}_f^*) = E\left\{\left|\mathbf{w}_f^{*H}\mathbf{z}'\right|^2\right\} \tag{4.22}$$

Expanding either 4.21 or 4.22 yields the same result, i.e.

$$\begin{aligned} MOE(\mathbf{w}_f^*) &= E\left\{\left|\mathbf{w}_f^{*H}\mathbf{z}_n^T\right|^2\right\} = E\left\{\left(\mathbf{w}_f^{*H}\mathbf{z}_n^T\right)\left(\mathbf{w}_f^{*H}\mathbf{z}_n^T\right)^H\right\} \\ &= E\left\{\mathbf{w}_f^{*H}\mathbf{z}_n^T(\mathbf{z}_n^T)^H\mathbf{w}_f^*\right\} \\ &= \mathbf{w}_f^{*H}E\left\{\mathbf{z}_n^T(\mathbf{z}_n^T)^H\right\}\mathbf{w}_f^* \\ &= \mathbf{w}_f^{*H}\mathbf{C}_f\mathbf{w}_f^* \end{aligned} \tag{4.23}$$

Substituting the CMOE solution given by 4.16 into 4.23 yields

$$\begin{aligned} MOE(\mathbf{w}_f^*) &= \left[\left(\tilde{\mathbf{c}}_1^H\mathbf{C}_f^{-1}\tilde{\mathbf{c}}_1\right)^{-1}\mathbf{C}_f^{-1}\tilde{\mathbf{c}}_1\right]^H\mathbf{C}_f\left[\left(\tilde{\mathbf{c}}_1^H\mathbf{C}_f^{-1}\tilde{\mathbf{c}}_1\right)^{-1}\mathbf{C}_f^{-1}\tilde{\mathbf{c}}_1\right] \\ &= \left(\tilde{\mathbf{c}}_1^H\mathbf{C}_f^{-1}\tilde{\mathbf{c}}_1\right)^{-1} \end{aligned} \tag{4.24}$$

It was shown in [22] that the MOE expression given in 4.24 can be maximized with respect to the effective FD signature sequence of the desired user $\tilde{\mathbf{c}}_1$ to estimate the effective FD signature, and in the process, the channel. Using this approach, 4.25 gives the optimization problem for the channel estimation, namely

$$\underset{\tilde{\mathbf{c}}_1}{\text{argmax}} \left\{ MOE(\mathbf{w}_f^*) \right\} = \underset{\tilde{\mathbf{c}}_1}{\text{argmax}} \left\{ \left(\tilde{\mathbf{c}}_1^H \mathbf{C}_f^{-1} \tilde{\mathbf{c}}_1 \right)^{-1} \right\} \tag{4.25}$$

Equivalently, one can minimize the reciprocal of 4.25 and therefore, the estimated effective signature is given by

$$\hat{\tilde{c}}_1 = \underset{\tilde{\mathbf{c}}_1}{\text{argmin}} \left\{ \left(\tilde{\mathbf{c}}_1^H \mathbf{C}_f^{-1} \tilde{\mathbf{c}}_1 \right) \right\} \tag{4.26}$$

Using the fact that $\tilde{\mathbf{c}}_1 = \mathbf{C_1 H}$ where $\mathbf{C_1} = diag(\mathbf{c}_1)$, $\mathbf{H} = \mathbf{F}_{M \times L}\mathbf{g}$ and the RLS estimate $\mathbf{\Phi}_f \approx \mathbf{C}_f^{-1}$, the channel response can be estimated by solving the optimization problem in equation (4-26), applying the substitutions expanding (4-26) yields

$$\hat{\mathbf{g}} = \underset{\mathbf{g}}{\text{argmin}} \left\{ \mathbf{g}^H \mathbf{F}_{M \times L}^H \mathbf{C}_1^H \mathbf{\Phi}_f \mathbf{C}_1 \mathbf{F}_{M \times L} \mathbf{g} \right\} \tag{4.27}$$

For a normalized channel impulse response $\mathbf{g}$ (i.e. $\|\mathbf{g}\| = 1$), the solution, unique up to a multiplicative complex constant, to 4.27 is the normalized eigenvector corresponding to the smallest eigenvalue of the matrix $\mathbf{F}_{M \times L}^H \mathbf{C}_1^H \mathbf{\Phi}_f \mathbf{C}_1 \mathbf{F}_{M \times L}$. The uniqueness of the solution is guaranteed if two conditions are met: (1) the composite matrix $[\tilde{\mathbf{c}}_1 | \tilde{\mathbf{c}}_2 | ... | \tilde{\mathbf{c}}_K]$ has rank equal to the number of linearly independent FD sequence used in the system U; (2) the channel estimation problem is solvable only if the number of linearly independent FD sequence used in the system U satisfy $L \leq M - U$ for a channel with a discrete time impulse response of length L [42] (this condition will be discussed again in more detail in Section 4.3.4). The second condition states that the maximum system capacity is reduced for multipath channels since rewriting condition (2) yields $U \leq M - L$. This is because in a multipath fading channel, only U out of a possible M linearly independent FD sequences can be used in the system. Therefore,

// Type I Blind TF-MC-CDMA CMOE RLS Receiver
// in Slowly Fading Rayleigh Multipath Channel

Initialization:

$\mathbf{\Phi}_f[0,0] = \mathbf{I}_{M\times M}$

In the p^{th} symbol, input matrix $\mathbf{Z}[p]$

Set $\mathbf{w}_t^* = \mathbf{a}_1$

for$(n = 1, 2, ..., N)$

Compute Kalman Gain:

$$\mathbf{k}_f[p,n] = \frac{\lambda^{-1}\mathbf{\Phi}_f[p,n-1]\mathbf{z}_n[p]^T}{1+\lambda^{-1}(\mathbf{z}_n[p]^T)^H\mathbf{\Phi}_f[p,n-1]\mathbf{z}_n[p]^T}$$

Compute Update:

$$\mathbf{\Phi}_f[p,n] = \lambda^{-1}\left(\mathbf{\Phi}_f[p,n-1] - \mathbf{k}_f\left(\mathbf{z}_n[p]^T\right)^H\mathbf{\Phi}_f[p,n-1]\right)$$

end for

Perform Channel Estimation:

Find smallest eigenvector $\hat{\mathbf{g}}$ corresponding to the smallest eigenvalue of $\mathbf{F}_{M\times L}^H\mathbf{C}_1^H\mathbf{\Phi}_f\mathbf{C}_1\mathbf{F}_{M\times L}$

Compute Estimated Effective FD Signature: $\tilde{\mathbf{c}}_1 = \mathbf{F}_{M\times L}\hat{\mathbf{g}}$

Compute FD Detector

$\mathbf{w}_f^* = \mathbf{\Phi}_f\tilde{\mathbf{c}}_1$

Perform detection

$\hat{b}_1[p] = \text{sgn}\left(\text{Re}\left\{\left(\mathbf{w}_t^{*H}\mathbf{Z}\right)^*\mathbf{w}_f^*\right\}\right)$

Table 4.1: Type I CMOE RLS Blind Receiver Algorithm

the maximum user capacity for TF-MC-CDMA system in a slowly fading multipath channel is now given by the product $N \times (M - L)$. The channel estimation solution is unique up to a multiplicative complex constant which means that only the magnitude of the channel impulse response can be uniquely estimated and there is an unknown phase. However, this can be resolved by using differential detection or phase tracking by periodical insertion of pilot symbols [22]. The algorithms we presented assume that this complex constant has been perfectly estimated; however, the algorithms can be easily modified using differential BPSK. Finally, the type I and type II CMOE RLS blind detection algorithm for TF-MC-CDMA are summarized in Table 4.1 and 4.2 respectively.

// Type II Blind TF-MC-CDMA CMOE RLS Receiver
// in Slowly Fading Rayleigh Multipath Channel

Initialization:

$\mathbf{\Phi}_f[0] = \mathbf{I}_{M\times M}$

In the p^{th} symbol, input matrix $\mathbf{Z}[p]$

Set $\mathbf{w}_t^* = \mathbf{a}_1$

Compute: $\mathbf{z}' = \mathbf{a}_1^H \mathbf{Z}[p]$

Compute Kalman Gain:

$\mathbf{k}_f[p] = \frac{\lambda^{-1}\mathbf{\Phi}_f[p-1]\mathbf{z}'^T}{1+\lambda^{-1}\left(\mathbf{z}'^T\right)^H \mathbf{\Phi}_f[p-1]\mathbf{z}'^T}$

Compute Update:

$\mathbf{\Phi}_f[p] = \lambda^{-1}\left(\mathbf{\Phi}_f[p-1] - \mathbf{k}_f\left(\mathbf{z}'^T\right)^H \mathbf{\Phi}_f[p-1]\right)$

Perform Channel Estimation:

Find smallest eigenvector $\hat{\mathbf{g}}$ corresponding to the smallest eigenvalue of $\mathbf{F}_{M\times L}^H \mathbf{C}_1^H \mathbf{\Phi}_f \mathbf{C}_1 \mathbf{F}_{M\times L}$

Compute Estimated Effective FD Signature: $\tilde{\mathbf{c}}_1 = \mathbf{F}_{M\times L}\hat{\mathbf{g}}$

Compute FD Detector

$\mathbf{w}_f^* = \mathbf{\Phi}_f \tilde{\mathbf{c}}_1$

Perform detection

$\hat{b}_1[p] = \mathrm{sgn}\left(\mathrm{Re}\left\{(\mathbf{w}_f^*)^H \mathbf{z}'^T\right\}\right)$

Table 4.2: Type II CMOE RLS Blind Receiver Algorithm

4.3.4 Blind Subspace Multiuser Detection

It was shown in [22, 25, 41, 42] that the blind subspace multiuser detection can be applied to MC-CDMA signals. In this section, we apply the blind subspace multiuser detection method for our proposed TF-MC-CDMA type I and type II FD multiuser detection in 4.9 and 4.14. The correlation matrices for the type I and type II detectors can be re-written as

$$\begin{aligned} \mathbf{C}_f &\equiv E\left\{\mathbf{z}_n^T \left(\mathbf{z}_n^T\right)^H\right\} = \tilde{\mathbf{S}}_f \left|\mathbf{A}\right|^2 \tilde{\mathbf{S}}_f^H + \sigma_f^2 \mathbf{I}_{M\times M} \\ \mathbf{C}_f &\equiv E\left\{\mathbf{z}'\mathbf{z}'^H\right\} = \tilde{\mathbf{S}}_f \left|\mathbf{A}\right|^2 \tilde{\mathbf{S}}_f^H + \sigma_f^2 \mathbf{I}_{M\times M} \end{aligned} \tag{4.28}$$

where

$$\tilde{\mathbf{S}}_f = [\tilde{\mathbf{c}}_1 | \tilde{\mathbf{c}}_2 | \ldots | \tilde{\mathbf{c}}_U] \tag{4.29}$$

contains the effective FDS signature waveforms of each user. Recall that the FD blind MUD for the TF-MC-CDMA type I and type II detector only differs in the number of interfering FD sequences. Therefore for type I detector, $U = K$ if $K < M$ and $U = M$ if $K > M$ and for type II detector, $U = \chi_1$. $|\mathbf{A}|^2$ denotes $diag(A_1^2, A_2^2, ..., A_U^2)$ where A_i is the total energy of all users using the same FD signature sequence, $i = 1, 2, ..., U$. The eigendecomposition of the correlation matrix then yields the subspace components [39]

$$\begin{aligned} \mathbf{C}_f &= \tilde{\mathbf{U}}_s^{(f)} \tilde{\mathbf{\Lambda}}_s^{(f)} \tilde{\mathbf{U}}_s^{(f)H} + \sigma_f^2 \tilde{\mathbf{U}}_n^{(f)} \tilde{\mathbf{U}}_n^{(f)H} \\ \tilde{\mathbf{\Lambda}}_s^{(f)} &= diag\left(\tilde{\lambda}_1^{(f)}, ..., \tilde{\lambda}_U^{(f)}\right) \end{aligned} \tag{4.30}$$

Then, based on the discussion of subspace detection in Section 3.3.3, the blind LMMSE detector for the type I and type II FD MUD is given by

$$\mathbf{w}_f^* = \tilde{\mathbf{U}}_s^{(f)} \left(\tilde{\mathbf{\Lambda}}_s^{(f)}\right)^{-1} \tilde{\mathbf{U}}_s^{(f)H} \tilde{\mathbf{c}}_1 \tag{4.31}$$

Estimating the effective FDS signature waveform is the last step to complete the blind subspace solution given by 4.31.

Blind Channel Estimation

It was shown in [42] that the effective signature waveform and the channel response can be jointly estimated by exploiting the orthogonality nature between the noise subspace and the signal subspace for MC-CDMA signals. For our proposed type I and type II detector joint channel estimation using the blind subspace method, we follow similar analysis as given in [42].

The orthogonal set of eigenvectors $\tilde{\mathbf{U}}_s^{(f)}$ from the eigendecomposition of the correlation matrix $\mathbf{C}_f$ spans the signal subspace of $\tilde{\mathbf{S}}_f = [\tilde{\mathbf{c}}_1|\tilde{\mathbf{c}}_2|\ldots|\tilde{\mathbf{c}}_U]$, then the orthogonality between the signal and noise subspace gives the result

$$\tilde{\mathbf{U}}_n^{(f)H}\tilde{\mathbf{c}}_1 = \mathbf{0} \tag{4.32}$$

Using this fact, the least squares method can be used to estimate the effective signature waveform and the unknown channel response

$$\hat{\tilde{c}}_1 = \underset{\tilde{\mathbf{c}}_1}{\operatorname{argmin}} \left\{ \left| \tilde{\mathbf{U}}_n^{(f)H}\tilde{\mathbf{c}}_1 \right|^2 \right\} \tag{4.33}$$

Using the definition of the effective signature waveform and expanding 4.33 yields an expression almost identical to 4.27.

$$\hat{\mathbf{g}} = \underset{\mathbf{g}}{\operatorname{argmin}} \left\{ \mathbf{g}^H \mathbf{F}_{M\times L}^H \mathbf{C}_1^H \hat{\mathbf{U}}_n^{(f)} \hat{\mathbf{U}}_n^{(f)H} \mathbf{C}_1 \mathbf{F}_{M\times L} \mathbf{g} \right\} \tag{4.34}$$

Upon restricting the solution to normalized $\mathbf{g}$, the solution for $\hat{\mathbf{g}}$ is given once again by the eigenvector corresponding to the smallest eigenvalue of the composite matrix $\mathbf{F}_{M\times L}^H \mathbf{C}_1^H \hat{\mathbf{U}}_n^{(f)} \hat{\mathbf{U}}_n^{(f)H} \mathbf{C}_1 \mathbf{F}_{M\times L}$. Such estimation is unique up to a complex constant as in the case with the channel estimation using the CMOE RLS estimates described in section 4.3.3. Using the subspace decomposition, the approach to channel estimation for both the CMOE RLS method and the subspace method relies on 4.32 being solvable. Recall that by definition, the matrix $\tilde{\mathbf{U}}_n^{(f)}$ contains all eigenvectors corresponding to the full eigenvalue decomposition of the sample data correlation

matrix that does not belong to the signal space collection. Suppose the signal space has rank U, then the matrix $\tilde{\mathbf{U}}_n^{(f)}$ contains $M-U$ eigenvectors. Also recall that the length of the unknown channel impulse response is L and hence the number of unknowns to solve for is also L. Therefore 4.32 contains $M-U$ equations and we are seeking for the solution for L unknowns. For the system of equations to be solvable, the number of equations must be greater than or equal to the number of unknowns and therefore, we arrive at the condition that $M-U \geq L$ which was stated without justification in Section 4.3.3. Hence, the maximum users that can be supported is limited by the channel impulse response length and the number of subcarriers used. Therefore, with M being fixed, the maximum number of users that can be supported in a slowly fading Rayleigh multipath channel is $N \times (M-L)$. For our proposed TF-MC-CDMA type I and type II detector, we present here two implementations for the blind subspace multiuser detection in slowly Rayleigh fading channel, namely, the singular value decomposition of the data matrix and adaptive subspace tracking using the PASTd algorithm introduced in Chapter 3, and investigate their performance in slowly fading Rayleigh multipath channel.

Singular Value Decomposition

The singular value decomposition implementation applies the exact eigendecomposition to the sample correlation matrix. The sample correlation matrix can be obtained either through batch sample averaging or an exponentially weighted recursive update with a forgetting factor which is more suitable for dynamic channels. The computation of subspace parameters using SVD need not be re-computed for every data sample. However, the interval between re-computation of the blind detector should accommodate to the changing dynamics of the channel such as the channel coherence time. The type I and type II detector implementation using the SVD method is

// Type I Blind TF-MC-CDMA Subspace (SVD) Receiver // in Slowly Fading Rayleigh Multipath Channel
In the p^{th} symbol, input matrix $\mathbf{Z}[p]$ Set $\mathbf{w}_t^* = \mathbf{a}_1$ **for**$(n = 1, 2, ..., N)$ Compute Update: $\hat{\mathbf{C}}_f[p, n] = \lambda \hat{\mathbf{C}}_f[p, n-1] + (\mathbf{z}_n[p]^T)(\mathbf{z}_n[p]^T)^H$ **end for** Apply Eigendecomposition to $\hat{\mathbf{C}}_f$ to get Subspace Eigenvectors: $\left\{\hat{\mathbf{u}}_j^{(f)}\right\}_{j=1}^{M}$ Subspace Eigenvalues: $\left\{\hat{\lambda}_j^{(f)}\right\}_{j=1}^{M}$ Form Subspace matrices: $\hat{\mathbf{U}}_s^{(f)}, \hat{\mathbf{\Lambda}}_s^{(f)}, \hat{\mathbf{U}}_n^{(f)}$ Perform Channel Estimation: Find smallest eigenvector $\hat{\mathbf{g}}$ corresponding to the smallest eigenvalue of $\mathbf{F}_{M\times L}^H \mathbf{C}_1^H \hat{\mathbf{U}}_n^{(f)} \hat{\mathbf{U}}_n^{(f)H} \mathbf{C}_1 \mathbf{F}_{M\times L}$ Compute Estimated Effective FD Signature: $\tilde{\mathbf{c}}_1 = \mathbf{F}_{M\times L}\hat{\mathbf{g}}$ Compute FD Detector $\mathbf{w}_f^* = \hat{\mathbf{U}}_s^{(f)}(\hat{\mathbf{\Lambda}}_s^{(f)})^{-1}\hat{\mathbf{U}}_s^{(f)H}\tilde{\mathbf{c}}_1$ Perform detection $\hat{b}_1[p] = \text{sgn}\left(\text{Re}\left\{\left(\mathbf{w}_t^{*H}\mathbf{Z}\right)^* \mathbf{w}_f^*\right\}\right)$

Table 4.3: Type I Blind Subspace (SVD) Receiver Algorithm

summarized in Table 4.3 and Table 4.4 respectively.

PASTd Adaptive Subspace Tracking

Alternatively, the subspace parameters can also be estimated using the PASTd adaptive subspace tracking algorithm used in Chapter 3. The adaptive subspace tracking using the PASTd algorithm offers a computation advantage over the singular value implementation method as discussed in Chapter 3. The adaptive algorithm need not be modified for the slowly fading channels. Again, the only added complexity comes from the joint channel estimation step which the channel coefficients are obtained once the subspace parameters are computed. However, we note that the PASTd algorithm only tracks the subspace eigenvectors belonging to the signal subspace but

// Type II Blind TF-MC-CDMA Subspace (SVD) Receiver
// in Slowly Fading Rayleigh Multipath Channel

In the p^{th} symbol, input matrix $\mathbf{Z}[p]$

Set $\mathbf{w}_t^* = \mathbf{a}_1$

Compute: $\mathbf{z}' = \mathbf{a}_1^H \mathbf{Z}[p]$

Compute Update:

$\hat{\mathbf{C}}_f[p] = \lambda \hat{\mathbf{C}}_f[p-1] + (\mathbf{z}'[p]^T)(\mathbf{z}'[p]^T)^H$

Apply Eigendecomposition to $\hat{\mathbf{C}}_f$ to get

Subspace Eigenvectors: $\left\{ \hat{\mathbf{u}}_j^{(f)} \right\}_{j=1}^{M}$

Subspace Eigenvalues: $\left\{ \hat{\lambda}_j^{(f)} \right\}_{j=1}^{M}$

Form Subspace matrices: $\hat{\mathbf{U}}_s^{(f)}, \hat{\mathbf{\Lambda}}_s^{(f)}, \hat{\mathbf{U}}_n^{(f)}$

Perform Channel Estimation:

Find smallest eigenvector $\hat{\mathbf{g}}$ corresponding to the smallest eigenvalue of $\mathbf{F}_{M\times L}^H \mathbf{C}_1^H \hat{\mathbf{U}}_n^{(f)} \hat{\mathbf{U}}_n^{(f)H} \mathbf{C}_1 \mathbf{F}_{M\times L}$

Compute Estimated Effective FD Signature: $\tilde{\mathbf{c}}_1 = \mathbf{F}_{M\times L} \hat{\mathbf{g}}$

Compute FD Detector

$\mathbf{w}_f^* = \hat{\mathbf{U}}_s^{(f)} (\hat{\mathbf{\Lambda}}_s^{(f)})^{-1} \hat{\mathbf{U}}_s^{(f)H} \tilde{\mathbf{c}}_1$

Perform detection

$\hat{b}_1[p] = \text{sgn}\left(\text{Re}\left\{ (\mathbf{w}_f^*)^H \mathbf{z}'^T \right\} \right)$

Table 4.4: Type II Blind Subspace (SVD) Receiver Algorithm

in fact we also need the estimate of the noise subspace eigenvectors as well. To do that, we invoke a orthogonality relationship relating the noise subspace eigenvectors and the signal subspace eigenvectors [23]

$$\mathbf{U}_n^{(f)}\mathbf{U}_n^{(f)H} = \mathbf{I} - \mathbf{U}_s^{(f)}\mathbf{U}_s^{(f)H} \tag{4.35}$$

Using 4.35, we do not have to explicitly update the noise subspace eigenvectors using the PASTd algorithm. It can be computed through the signal subspace. The algorithms for type I and type II detectors using PASTd adaptive subspace tracking are summarized in Table 4.4 and 4.5 respectively.

4.4 Performance Evaluation Measure

The performance evaluation criteria for blind multiuser receivers presented in Section 3.4 applies to the slowly fading channel as well. The output SINR is defined as in section 3.4 except that the expectation is now over all channel realizations for a given Doppler rate and delay profile.

$$SINR(\mathbf{w}_t, \mathbf{w}_f) = \frac{E\left\{\mathbf{w}_t^H\mathbf{Z}[p]\mathbf{w}_f|b_1[\mathrm{p}]\right\}^2}{E\left\{Var\left(\mathbf{w}_t^H\mathbf{Z}[p]\mathbf{w}_f|b_1[\mathrm{p}]\right)\right\}} \tag{4.36}$$

Furthermore, because our blind multiuser receivers perform joint channel estimation, we also evaluate the mean square error in the channel estimation. This is defined as the variance of the channel estimation error as a function of the number of samples processed. This is defined as,

$$\varepsilon(\hat{\mathbf{g}}) = E\left\{\|\hat{\mathbf{g}} - \mathbf{g}\|^2\right\} \tag{4.37}$$

4.4.1 Receiver Complexity

The receiver computational complexity in the downlink slowly fading Rayleigh multipath channel is slightly different from the AWGN channel case discussed in Chapter

// Type I Blind TF-MC-CDMA Subspace (PASTd) Receiver
// in Slowly Fading Rayleigh Multipath Channel

In the p^{th} symbol, input matrix $\mathbf{Z}[p]$ and previous estimates $\left\{\hat{\lambda}_k^{(f)}, \hat{\mathbf{u}}_k^{(f)}\right\}_{k=1}^{U}$

Set $\mathbf{w}_t^* = \mathbf{a}_1$

for$(n = 1, 2, ..., N)$

  Input $\mathbf{z}_n[p]^T$

  Set $\mathbf{x}_1^{(f)} = \mathbf{z}_n[p]^T$

  for$(k = 1, 2, ..., U)$

    Projection Approximation: $y_k^{(f)} = \hat{\mathbf{u}}_k^{(f)}[p, n-1]^H \mathbf{x}_k^{(f)}$

    Eigenvalue Update: $\hat{\lambda}_k^{(f)}[p, n] = \gamma \hat{\lambda}_k^{(f)}[p, n-1] + \left|y_k^{(f)}\right|^2$

    Eigenvector Update:

    $$\hat{\mathbf{u}}_k^{(f)}[p, n] = \hat{\mathbf{u}}_k^{(f)}[p, n-1] + \left(\frac{y_k^{(f)*}}{\hat{\lambda}_k^{(f)}[p,n]}\right)\left(\mathbf{x}_k^{(f)} - \hat{\mathbf{u}}_k^{(f)}[p, n-1] y_k^{(f)}\right)$$

    Deflation: $\mathbf{x}_{k+1}^{(f)} = \mathbf{x}_k^{(f)} - \hat{\mathbf{u}}_k^{(f)}[p, n] y_k^{(f)}$

  end for

end for

Form Signal Subspace Matrices: $\hat{\mathbf{U}}_s^{(f)}, \hat{\mathbf{\Lambda}}_s^{(f)}$

Compute: $\hat{\mathbf{U}}_n^{(f)} \hat{\mathbf{U}}_n^{(f)H} = \mathbf{I} - \hat{\mathbf{U}}_s^{(f)} \hat{\mathbf{U}}_s^{(f)H}$

Perform Channel Estimation:

  Find smallest eigenvector $\hat{\mathbf{g}}$ corresponding to the smallest eigenvalue of $\mathbf{F}_{M\times L}^H \mathbf{C}_1^H \hat{\mathbf{U}}_n^{(f)} \hat{\mathbf{U}}_n^{(f)H} \mathbf{C}_1 \mathbf{F}_{M\times L}$

  Compute Estimated Effective FD Signature: $\tilde{\mathbf{c}}_1 = \mathbf{F}_{M\times L} \hat{\mathbf{g}}$

Compute FD Detector

  $\mathbf{w}_f^* = \hat{\mathbf{U}}_s^{(f)} (\hat{\mathbf{\Lambda}}_s^{(f)})^{-1} \hat{\mathbf{U}}_s^{(f)H} \tilde{\mathbf{c}}_1$

Perform detection

  $\hat{b}_1[p] = \text{sgn}\left(\text{Re}\left\{\left(\mathbf{w}_t^{*H} \mathbf{Z}\right)^* \mathbf{w}_f^*\right\}\right)$

Table 4.5: Type I Blind Subspace PASTd Receiver Algorithm

// Type II Blind TF-MC-CDMA Subspace (PASTd) Receiver
// in Slowly Fading Rayleigh Multipath Channel

In the p^{th} symbol, input matrix $\mathbf{Z}[p]$ and previous estimates $\left\{\hat{\lambda}_k^{(f)}, \hat{\mathbf{u}}_k^{(f)}\right\}_{k=1}^{U}$

Set $\mathbf{w}_t^* = \mathbf{a}_1$

Compute: $\mathbf{z}' = \mathbf{a}_1^H \mathbf{Z}[p]$

Input $\mathbf{z}'[p]^T$

Set $\mathbf{x}_1^{(f)} = \mathbf{z}'[p]^T$

for$(k = 1, 2, ..., U)$

Projection Approximation: $y_k^{(f)} = \hat{\mathbf{u}}_k^{(f)}[p-1]^H \mathbf{x}_k^{(f)}$

Eigenvalue Update: $\hat{\lambda}_k^{(f)}[p] = \gamma \hat{\lambda}_k^{(f)}[p-1] + \left|y_k^{(f)}\right|^2$

Eigenvector Update:

$$\hat{\mathbf{u}}_k^{(f)}[p] = \hat{\mathbf{u}}_k^{(f)}[p-1] + \left(\frac{y_k^{(f)*}}{\hat{\lambda}_k^{(f)}[p]}\right)\left(\mathbf{x}_k^{(f)} - \hat{\mathbf{u}}_k^{(f)}[p-1] y_k^{(f)}\right)$$

Deflation: $\mathbf{x}_{k+1}^{(f)} = \mathbf{x}_k^{(f)} - \hat{\mathbf{u}}_k^{(f)}[p] y_k^{(f)}$

end for

Form Signal Subspace Matrices: $\hat{\mathbf{U}}_s^{(f)}, \hat{\mathbf{\Lambda}}_s^{(f)}$

Compute: $\hat{\mathbf{U}}_n^{(f)} \hat{\mathbf{U}}_n^{(f)H} = \mathbf{I} - \hat{\mathbf{U}}_s^{(f)} \hat{\mathbf{U}}_s^{(f)H}$

Perform Channel Estimation:

Find smallest eigenvector $\hat{\mathbf{g}}$ corresponding to the smallest eigenvalue of $\mathbf{F}_{M\times L}^H \mathbf{C}_1^H \hat{\mathbf{U}}_n^{(f)} \hat{\mathbf{U}}_n^{(f)H} \mathbf{C}_1 \mathbf{F}_{M\times L}$

Compute Estimated Effective FD Signature: $\tilde{\mathbf{c}}_1 = \mathbf{F}_{M\times L} \hat{\mathbf{g}}$

Compute FD Detector

$\mathbf{w}_f^* = \hat{\mathbf{U}}_s^{(f)} (\hat{\mathbf{\Lambda}}_s^{(f)})^{-1} \hat{\mathbf{U}}_s^{(f)H} \tilde{\mathbf{c}}_1$

Perform detection

$$\hat{b}_1[p] = \text{sgn}\left(\text{Re}\left\{(\mathbf{w}_f^*)^H \mathbf{z}'^T\right\}\right)$$

Table 4.6: Type II Blind Subspace PASTd Receiver Algorithm

3 even though the methods used in both cases are inherently the same (CMOE RLS, blind subspace using SVD, and blind subspace using PASTd subspace tracking). The difference stems from the fact that in slowly fading downlink channels, matched filtering is applied for the time domain detection because orthogonality of the TD signature sequence are preserved in slowly fading channels. Furthermore, there is added complexity for receivers in slowly fading downlink channel coming from the joint channel estimation computations. The CMOE RLS channel estimation involves computing an eigendecomposition of a L by L matrix to find the eigenvector corresponding to the smallest eigenvector; this has complexity $O(L^3)$. Both the blind subspace methods using SVD and adaptive subspace tracking PASTd also involve computing an EVD of a L by L matrix to find the eigenvector corresponding to the smallest eigenvector to estimate the channel. The FD detector computation for both CMOE RLS type I and type II detectors have the same complexity as in the AWGN channel case which is $O(M^2)$ per update. Because there are N updates per symbol for type I, the total complexity for type I is $O(NM^2)$. For type II, only one update is computed per symbol, hence the total complexity of type II CMOE RLS is $O(M^2)$. Hence in this case, there is a computational advantage going from type I to type II for the CMOE RLS implementation. The FD detector computation using blind subspace method through SVD is based on the data autocorrelation matrix rank. For type I, this is $\min\{K, M\}$. In most realistic situations, M will be less than K since one of the main motivations for using TF-MC-CDMA is to use short signature codes [17]. For type II, this is χ_1 and as discussed before, $\chi_1 \leq M$. Using SVD, the complexity for the type I blind subspace detector computation is $O(M^3)$ and for the type II detector $O(\chi_1^3)$. In this case, when the system is below full capacity, there is computation advantage going from type I to type II. The frequency domain detector computation using blind subspace method using PASTd adaptive subspace tracking is also based

Multiuser Detector	Type	Complexity
CMOE RLS	Type I	$O(NM^2 + L^3)$
CMOE RLS	Type II	$O(M^2 + L^3)$
Subspace SVD	Type I	$O(M^3 + L^3)$
Subspace SVD	Type II	$O(\chi_1^3 + L^3)$
Subspace PASTd	Type I	$O(NM^2 + L^3)$
Subspace PASTd	Type II	$O(\chi_1 M + L^3)$

Table 4.7: Summary of TF-MC-CDMA Blind Multiuser detection complexity for slowly fading Rayleigh multipath channels

on the sample correlation matrix rank. Using the PASTd adaptive subspace tracking, the complexity for the type I blind subspace detector computation is $O(M^2)$ under normal system capacity and for the type II detector is $O(\chi_1 M)$ per update. For type I using PASTd, there are N updates per symbol, therefore, the total complexity for type I receiver is $O(NM^2)$. However, for type II, there is only one update per symbol, therefore the total complexity for type II PASTd detector is $O(\chi_1 M)$. We also see that using the PASTd subspace tracking algorithm, there is computation advantage going from type I to type II. Together with the joint channel estimation estimates, the detector complexities for the multiuser detection methods considered are summarized in Table 4.7.

4.5 Simulation Results

Computer simulations were carried out to illustrate the performance of the following multiuser receivers in downlink slowly fading Rayleigh multipath channels: CMOE RLS, subspace SVD, and the adaptive subspace tracking using PASTD implemented in both type I and type II architectures. The channel model used in our simulation is the ITU-A model for evaluating outdoor/indoor pedestrian environment. The power delay profile for the ITU-A model is given in Table 4.8. The TF-MC-CDMA chip period is chosen to be 100ns. For simplicity, we round the relative delays of the delay

Tap	Relative Delay (ns)	Average Power (dB)	Doppler Spectrum
1	0	0	$\frac{\sigma_h^2}{\pi f_d \sqrt{1-\left(\frac{\upsilon}{f_d}\right)^2}}$
2	110	-9.7	$\frac{\sigma_h^2}{\pi f_d \sqrt{1-\left(\frac{\upsilon}{f_d}\right)^2}}$
3	190	-19.2	$\frac{\sigma_h^2}{\pi f_d \sqrt{1-\left(\frac{\upsilon}{f_d}\right)^2}}$
4	410	-22.8	$\frac{\sigma_h^2}{\pi f_d \sqrt{1-\left(\frac{\upsilon}{f_d}\right)^2}}$

Table 4.8: ITU-A Pedestrian Rayleigh Fading Channel Power delay profile

TD Spreading Gain	8
FD Spreading Gain	16
Number of Subcarriers	16
TDS Sequence	Walsh-Hadamard
FDS Sequence	Walsh-Hadamard
Number of FDS Sequence used	11

Table 4.9: Simulation parameters

profile to the nearest 100ns. Furthermore, we assume the mobile user is moving at speed of 3km/hr which corresponds to normal walking pace in urban areas. The system parameters chosen are shown in Table 4.9.

We consider three levels of system loading, light moderate (35 users), moderate (55 users) and high (75 users). The BER performance curves for 35 users, 55 users and 75 users are presented in Figures 4.3, 4.4, and 4.5. It can be seen from the BER figures that the TF-MC-CDMA type I detectors are far inferior in performance to the type II detectors especially in the 35 and 55 users case. This result is not surprising given that the type II cascade processing eliminates interferers from other time-groups by matched filtering while type I detectors do not enjoy this property. There is a large difference in performance between type I and type II blind subspace PASTd detectors and it can be seen that type I blind subspace PASTd detector has the poorest performance among all receivers considered. For light to moderate loads (i.e.

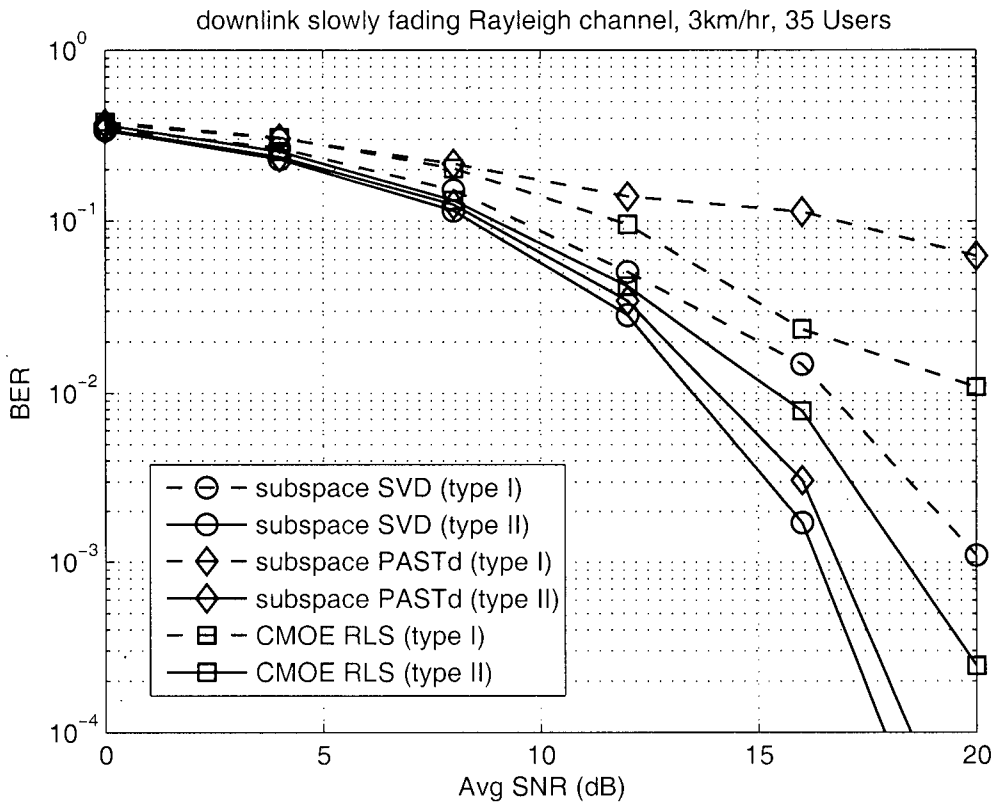

Figure 4.3: BER performance for 35 users case

the 35 users and 55 users case), it can be seen that the type II blind subspace PASTd detector's performance matches closely to that of the type II blind subspace SVD although there is a slight (<1dB) penalty for using an adaptive tracking algorithm instead of computing the SVD. However, at higher system loading, the blind subspace SVD detector has a better good performance.

For the type II detectors (in the 35 users and 55 users case), we see similar trends as in Chapter 3 for the TF-MC-CDMA blind multiuser detection problem in AWGN. We see that the subspace detection using SVD provides the best performance and the subspace detection using PASTd subspace tracking but provides fairly good performance.

We also present output SINR plots to confirm our BER performance results and to look into the convergence of the proposed detectors. Figures 4.6, 4.7 and 4.8 provide

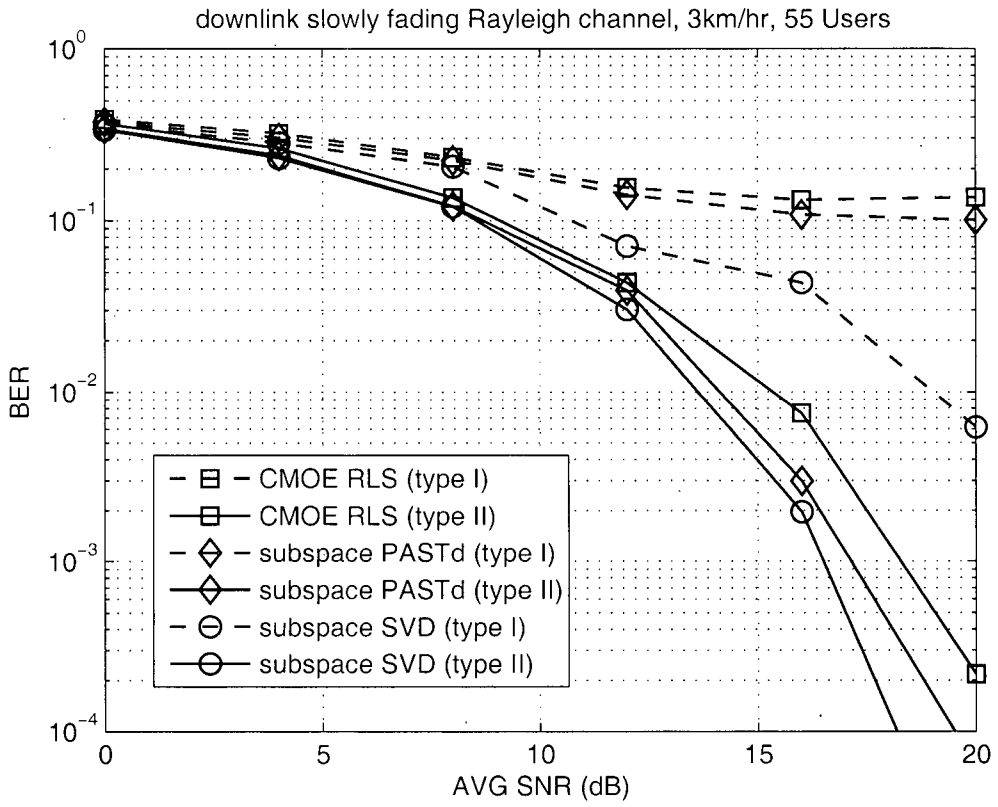

Figure 4.4: BER performance for 55 users case

the output SINR versus data samples plot for 35 users, 55 users, and the 75 users system load. The convergence of the blind subspace PASTd algorithm is relatively slow compared to the other two. This is expected since we have already observed this relatively slow convergence in Chapter 3. In our simulations, the PASTd algorithm has been accelerated by applying a batch SVD decomposition to the first 50 data samples. The SINR plots confirm that type II detectors outperform type I detectors.

We also studied the channel estimation capabilities for our proposed detectors. The sampled mean square channel estimation error is plotted against the data samples in Fig. 4.9 for type I and type II CMOE RLS, blind subspace SVD, and blind subspace PASTd adaptive subspace tracking detectors. Again, the channel estimation error plots confirm the type II detectors estimates the channel much better than type II detectors. The cascade implementation of type II detectors remove MAI using the

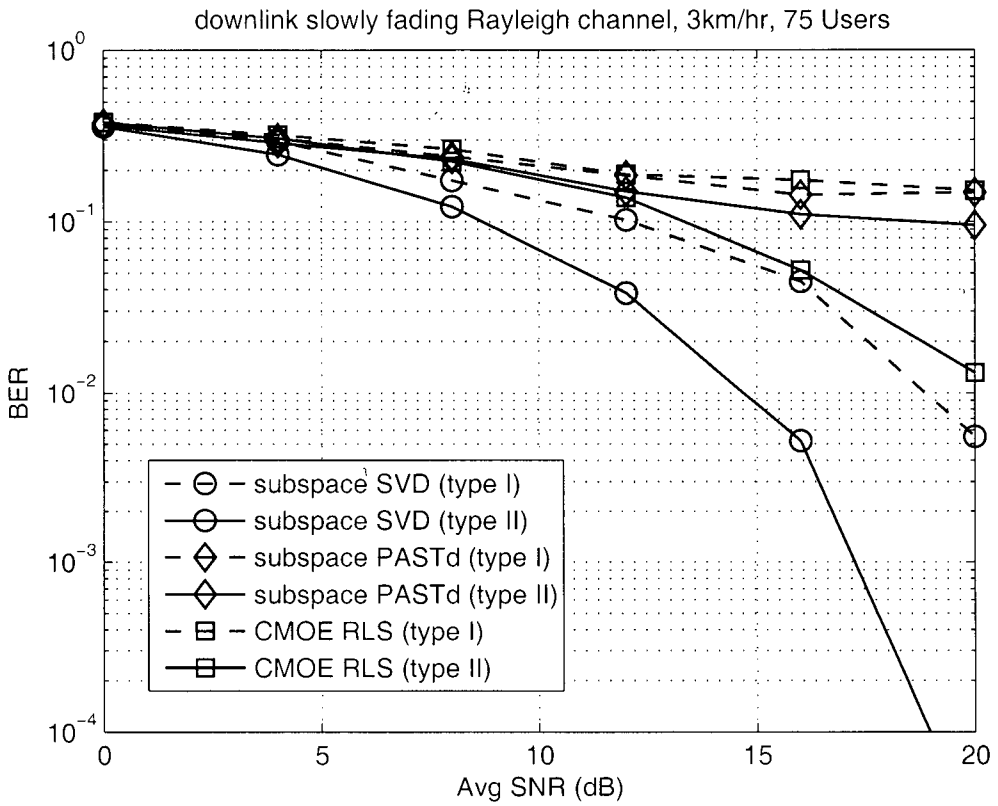

Figure 4.5: BER performance for 75 users case

orthogonality of the TD spreading codes thus giving better joint channel estimation during the FD detection stage.

4.6 Summary

In this chapter, the TF-MC-CDMA blind multiuser detection problem in a downlink slowly fading Rayleigh multipath channel was investigated. Two types of blind multiuser detectors were proposed and investigated. The first type, known as type I detector, retains the same parallel processing form as the blind multiuser detector for the AWGN channel with MAI by using the decoupling method discussed in Chapter 3. The second type, known as type II detector, uses cascade processing where the output of the TD processing is used as the input to the frequency domain processing.

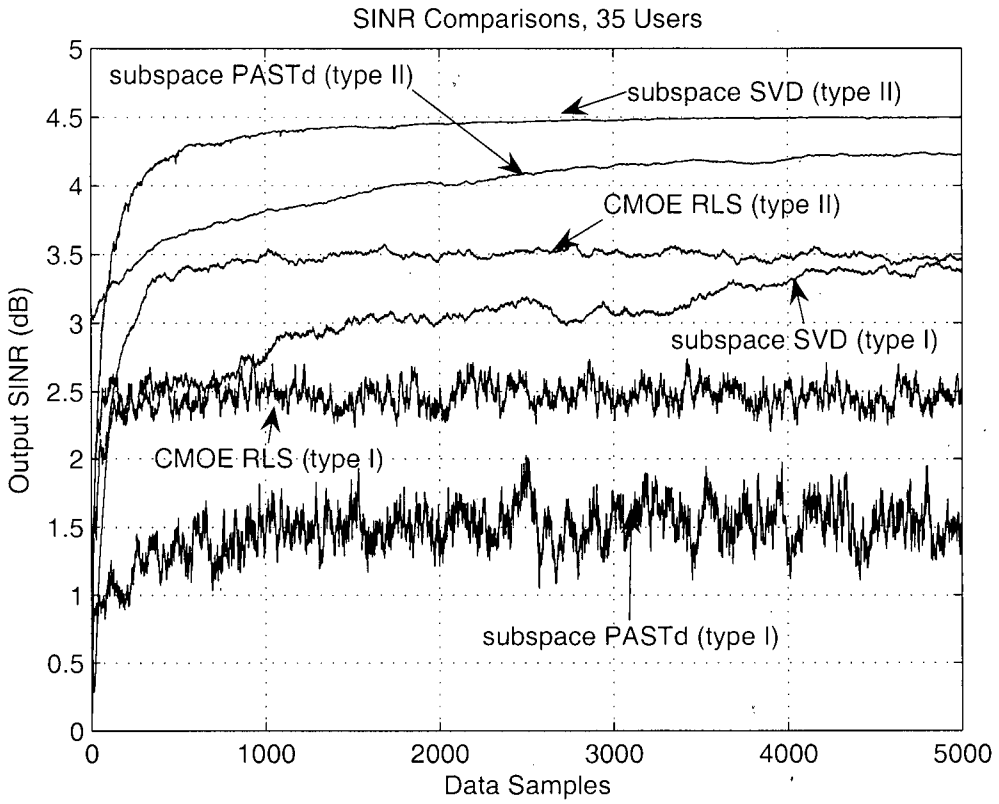

Figure 4.6: Output SINR for 35 users case at SNR 12dB

It was found that both methods involve solving an equivalent MC-CDMA multiuser detection problem (that differ only in the number of FD interfering sequences in slowly fading channel for the FD multiuser detector coefficients. The type I and type II detectors were then applied with three multiuser detection methods, namely, the CMOE RLS method, blind subspace method using SVD and blind subspace method using PASTd adaptive subspace tracking. Computer simulation results show that type II detectors outperform type I detectors. The cascade implementation of the type II detector reduces the amount of interference going into the FD MUD stage by applying matched filtering in the TD detection.

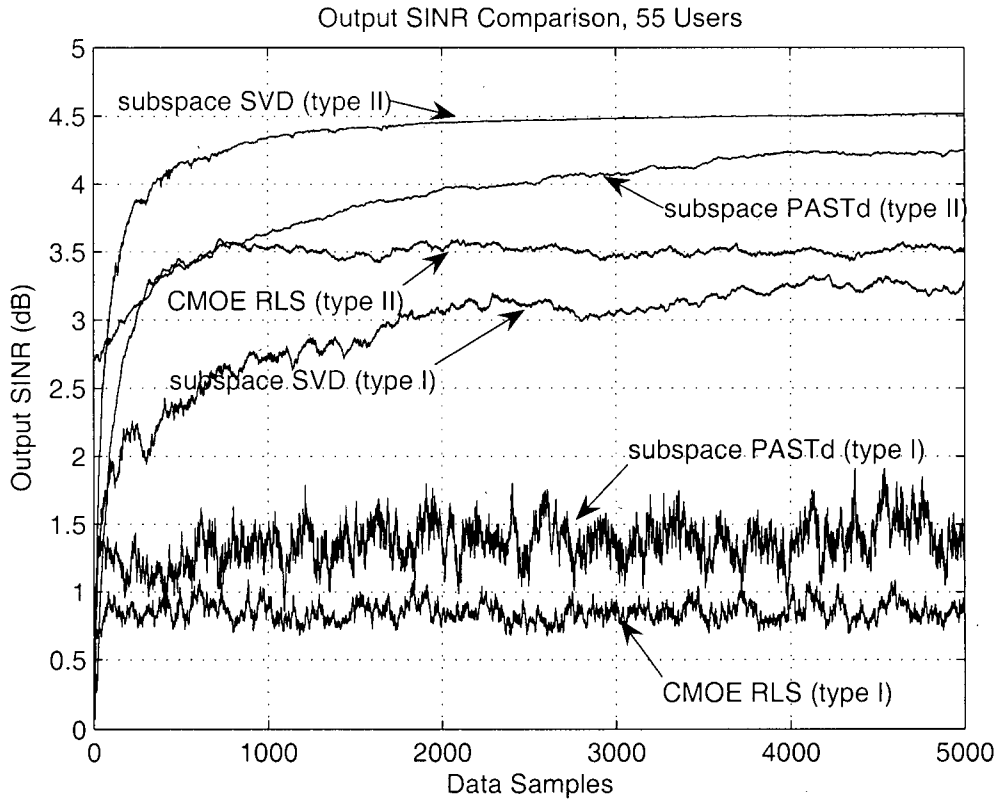

Figure 4.7: Output SINR for 55 users case at SNR 12dB

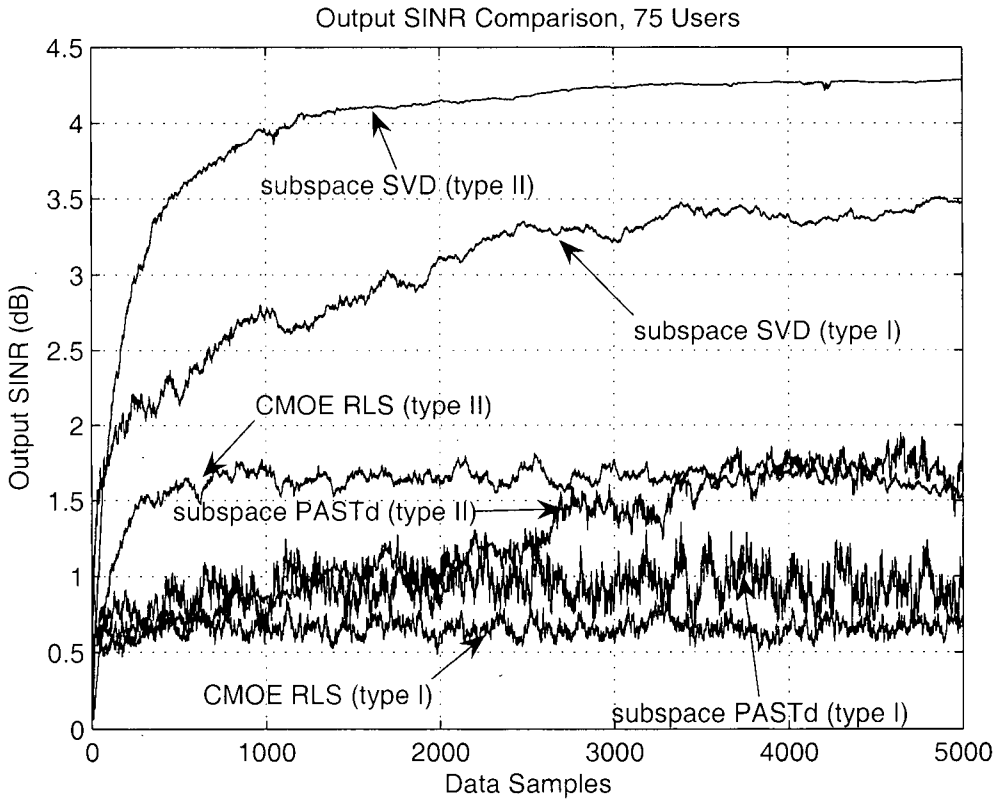

Figure 4.8: Output SINR for 75 users case at SNR 12dB

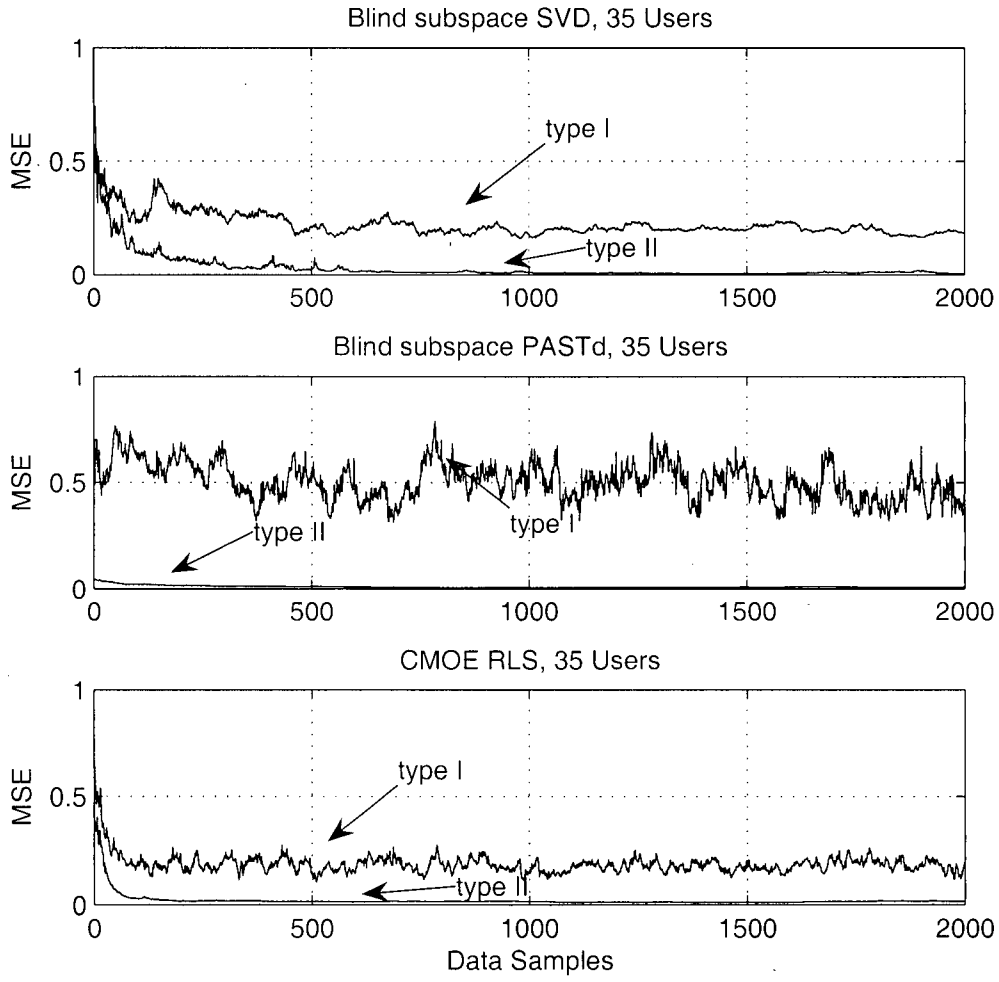

Figure 4.9: Mean square channel estimation error for 35 users at SNR 16dB

Chapter 5

TF-MC-CDMA Blind Multiuser Detection in Downlink Mobile Rayleigh Fading Channel with Doppler Induced ICI

5.1 Introduction

In this chapter, the random frequency offset caused by mobile Doppler shifts in downlink multipath fading channels is investigated. Previous discussions in Chapters 3 and 4 have implicitly assumed that any frequency offset is compensated exactly at the receiver. Frequency offset is a result of the mismatch in frequency between the detected signal and the demodulator's oscillators. Perfect frequency matching is important in multicarrier based modulation because subcarrier frequency offset or mismatch results in leakage from one subcarrier to other subcarrier as a result of loss of orthogonality creating intercarrier interference (ICI). Random frequency mismatch is caused by the Doppler shift in mobile communication multipath channels and the effect of in-

tercarrier interference is most severe when subchannels or subcarriers have minimal separation. The result is a loss of orthogonality in the FDS codes. In this chapter, we investigate the performance of the TF-MC-CDMA blind multiuser detectors proposed in Chapter 4 in multipath fading channels with Doppler induced ICI.

The roadmap of this chapter is as follows: section 5.2 discusses the mathematical model of ICI in TF-MC-CDMA and its analysis in TF-MC-CDMA downlink transmission. Section 5.3 discusses the blind multiuser detection algorithms used in combating ICI in downlink multipath fading channels. Section 5.4 presents computer simulation results. A Summary of the chapter is provided in Section 5.5.

5.2 Modeling Intercarrier Interference

In this section, a mathematical model for ICI in TF-MC-CDMA caused by mobile Doppler shifts as a result of user mobility is discussed. It is shown in [26] that intercarrier interference (ICI) in OFDM systems caused by mobile Doppler shifts can be modeled as a frequency shift within the channel impulse response. Because of multipath propagation, each path arrives at the mobile receiver isotropic antenna with incident angle θ_i and experiences a Doppler shift ν_i(Hz). In [43], it was shown that if the Doppler shift is considered into the tapped delay line channel model, then the continuous time varying channel impulse response for a L path multipath channel is given by

$$h(\tau,t)=\sum_{l=0}^{L-1} g_l(t)e^{j2\pi\upsilon_l(t)(t-\tau_l(t))}\delta\left(\tau-\tau_l(t)\right) \tag{5.1}$$

If the channel is assumed to be changing slowly with respect to the transmission rate so that the complex channel gains, path delays and Doppler frequency shifts are relatively constant over at least an OFDM data block, then we can rewrite 5.1 as

$$h(\tau,t)=\sum_{l=0}^{L-1} g_l e^{j2\pi\upsilon_l(t-\tau_l)}\delta\left(\tau-\tau_l\right) \tag{5.2}$$

The Fourier transform with respect to the delay variable τ gives the function

$$\bar{h}(f,t) = \sum_{l=0}^{L-1} g_l e^{j2\pi\upsilon_l(t-\tau_l)} e^{-j2\pi f\tau_l} \tag{5.3}$$

An important result in [27] showed that using a time domain analysis from the received signal, the effect of Doppler induced ICI in MC-CDMA systems can be viewed as a form of weighted sampling in the frequency domain. Using this result and sampling the channel frequency response given in 5.3 with integer multiples of the frequency separation between subcarriers f_s, the Doppler induced ICI weight coefficients can be found. Assuming that M subcarriers are used, this yields

$$\bar{h}(m_0 f_s,t) = \sum_{l=0}^{L-1} g_l e^{j2\pi\upsilon_l(t-\tau_l)} e^{-j2\pi m_0 f_s\tau_l} \tag{5.4}$$

where $f_s = \frac{1}{T_s M}$ is the subcarrier frequency spacing and T_s is the duration of an OFDM symbol transmission. Samples of the channel impulse response in the t variable at multiples of T_s is yields the discrete channel impulse response

$$\bar{h}(m_0 f_s,iT_s) = \sum_{l=0}^{L-1} g_l e^{j2\pi\upsilon_l(iT_s-\tau_l)} e^{-j2\pi m_0 f_s\tau_l} \tag{5.5}$$

If we approximate and discretize the path delays to integer multiples of T_s, and let $\varepsilon_l = \frac{\upsilon_l}{f_s}$ be the normalized Doppler offset of the l path, then we can rewrite 5.5 as

$$\begin{aligned}\bar{h}(m_0,i) &= \sum_{l=0}^{L-1} g_l \exp\left(\frac{j2\pi i\varepsilon_l}{M}\right)\exp\left(\frac{-j2\pi\varepsilon_l l}{M}\right)\exp\left(\frac{-j2\pi m_0 l}{M}\right)\\ &= \sum_{l=0}^{L-1} g_l \exp\left(\frac{j2\pi\varepsilon_l(i-l)}{M}\right)\exp\left(\frac{-j2\pi m_0 l}{M}\right)\end{aligned} \tag{5.6}$$

The frequency domain channel transfer function is then the M point DFT of $\bar{h}(n,i)$ with respect to the variable i.

$$\begin{aligned}H(m_0,m) &= \frac{1}{M}\sum_{i=0}^{M-1}\sum_{l=0}^{L-1} g_l \exp\left(\frac{j2\pi\varepsilon_l(i-l)}{M}\right)\exp\left(\frac{-j2\pi m_0 l}{M}\right)\exp\left(\frac{-j2\pi mi}{M}\right)\\ &= \frac{1}{M}\sum_{i=0}^{M-1}\sum_{l=0}^{L-1} g_l \exp\left(\frac{j2\pi((\varepsilon_l-m)i-\varepsilon_l l)}{M}\right)\exp\left(\frac{-j2\pi m_0 l}{M}\right)\end{aligned} \tag{5.7}$$

It is shown in [28] that using OFDM based transmission, the DFT demodulated received signal is weighted by the frequency domain channel transfer function $H(m_0, m-m_0)$. Applying this result to the TF-MC-CDMA received signal yields

$$r_{LP}[m_0] = \sqrt{\frac{P}{M}} \sum_{k=1}^{K} b_k a_k[n] \sum_{m=0}^{M-1} c_k[m] H(m_0, m-m_0) + W[m_0] \tag{5.8}$$

The term $H(m_0, m-m_0)$ weighted by the frequency domain spreading chip sequence $c_k[m]$ is the ISI induced by the channel and represents the leakage of energy from the m^{th} subcarrier to the ${m_0}^{th}$ subcarrier. Expanding 5.8 yields

$$\begin{aligned} r_{LP}[m_0] &= \sqrt{\tfrac{P}{M}} \sum_{k=1}^{K} b_k a_k[n] \sum_{m=0}^{M-1} c_k[m] \\ &\times \left(\tfrac{1}{M} \sum_{i=0}^{M-1} \sum_{l=0}^{L-1} g_l \exp\left(\tfrac{j2\pi((\varepsilon_l - (m-m_0))i - \varepsilon_l l)}{M} \right) \exp\left(\tfrac{-j2\pi m_0 l}{M} \right) \right) + W[m_0] \end{aligned} \tag{5.9}$$

Equation (5-10) is the received TF-MC-CDMA signal model that includes both the effects of both multipath fading and Doppler induced ICI. This result can be used to model TF-MC-CDMA signals in downlink mobile fading channels. If the mobile receiver is stationary relative to the transmitting basestation and as a result, no Doppler frequency shifts, then we can set $\varepsilon_l = 0$ for $l = 1, 2, ..., L$. By doing this, then we have

$$\begin{aligned} r_{LP}[m_0] &= \sum_{k=1}^{K} b_k a_k[n] \sum_{m=0}^{M-1} c_k[m] \\ &\times \left(\tfrac{1}{M} \sum_{l=0}^{L-1} \sum_{i=0}^{M-1} g_l \exp\left(\tfrac{j2\pi(m_0 - m)i}{M} \right) \exp\left(\tfrac{-j2\pi m_0 l}{M} \right) \right) + W[m_0] \\ &= \sum_{k=1}^{K} b_k a_k[n] \sum_{m=0}^{M-1} c_k[m] \delta_{mm_0} \sum_{l=0}^{L-1} g_l \exp\left(\tfrac{-j2\pi m_0 l}{M} \right) + W[m_0] \end{aligned} \tag{5.10}$$

which is the received signal model for the slowly fading Rayleigh multipath channel discussed in Chapter 2 and Chapter 4.

We now define the effective frequency domain chip sequence (as a result of ICI) as

$$G_k[m_0] \equiv \sum_{m=0}^{M-1} c_k[m] H(m_0, m-m_0) \tag{5.11}$$

Equation (5-8) can be rewritten as

$$r_{LP}[m_0] = \sum_{k=1}^{K} b_k a_k[n] G_k[m_0] + W[m_0] \tag{5.12}$$

or in a more familiar form

$$r_{LP}[m_0] = \sum_{k=1}^{K} b_k a_k[n] \left(\frac{G_k[m_0]}{c_k[m_0]} \right) c_k[m_0] + W[m_0] \tag{5.13}$$

Defining the effective frequency domain complex subchannel gain as

$$G'_k[m_0] \equiv \frac{G_k[m_0]}{c_k[m_0]} \tag{5.14}$$

Using (5-14) and (5-15), the received signal can be written as

$$r_{LP}[m_0] = \sum_{k=1}^{K} b_k a_k[n] G'_k[m_0] c_k[m_0] + W[m_0] \tag{5.15}$$

which is an equation identical in form to 4.4 with the exception that 5.15 is a quasi-uplink synchronous model (even though we are analyzing a downlink channel) since each user experiences a user dependent channel gain $G'_k[m_0]$ instead of a common channel gain. As a result, we can also define an equivalent channel impulse response $\mathbf{g}' = IDFT(\mathbf{G}'_\mathbf{k})$.

Based on the above discussion of the modeling of ICI due to Doppler shifts in a mobile communication channel, we can summarize two important effects of ICI in TF-MC-CDMA: (1) it destroys the orthogonality of the FDS codes and (2) it transforms a downlink synchronous model into a quasi-uplink synchronous model.

5.3 Blind Multiuser Detection

This section discusses using the blind multiuser detection methods proposed in Chapter 4 to the TF-MC-CDMA signal given by 5.15 without knowledge of the ICI coefficients, the Doppler frequencies, and other interfering users' time and frequency

domain signature sequences. Since it was shown in Chapter 4 that type II detectors out-performs type I detectors, we only discuss type II detectors. In particular, we revisit the CMOE RLS method and the subspace blind multiuser detection method using SVD and adaptive subspace tracking through the PASTd algorithm to show that all these algorithms gives robust performance in mobile multipath fading channels with Doppler induced ICI.

5.3.1 Type II Detection Formulation

Based on the previous discussion of the type II detectors in Chapter 4, we begin by rewriting the TF-MC-CDMA received signal given by 5.15 using the groupings of TDS sequences, with all users sharing the same time domain signature sequence forming a group. This gives

$$r_{LP}[m_0] = Z_n[m_0] = \sqrt{P}\sum_{j=1}^{N}\sum_{\kappa=1}^{\chi_j} b_{n\kappa}a_n[j]c_\kappa[m_0]G'_\kappa[m_0] + W_n[m_0] \tag{5.16}$$

Using vector notation, 5.16 can be re-written as

$$\mathbf{z}[m_0] = \sqrt{P}\sum_{j=1}^{N}\sum_{\kappa=1}^{\chi_j} b_{j\kappa}c_\kappa[m_0]G'_\kappa[m_0]\mathbf{a}_j + \mathbf{W}[m_0] \tag{5.17}$$

The orthogonality of the TDS sequences is preserved when the channel is varying slowly with respect to the transmission rate and thus we can simplify 5.17 by applying matched filtering for the time domain detection

$$\begin{aligned}\mathbf{a}_1^H\mathbf{z}[m_0] = z'[m_0] &= \sqrt{P}\sum_{j=1}^{N}\sum_{\kappa=1}^{\chi_j} b_{j\kappa}c_\kappa[m_0]G'_\kappa[m_0]\mathbf{a}_1^H\mathbf{a}_j + \mathbf{a}_1^H\mathbf{W}[m_0] \\ &= \sqrt{P}\sum_{\kappa=1}^{\chi_1} b_{1\kappa}c_\kappa[m_0]G'_\kappa[m_0] + w'\end{aligned} \tag{5.18}$$

Re-writing 5.18 using vectors yields

$$\mathbf{z}' = \begin{bmatrix} z'[1] \\ \vdots \\ z'[M] \end{bmatrix} = \sqrt{P}\sum_{\kappa=1}^{\chi_1} b_{1\kappa}\tilde{\mathbf{c}}_\kappa + \mathbf{w}' \tag{5.19}$$

where now the effective FDS waveform is given by

$$\begin{aligned}
\tilde{\mathbf{c}}_k &= diag(\mathbf{c}_k)\mathbf{G'}_k \\
\mathbf{G'}_k &= \begin{bmatrix} G'_k[1] & G'_k[2] & \dots & G'_k[M] \end{bmatrix}^T \\
diag(\mathbf{c}_k) &= \begin{bmatrix} c_k[1] & & \\ & \ddots & \\ & & c_k[M] \end{bmatrix}
\end{aligned} \tag{5.20}$$

Then, the same optimization problem for the type II blind LMMSE detector as in Chapter 4 (see equation 4.14) is obtained with the slight difference in the effective FDS signature since the complex channel gain vector is now user dependent. However, the FD blind LMMSE optimization problem remains the same as before, i.e.

$$\mathbf{w}_f^* = \underset{\mathbf{w}_f \in \mathbb{C}^{M\times 1}}{\operatorname{argmin}} \; E\left\{ \left\| \sqrt{P}\,(b_{11}) - \mathbf{w}_f^H \mathbf{z}' \right\|^2 \right\} \tag{5.21}$$

5.3.2 CMOE RLS Blind Detector

In this section, we show the CMOE RLS blind detector for blind multiuser detection can be applied in mobile Rayleigh fading channel with Doppler shift induced ICI. Since the optimization problem in 5.21 is similar to that in 4.14 except the effective FDS waveform has a quasi-uplink interpretation. Using this fact, the CMOE RLS algorithm remains the same as that in chapter four, namely

$$\mathbf{w}_f^* = \left(\tilde{\mathbf{c}}_1^H \mathbf{C}_f^{-1} \tilde{\mathbf{c}}_1\right)^{-1} \mathbf{C}_f^{-1} \tilde{\mathbf{c}}_1 \tag{5.22}$$

where $\mathbf{C}_f^{-1}$ is approximated recursively using the matrix inversion lemma, i.e.

$$\mathbf{C}_f^{-1}[j] \approx \mathbf{\Phi}_f[j] = \lambda^{-1}\mathbf{\Phi}_f[j-1] - \frac{\lambda^{-2}\mathbf{\Phi}_f[j-1]\mathbf{z}'\mathbf{z}'^H\mathbf{\Phi}_f[j-1]}{1+\lambda^{-1}\mathbf{z}'^H\mathbf{\Phi}_f[j-1]\mathbf{z}'} \tag{5.23}$$

Using the results in Section 4.3.3, the effective FDS sequence, and hence the effective frequency domain channel gain for the desired user can be estimated using the MOE expression and then maximizing it with respect to the desired user's effective FD

// Type II Blind TF-MC-CDMA CMOE RLS Receiver
// in Slowly Fading Rayleigh Multipath Channel
// with Doppler induced ICI

Initialization:

$\mathbf{\Phi}_f[0] = \mathbf{I}_{M\times M}$

In the p^{th} symbol, input matrix $\mathbf{Z}[p]$

Set $\mathbf{w}_t^* = \mathbf{a}_1$

Compute: $\mathbf{z}' = \mathbf{a}_1^H \mathbf{Z}[p]$

Compute Kalman Gain:

$$\mathbf{k}_f[p] = \frac{\lambda^{-1}\mathbf{\Phi}_f[p-1]\mathbf{z}'^T}{1+\lambda^{-1}\left(\mathbf{z}'^T\right)^H \mathbf{\Phi}_f[p-1]\mathbf{z}'^T}$$

Compute Update:

$$\mathbf{\Phi}_f[p] = \lambda^{-1}\left(\mathbf{\Phi}_f[p-1] - \mathbf{k}_f\left(\mathbf{z}'^T\right)^H \mathbf{\Phi}_f[p-1]\right)$$

Perform Channel Estimation:

Find smallest eigenvector $\hat{\mathbf{g}}'$ corresponding to the smallest eigenvalue of $\mathbf{F}_{M\times L}^H \mathbf{C}_1^H \mathbf{\Phi}_f \mathbf{C}_1 \mathbf{F}_{M\times L}$

Compute Estimated Effective FD Signature: $\tilde{\mathbf{c}}_1 = \mathbf{F}_{M\times L}\hat{\mathbf{g}}'$

Compute FD Detector

$\mathbf{w}_f^* = \mathbf{\Phi}_f \tilde{\mathbf{c}}_1$

Perform detection

$\hat{b}_1[p] = \mathrm{sgn}\left(\mathrm{Re}\left\{(\mathbf{w}_f^*)^H \mathbf{z}'^T\right\}\right)$

Table 5.1: Type II CMOE RLS Blind Receiver Algorithm for multipath fading channels with Doppler induced ICI

signature. This again ends up being a familiar problem to find the normalized eigenvector corresponding to the smallest eigenvalue of the matrix $\mathbf{F}_{M\times L}^H \mathbf{C}_1^H \mathbf{\Phi}_f \mathbf{C}_1 \mathbf{F}_{M\times L}$. The algorithm is summarized in Table 5.1.

5.3.3 Blind Subspace Multiuser Detection

The blind subspace multiuser detector for TF-MC-CDMA signal in mobile fading channel with Doppler induced ICI can be formulated in the same way as presented in Section 4.3.4. The data correlation matrix from the TF-MC-CDMA multiuser detection problem in 5.15 can be expanded into

$$\mathbf{C}_f \equiv E\left\{\mathbf{z}'\mathbf{z}'^H\right\} = \tilde{\mathbf{S}}_f |\mathbf{A}|^2 \tilde{\mathbf{S}}_f^H + \sigma_f^2 \mathbf{I}_{M\times M} \tag{5.24}$$

where

$$\tilde{\mathbf{S}}_f = [\tilde{\mathbf{c}}_1 | \tilde{\mathbf{c}}_2 | \dots | \tilde{\mathbf{c}}_{\chi_1}] \tag{5.25}$$

contains the effective FD signatures of the users within the same time domain signature group as the desired user (user 1). Applying the eigendecomposition to $\mathbf{C}_f$ gives the signal and noise subspace decomposition

$$\begin{aligned} \mathbf{C}_f &= \tilde{\mathbf{U}}_s^{(f)} \tilde{\mathbf{\Lambda}}_s^{(f)} \tilde{\mathbf{U}}_s^{(f)H} + \sigma_f^2 \tilde{\mathbf{U}}_n^{(f)} \tilde{\mathbf{U}}_n^{(f)H} \\ \tilde{\mathbf{\Lambda}}_s^{(f)} &= diag\left(\tilde{\lambda}_1^{(f)}, ..., \tilde{\lambda}_{\chi_1}^{(f)}\right) \end{aligned} \tag{5.26}$$

The solution to the type II FD blind LMMSE detector is given by

$$\mathbf{w}_f^* = \tilde{\mathbf{U}}_s^{(f)} \left(\tilde{\mathbf{\Lambda}}_s^{(f)}\right)^{-1} \tilde{\mathbf{U}}_s^{(f)H} \tilde{\mathbf{c}}_1 \tag{5.27}$$

The effective FD signature can be estimated using the exact same procedure as in Section 4.3.4 by exploiting the orthogonality nature between the noise subspace and the signal subspace. Combined with the least squares estimation, we arrive again at the familiar optimization problem for the channel estimation

$$\hat{\mathbf{g}}' = \underset{\mathbf{g}}{\operatorname{argmin}} \left\{ \mathbf{g}^H \mathbf{F}_{M\times L}^H \mathbf{C}_1^H \hat{\mathbf{U}}_n^{(f)} \hat{\mathbf{U}}_n^{(f)H} \mathbf{C}_1 \mathbf{F}_{M\times L} \mathbf{g} \right\} \tag{5.28}$$

Solving the optimization problem in 5.28 again requires finding the normalized eigenvector corresponding to the smallest (least dominant) eigenvalue of the composite matrix $\mathbf{F}_{M\times L}^H \mathbf{C}_1^H \hat{\mathbf{U}}_n^{(f)} \hat{\mathbf{U}}_n^{(f)H} \mathbf{C}_1 \mathbf{F}_{M\times L}$. As in Chapter 4 where it was implicitly assumed that the channel ICI has been perfectly compensated, the channel estimation in this case is also unique up to a multiplicative complex constant for the same reasoning discussed in Section 4.3.4. Therefore, the maximum user capacity for the TF-MC-CDMA downlink system in a multipath fading channel with Doppler induced ICI is also $N \times (M - L)$ as long as the two conditions stated in Section 4.3.3 are satisfied. Therefore, assuming the two conditions are satisfied, the Doppler induced ICI effect

// Type II Blind TF-MC-CDMA Subspace (SVD) Receiver
// in Slowly Fading Rayleigh Multipath Channel
// with Doppler induced ICI

In the p^{th} symbol, input matrix $\mathbf{Z}[p]$
Set $\mathbf{w}_l^* = \mathbf{a}_1$
Compute: $\mathbf{z}' = \mathbf{a}_1^H \mathbf{Z}[p]$
Compute Update:
$\hat{\mathbf{C}}_f[p] = \lambda \hat{\mathbf{C}}_f[p-1] + (\mathbf{z}'[p]^T)(\mathbf{z}'[p]^T)^H$
Apply Eigendecomposition to $\hat{\mathbf{C}}_f$ to get
Subspace Eigenvectors: $\left\{\hat{\mathbf{u}}_j^{(f)}\right\}_{j=1}^{\min\{K,M\}}$
Subspace Eigenvalues: $\left\{\hat{\lambda}_j^{(f)}\right\}_{j=1}^{\min\{K,M\}}$
Form Subspace matrices: $\hat{\mathbf{U}}_s^{(f)}, \hat{\mathbf{\Lambda}}_s^{(f)}, \hat{\mathbf{U}}_n^{(f)}$
Perform Channel Estimation:
Find smallest eigenvector $\hat{\mathbf{g}}'$ corresponding to the smallest eigenvalue of $\mathbf{F}_{M\times L}^H \mathbf{C}_1^H \hat{\mathbf{U}}_n^{(f)} \hat{\mathbf{U}}_n^{(f)H} \mathbf{C}_1 \mathbf{F}_{M\times L}$
Compute Estimated Effective FD Signature: $\tilde{\mathbf{c}}_1 = \mathbf{F}_{M\times L}\hat{\mathbf{g}}'$
Compute FD Detector
$\mathbf{w}_f^* = \hat{\mathbf{U}}_s^{(f)}(\hat{\mathbf{\Lambda}}_s^{(f)})^{-1}\hat{\mathbf{U}}_s^{(f)H}\tilde{\mathbf{c}}_1$
Perform detection
$\hat{b}_1[p] = \mathrm{sgn}\left(\mathrm{Re}\left\{(\mathbf{w}_f^*)^H \mathbf{z}'^T\right\}\right)$

Table 5.2: Type II Blind Subspace (SVD) Receiver Algorithm

does not change the user capacity of the system as the system is still capable of suppressing $N \times (M - L) - 1$ interferers. However, there is a penalty to pay in terms of BER performance because ICI reduces the average output SINR as a result of the leakage of subcarrier energy. The subspace parameters can be obtained using the SVD method or the PASTd adaptive subspace tracking. Both methods require no modification for the Doppler induced ICI channel. We summarize the both the type II blind subspace detector algorithm using SVD and using PASTd adaptive subspace tracking in Table 5.2 and 5.3 respectively.

// Type II Blind TF-MC-CDMA Subspace (PASTd) Receiver
// in Slowly Fading Rayleigh Multipath Channel
// with Doppler induced ICI

In the p^{th} symbol, input matrix $\mathbf{Z}[p]$ and previous estimates $\left\{\hat{\lambda}_k^{(f)}, \hat{\mathbf{u}}_k^{(f)}\right\}_{k=1}^{\chi_1}$

Set $\mathbf{w}_t^* = \mathbf{a}_1$

Compute: $\mathbf{z}' = \mathbf{a}_1^H \mathbf{Z}[p]$

Input $\mathbf{z}'[p]^T$

Set $\mathbf{x}_1^{(f)} = \mathbf{z}'[p]^T$

for$(k = 1, 2, ..., \chi_1)$

Projection Approximation: $y_k^{(f)} = \hat{\mathbf{u}}_k^{(f)}[p-1]^H \mathbf{x}_k^{(f)}$

Eigenvalue Update: $\hat{\lambda}_k^{(f)}[p] = \gamma \hat{\lambda}_k^{(f)}[p-1] + \left|y_k^{(f)}\right|^2$

Eigenvector Update:

$$\hat{\mathbf{u}}_k^{(f)}[p] = \hat{\mathbf{u}}_k^{(f)}[p-1] + \left(\frac{y_k^{(f)*}}{\hat{\lambda}_k^{(f)}[p]}\right)\left(\mathbf{x}_k^{(f)} - \hat{\mathbf{u}}_k^{(f)}[p-1] y_k^{(f)}\right)$$

Deflation: $\mathbf{x}_{k+1}^{(f)} = \mathbf{x}_k^{(f)} - \hat{\mathbf{u}}_k^{(f)}[p] y_k^{(f)}$

end for

Form Signal Subspace Matrices: $\hat{\mathbf{U}}_s^{(f)}, \hat{\mathbf{\Lambda}}_s^{(f)}$

Compute: $\hat{\mathbf{U}}_n^{(f)} \hat{\mathbf{U}}_n^{(f)H} = \mathbf{I} - \hat{\mathbf{U}}_s^{(f)} \hat{\mathbf{U}}_s^{(f)H}$

Perform Channel Estimation:

Find smallest eigenvector $\hat{\mathbf{g}}'$ corresponding to the smallest eigenvalue of $\mathbf{F}_{M\times L}^H \mathbf{C}_1^H \hat{\mathbf{U}}_n^{(f)} \hat{\mathbf{U}}_n^{(f)H} \mathbf{C}_1 \mathbf{F}_{M\times L}$

Compute Estimated Effective FD Signature: $\tilde{\mathbf{c}}_1 = \mathbf{F}_{M\times L} \hat{\mathbf{g}}'$

Compute FD Detector

$\mathbf{w}_f^* = \hat{\mathbf{U}}_s^{(f)} (\hat{\mathbf{\Lambda}}_s^{(f)})^{-1} \hat{\mathbf{U}}_s^{(f)H} \tilde{\mathbf{c}}_1$

Perform detection

$\hat{b}_1[p] = \text{sgn}\left(\text{Re}\left\{(\mathbf{w}_f^*)^H \mathbf{z}'^T\right\}\right)$

Table 5.3: Type II Blind Subspace PASTd Receiver Algorithm

TD spreading gain	8
FD spreading gain	16
Number of subcarriers	16
TDS sequence type	Walsh-Hadamard
FDS sequence type	Walsh-Hadamard
Number of FDS sequence used	11
Carrier frequency	1.9 GHz

Table 5.4: Summary of simulation parameters

5.4 Simulation Results

Computer simulations were carried out to illustrate the performance of the proposed TF-MC-CDMA type II CMOE RLS receiver, blind subspace receiver using SVD, and the blind subspace receiver using PASTd adaptive subspace tracking for downlink slowly fading Rayleigh multipath channels with Doppler induced ICI. The channel model used is again the ITU-A 4 path model for evaluating outdoor/indoor pedestrian test environments provided in Table 4.5. The TF-MC-CDMA chip period is 100ns. Again, for simplicity, the relative delays of the multipath arrivals are rounded to the nearest 100ns and we do not modify the average receiving powers. The mobile speed considered here is pedestrian speed which corresponds to 3km/hr. The simulation parameters are summarized in Table 5.4.

Three types of system loading are considered: 35 users (light moderate load), 55 users (moderate load), and 75 users (high load). Figures 5.1, 5.2 and 5.3 show the BER performance curves for the 35 users, 55 users, and 75 users load respectively. Comparing the 35 users case and 55 users case with the simulation results in Chapter 4 (perfect frequency offset correction), it can be seen that the performance is still very good for all three type II detection methods. In particular, we once again see the closeness in performance between the type II blind subspace SVD and the blind subspace PASTd detectors for the 35 users and 55 users case. However, as the system

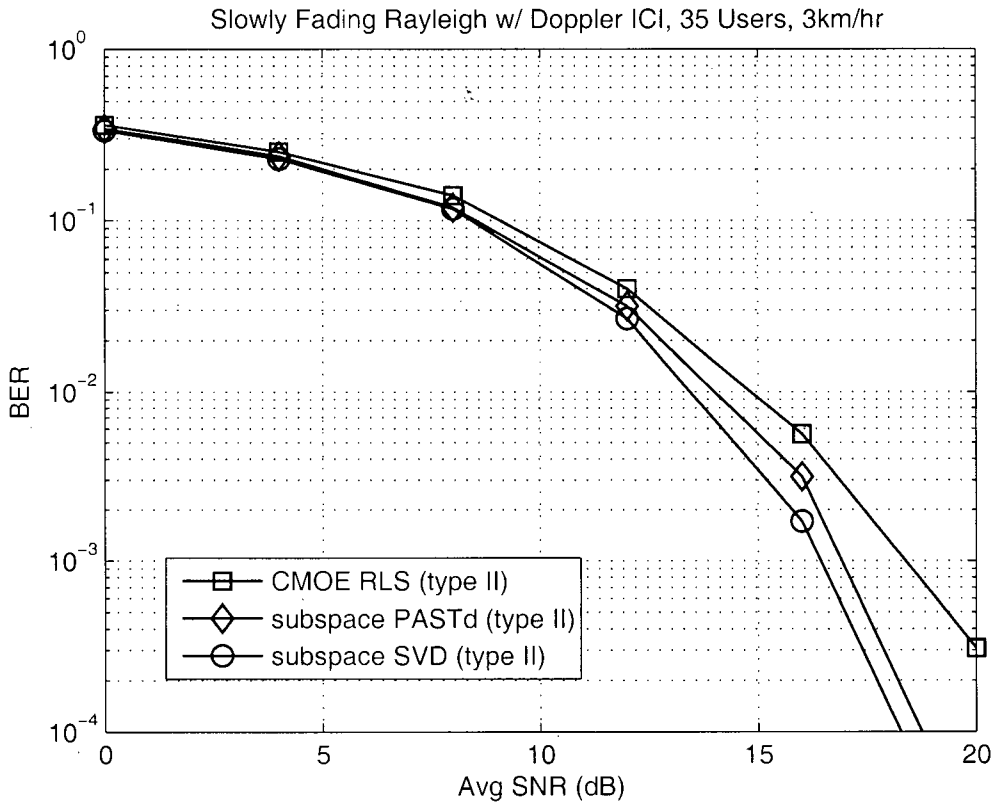

Figure 5.1: BER performance for 35 users case

reaches a high user loading, the type II blind subspace PASTd detector degrades significantly. This observation is also consistent with the simulation results from Chapter 4. From the BER performance simulation results, we can see that without using any frequency offset corrections, the type II blind subspace SVD, PASTd detectors and the CMOE RLS detector are robust to Doppler induced ICI in the channel.

We next present the output SINR results. Figures 5.4, 5.5 and 5.6 show the output SINR against the number of data samples processed for the 35 users, 55 users and 75 users case respectively. The output SINR results show that in all three system load cases, the slowest to converge is the blind subspace PASTd algorithm. The convergence speeds of the CMOE RLS detector and the blind subspace SVD algorithm are similar. In all user load cases, the blind subspace SVD performs the best which confirms the result of the BER performance results above. At high user

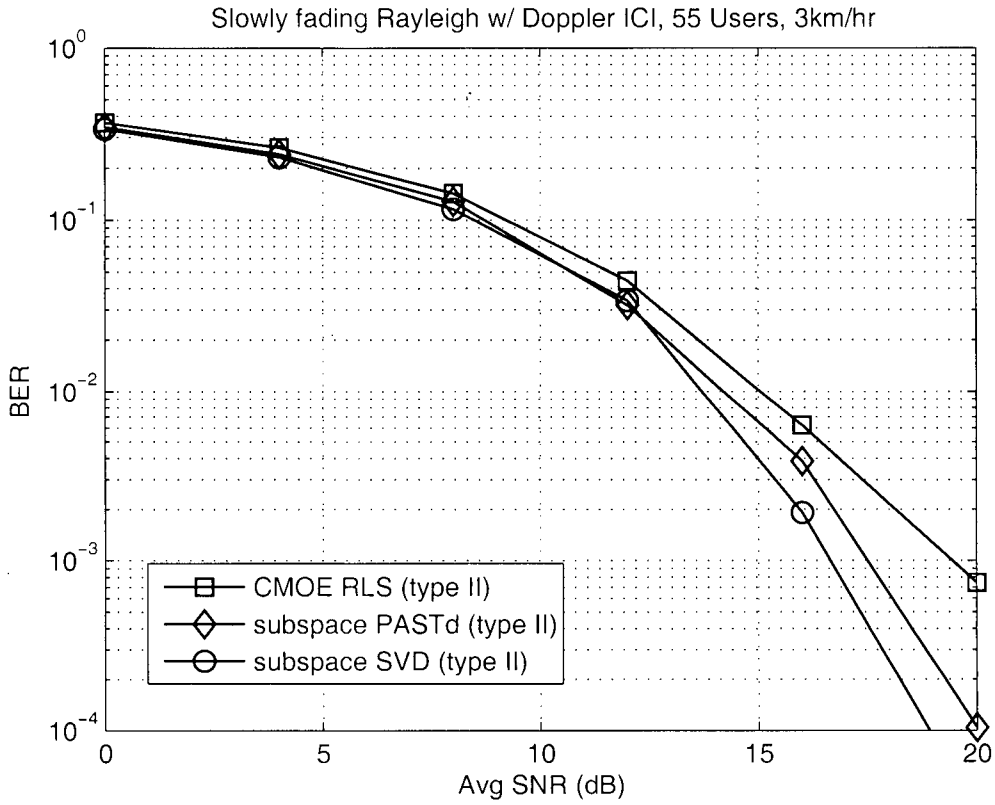

Figure 5.2: BER performance for 55 users case

loading, the PASTd does not perform well.

Finally, we present the mean square channel estimation error plots in Fig. 5.7 for all three type II detector implementation methods. This channel estimation is different from the channel estimation in Chapter 4 where we are truly estimating the channel's path gains. The channel estimation here estimates the effective frequency domain complex subchannel gains given in 5.14. It can be seen from Fig. 5.7 that all three detector schemes give similar channel estimation performance.

5.5 Summary

In this chapter, the mobile Doppler shift induced ICI is analyzed and derived for the TF-MC-CDMA slowly fading downlink model. This was shown to have two important

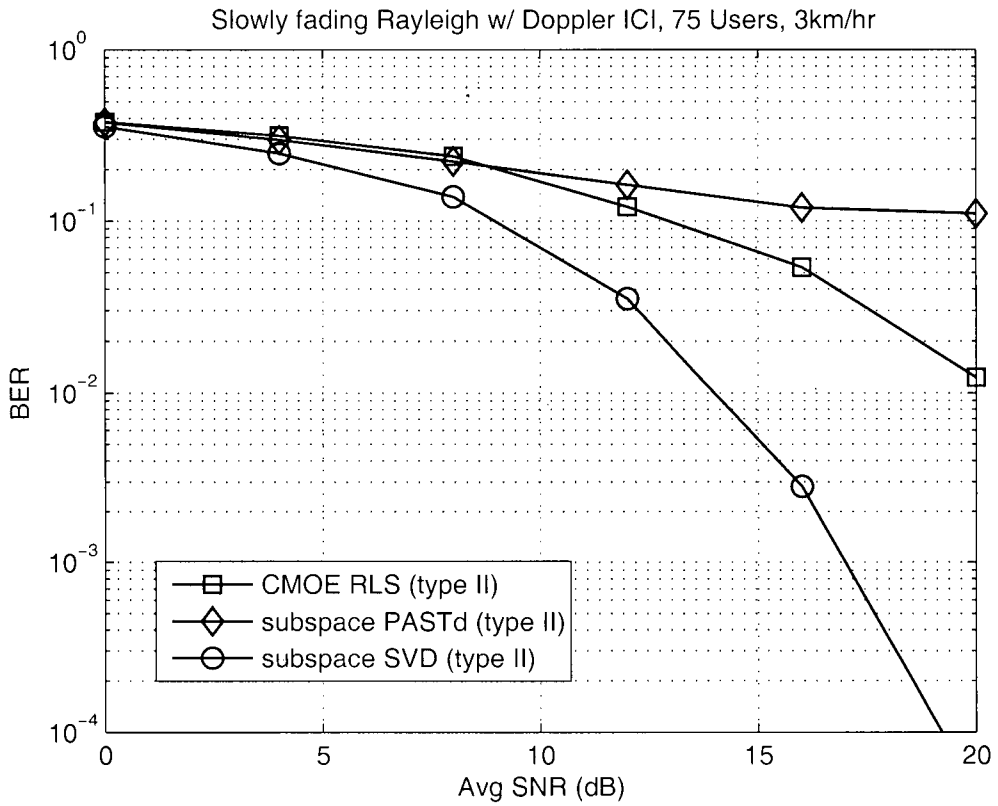

Figure 5.3: BER performance for 75 users case

effects: (1) the loss of orthogonality of the FDS sequences and (2) due to ICI, the pure downlink model becomes a quasi-uplink synchronous blind multiuser detection problem. We also show that we need not modify the TF-MC-CDMA type II CMOE RLS method and the blind subspace method proposed in Chapter 4. It is shown that they can be directly applied as long as the rank criteria is fulfilled. However, computer simulation results confirms that due to Doppler induced ICI, there is a performance degradation as compared to the performance without ICI.

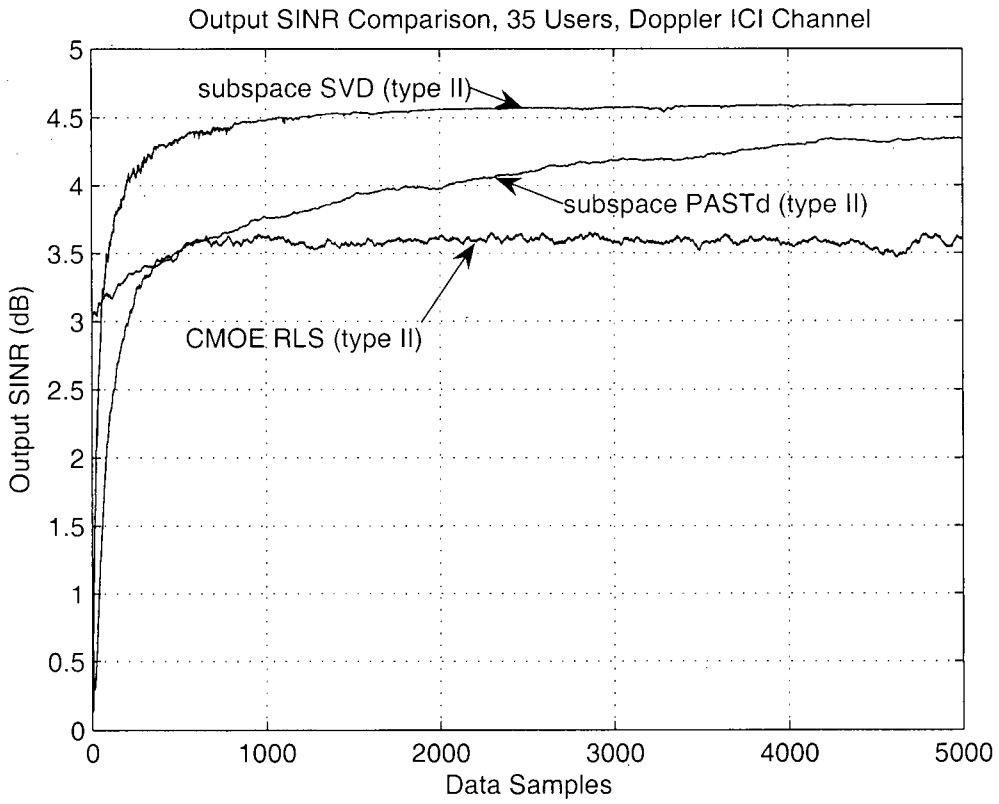

Figure 5.4: Output SINR for 35 users case at SNR 12dB

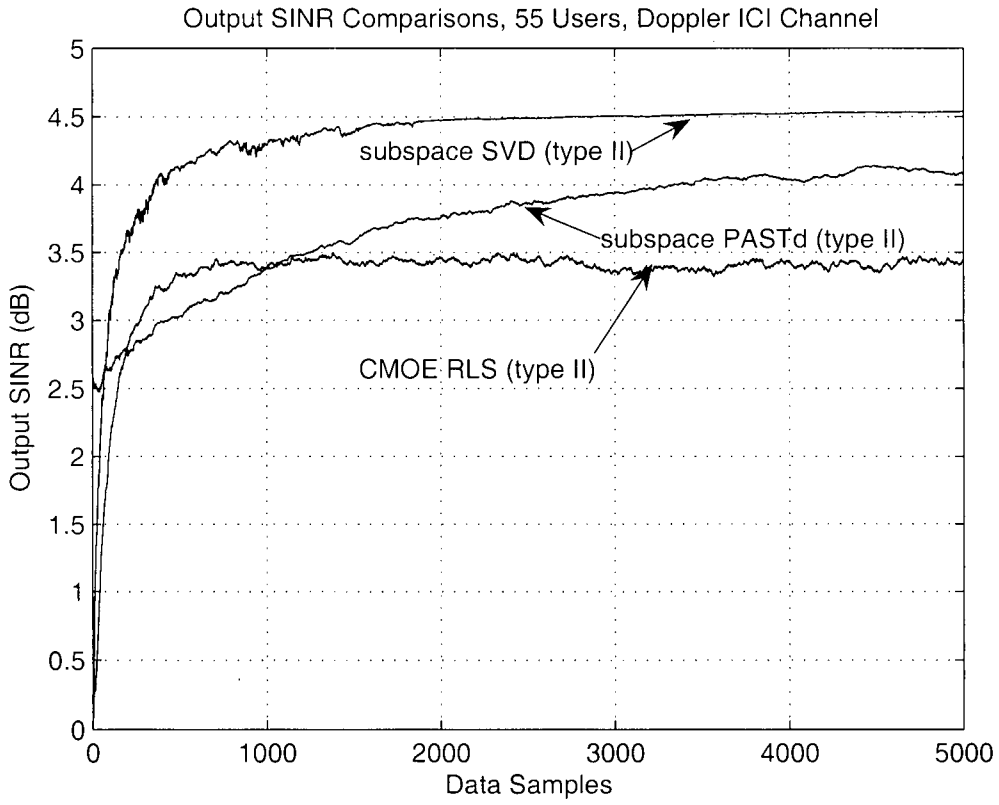

Figure 5.5: Output SINR for 55 users case at SNR 12dB

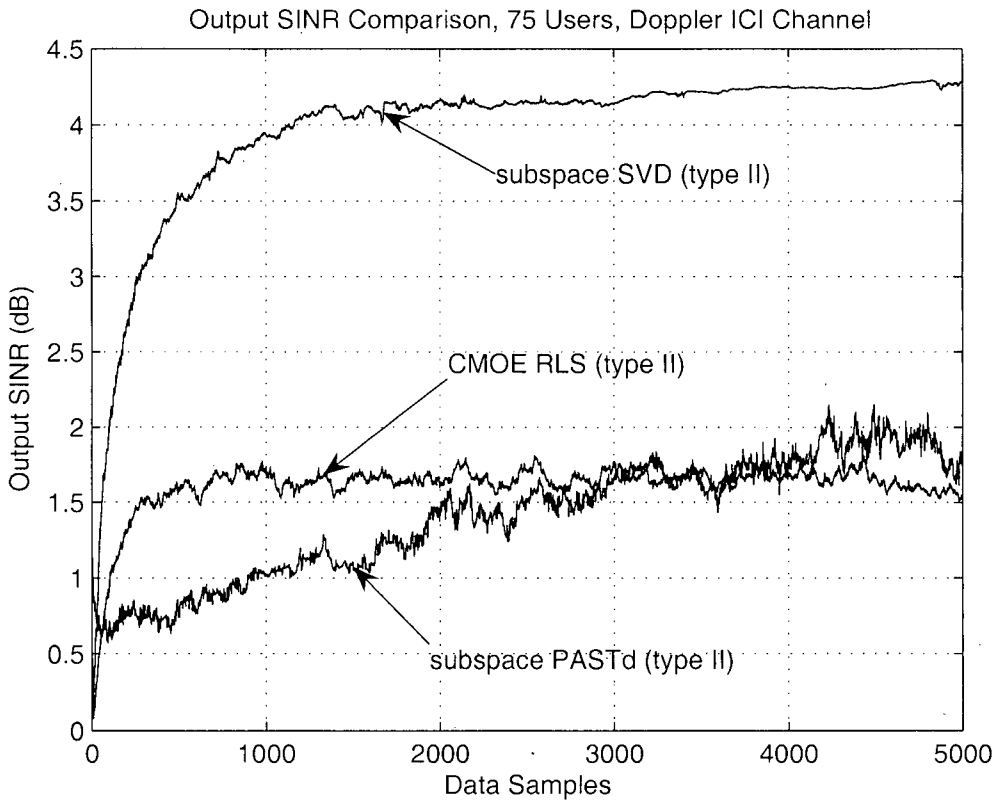

Figure 5.6: Output SINR for 75 users case at SNR 12dB

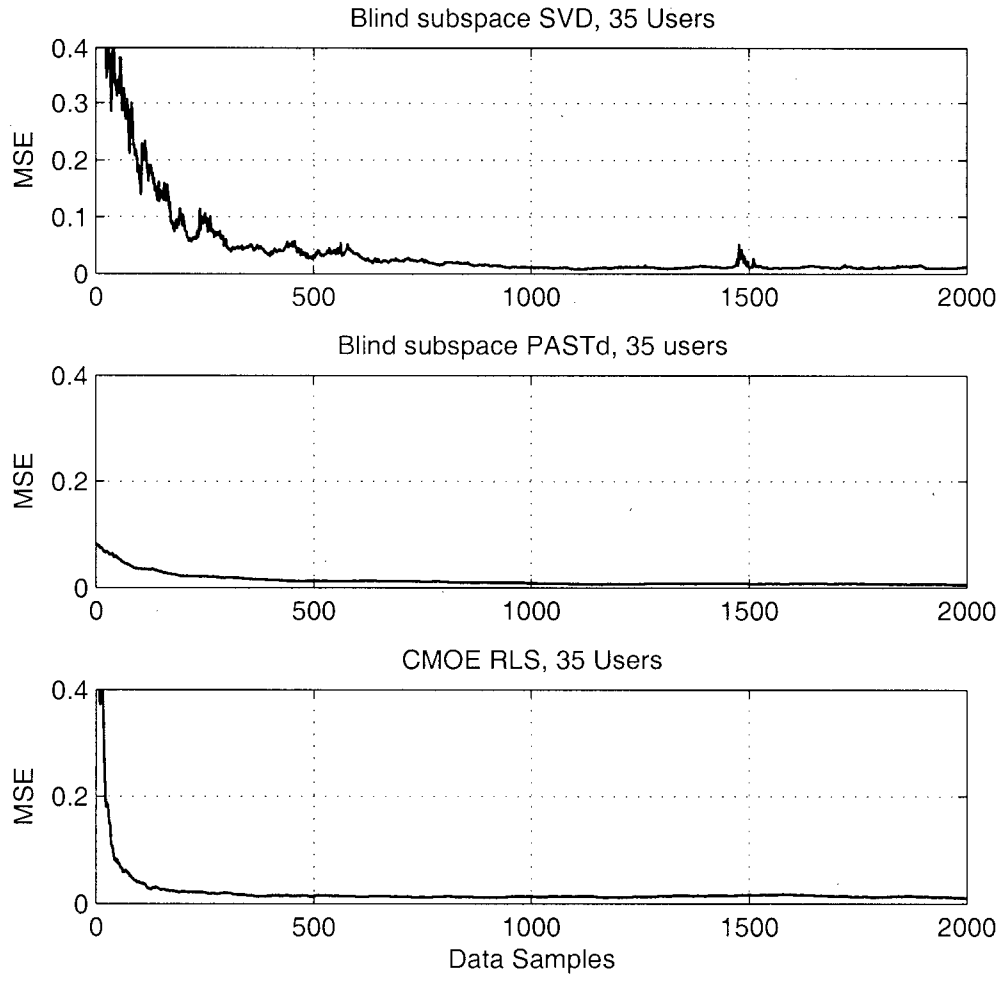

Figure 5.7: Mean square channel estimation error for 35 users at SNR 16dB

Chapter 6

Conclusion and Future Research

6.1 Conclusion

TF-MC-CDMA has shown significant promise to accommodate the demands of 4G broadband mobile communication systems. It combines the benefits of DS-CDMA and MC-CDMA that are high user capacity, robust to frequency selective fading, and flexibility in providing a framework for adaptive resource allocation. Any system using CDMA based multiple access is interference limited, and this is no different for TF-MC-CDMA. In fact, TF-MC-CDMA must contend with interference in both the spreading in time and frequency. The method of multiuser detection mitigates the near far problem and suppresses the multiple access interference thus providing much better performance than single user matched filter detection. Non-blind multiuser detection requires the knowledge of the spreading sequences of all users and accurate channel information. Blind multiuser detection methods avoid the use of pilot symbols and training sequences to acquire this information and provide much superior bandwidth utilization than non-blind multiuser detection. This is especially important in receivers operating in next generation mobile handsets. This thesis is focused on extending the applicability of blind multiuser detection methods to TF-MC-CDMA

systems in three different channels: (1) the AWGN, (2) the downlink slowly fading multipath Rayleigh channel, and (3) the downlink slowly fading multipath mobile Rayleigh channel with Doppler shift induced ICI.

In Chapter 2, the modeling of TF-MC-CDMA transmission and demodulation is considered. The WSSUS channel model is also discussed and the equivalent frequency domain channel transfer function for a frequency selective channel is obtained for system using multicarrier based transmission. One of the key results developed in Chapter 2 is that a systematic allocation of the time and frequency domain signature sequences for TF-MC-CDMA so as to reduce the total multiple access interference by minimizing the number of users sharing the same TD signature (and the same FD signature). This allocation scheme is not specified in [17].

In Chapter 3, the blind linear multiuser detection problem for TF-MC-CDMA in AWGN with MAI is discussed. The key result of Chapter 3 is that one can suboptimally decouple the TF-MC-CDMA multiuser detection problem into two separate blind multiuser DS-CDMA problems, one for the TD spreading and one for the FD spreading. This has the advantage of utilizing parallel processing. The blind DMI algorithm, blind CMOE RLS algorithm, the blind subspace algorithm using SVD, and the blind adaptive subspace algorithm using PASTd were applied to the proposed decouple detector and their performances were investigated.

In Chapter 4, the blind multiuser detection problem for TF-MC-CDMA in a slowly fading downlink multipath Rayleigh channel is discussed. The key result is that two types of TF-MC-CDMA blind detectors are proposed based on the results developed in Chapter 3. The first type, known as the type I detector, follows the same decoupled processing method as in Chapter 3 for the TF-MC-CDMA blind detection in the AWGN. The second type, known as the type II detector, uses a cascade processing with the output of the TD processing serving as input to the FD

processing. Computer simulations have shown that type II detectors outperform type I detectors. The type II detector takes advantage of the orthogonality of the time domain spreading sequences to eliminate interference from users belonging to other time domain signature groups. Therefore, the signal coming from the time domain detector only contains interferers from users within the same time domain user groups which is guaranteed to be less than or equal to the frequency domain spreading gain.

In Chapter 5, the TF-MC-CDMA blind multiuser detection problem in slowly fading downlink multipath Rayleigh channel with Doppler shift induced ICI is discussed. We first presented the modeling of Doppler shift induced ICI in a WSSUS multipath fading channel. There are several important results that came from the analysis: firstly, the ICI creates leakage of energy from one subcarrier to another that results in a loss of orthogonality in the frequency domain spreading codes; and secondly, the downlink multiuser detection problem becomes a quasi-uplink problem.

6.2 Future Research

The results presented this thesis on blind multiuser detection for TF-MC-CDMA provide a glimpse of the immense possibilities and potential applications of TF-MC-CDMA systems in future mobile communication systems. There are many interesting research areas that can be branched off into various directions in conjunction with other currently new research results in the areas of MIMO, Bayesian Monte Carlo methods, and signal processing techniques for fast fading channels.

6.2.1 MIMO TF-MC-CDMA Multiuser Detection

MIMO using multiple transmit and receive antennas can further increase the capacity of TF-MC-CDMA systems. Such a system can fully utilize time, frequency, and spatial diversity. Some ground work has been laid in [21] investigating the perfor-

mance of un-coded TF-MC-CDMA subspace detection using multiple antennas. The integration of transmit diversity with space-time coding methods such as space-time trellis coding and space-time block coding can further improve the performance of TF-MC-CDMA systems. The addition of MIMO transmission and reception will increase the complexity receiver, hence the challenge remains to design receivers that incorporates spatial diversity in TF-MC-CDMA systems while maintaining a practical level of complexity.

6.2.2 Bayesian Monte-Carlo Blind Multiuser Detection for TF-MC-CDMA

The Bayesian Monte-Carlo technique is a new signal processing technique that can be used in any type of statistical inference problems. In the communications area, blind multiuser detection, blind equalization are all special types of statistical inference problem. The main idea of Bayesian Monte-Carlo signal processing is to approximate the solution by simulating samples from the posterior distribution. There are two popular Bayesian Monte-Carlo techniques used for such applications: (1) Markov chain Monte Carlo (MCMC) which is a batch processing method and (2) Sequential Monte Carlo (SMC) which is a recursive processing method. It was shown in [44] that near optimal results can be obtained by applying the SMC technique to blind detection in OFDM systems. Such detectors have the potential to achieve near optimal performance because this type of detection method approximates the optimal MAP estimate that truly minimizes the probability of error. Another advantage of such methods is that they can be incorporated into any model with a fully blind approach with all unknown parameters jointly estimated.

6.2.3 TF-MC-CDMA Blind Multiuser Detection in Fast Fading Channels

The blind multiuser detection techniques discussed in this thesis applies to slowly fading channels. That is, the channel is approximately constant for at least the duration of an OFDM symbol. However, if the channel changes rapidly within an information symbol, then other techniques must be used. Several challenging issues arise in fast fading: (1) The fast fading channel gain need to be tracked for each subcarrier stream in order to perform multiuser detection. (2) One can not rely on the orthogonality of the time domain signature grouping of the users since in fast fading channel, the orthogonality of the time domain signature will in almost all cases be lost. (3) the decoupling technique will not be very effective for the two reasons previously stated.

Bibliography

[1] T. S. Rappaport, *Wireless Communications: Principles and Practice (2nd Edition)*. Prentice Hall PTR, 2002.

[2] S. Glisic, *Advanced Wireless Communications: 4G Technologies*. John Wiley and Sons, 2004.

[3] R. Chang, "Synthesis of band-limited orthogonal signals for multi-channel data transmission," *The Bell System Technical Journal*, vol. 45, Dec. 1966.

[4] S. Weinstein and P. Ebert, "Data transmission by frequency divison multiplexing using the discrete fourier transform," *IEEE Transactions on Communications*, vol. 19, pp. 628–634, Oct. 1971.

[5] M. Dohler, S. McLaughlin, P. Sweeney, and L. Hanzo, "Implementable wireless access for b3g networks - part iii: complexity reducing transceiver structures," *IEEE Communications Magazine*, vol. 45, pp. 98–104, Mar. 2007.

[6] N. Yee, J. Linnartz, and G. Fettweis, "Multicarrier cdma in indoor wireless radio networks," in *IEEE Symposium on Personal, Indoor, and Mobile Radio Communications*, vol. 2, pp. 109–113, 1993.

[7] N. Yee and J. Linnartz, "Wiener filtering of multi-carrier cdma in rayleigh fading channel," in *IEEE Symposium on Personal, Indoor, and Mobile Radio Communications*, vol. 4, pp. 1344–1347, 1994.

[8] S. Hara and R. Prasad, "Overview of multicarrier cdma," *IEEE Communications Magazine*, vol. 35, pp. 126–133, Dec. 1997.

[9] L. Hanzo, L. Yang, E. Kuan, and K. Yen, *Single and Multicarrier DS-CDMA: Multi-User detection, space-time spreading, synchronization and standards*. Wiley IEEE Press, 2003.

[10] C. You and D. Hong, "Multicarrier cdma systems using time-domain and frequency-domain spreading codes," *IEEE Transactions on Communications*, vol. 51, pp. 17–21, Jan. 2003.

[11] L. Yang, W. Hua, and L. Hanzo, "A multicarrier ds-cdma system using both time-domain and frequency-domain spreading," in *IEEE Vehicular Technology Conference*, vol. 4, pp. 2426–2430, Oct. 2003.

[12] W. Sheen and J. Sheu, "On the adaptability of ofdm-cdma forward link with time-frequency spreading in multipath fading channels," in *IEEE Vehicular Technology Conference*, vol. 1, pp. 617–621, Sept. 2005.

[13] S. Verdu, *Multiuser Detection*. Cambridge University Press, 1998.

[14] M. Honig, U. Madhow, and S. Verdu, "Blind adaptive multiuser detection," *IEEE Transactions on Information Theory*, vol. 41, pp. 944–960, July 1995.

[15] Y. Teng, K. Naito, K. Mori, and H. Kobayashi, "Performances of multi-carrier system with time and frequency domain spreading for wireless communications," in *IEEE Wireless and Communications Networking Conference*, vol. 1, pp. 558–563, June 2005.

[16] L. Yang, W. Hua, and L. Hanzo, "Multiuser detection in multicarrier cdma systems employing both time-domain and frequency-domain spreading," in *IEEE Symposium on Personal, Indoor, and Mobile Radio Communications*, vol. 2, pp. 1840–1844, Sept. 2003.

[17] L. Yang, W. Hua, and L. Hanzo, "Multiuser detection assisted time- and frequency-domain spread multicarrier code division multiple access," *IEEE Transactions on Vehicular Technology*, vol. 55, pp. 397–404, Jan. 2006.

[18] J. Schodorf and D. Williams, "A constrained optimization approach to multiuser detection," *IEEE Transactions on Signal Processing*, vol. 45, pp. 258–262, Jan. 1997.

[19] M. Honig and M. Tsatsanis, "Adaptive techniques for multiuser cdma receivers: enhanced signal processing with short spreading codes," *IEEE Signal Processing Magazine*, vol. 17, pp. 49–61, May 2000.

[20] X. Wang and V. Poor, "Blind multiuser detection: A subspace approach," *IEEE Transactions on Information Theory*, vol. 44, pp. 677–690, Mar. 1998.

[21] B. Hu, L. Yang, and L. Hanzo, "Subspace-based blind and group-blind space-time multiuser detection for the generalized multicarrier ds-cdma uplink," in *IEEE Vehicular Technology Conference*, vol. 1, pp. 1–5, Sept. 2006.

[22] C. Hui, "New channel estimation and multiuser detection algorithms for multi-carrier (mc)-cdma communications systems," 2005.

[23] X. Wang and V. Poor, "Subspace methods for blind joint channel estimation and multiuser detection in cdma systems," *Wireless Networks*, vol. 6, pp. 59–71, Feb. 2000.

[24] X. Wang and V. Poor, "Blind adaptive multiuser detection in multipath cdma channels based on subspace tracking," *IEEE Transactions on Signal Processing*, vol. 46, pp. 3030–3044, Nov. 1998.

[25] J. Wu, Y. Wang, and K. Cheng, "Blind channel estimation based on subspace for multicarrier cdma," in *IEEE Vehicular Technology Conference*, vol. 4, pp. 2374–2378, Aug. 2001.

[26] Y. Zhao and S. Haggman, "Sensitivity to doppler shift and carrier frequency errors in ofdm systems - the consequences and solutions," in *IEEE Vehicular Technology Conference*, vol. 3, pp. 1564–1568, May 1996.

[27] J. Linnartz, "Performance analysis of synchronous mc-cdma in mobile rayleigh channel with both delay and doppler spreads," *IEEE Transactions on Vehicular Technology*, vol. 50, pp. 1375–1387, Nov. 2001.

[28] M. Russell and G. Stuber, "Interchannel interference analysis of ofdm in a mobile environment," in *IEEE Vehicular Technology Conference*, vol. 2, pp. 820–824, July 1995.

[29] H. Wang, X. Chen, S. Zhou, M. Zhao, and Y. Yao, "Low-complexity ici cancellation in frequency domain for ofdm systems in time-varying multipath channels," *IEICE Transactions on Communiations*, vol. 89, pp. 1020–1023, Mar. 2006.

[30] S. Chen and T. Yao, "An inter-carrier interference suppression scheme for ofdm systems in time-varying fading channels," *IEEE Transactions on Consumer Electronics*, vol. 50, pp. 429–435, May 2004.

[31] W. Hou and B. Chen, "Ici cancellation for ofdm communication systems in time-varying multipath fading channels," *IEEE Transactions on Wireless Communications*, vol. 4, pp. 2100–2110, Sept. 2005.

[32] A. Goldsmith, *Wireless Communications.* Cambridge University Press, 2005.

[33] J. Proakis, *Digital Communications (4th Edition).* McGraw Hill, 2001.

[34] A. Molisch, *Wireless Communications.* Wiley IEEE Press, 2005.

[35] B. Sklar, "Rayleigh fading channels in mobile digital communication systems part i: characterization," *IEEE Communications Magazine*, vol. 35, pp. 90–100, July 1997.

[36] B. Sklar, "Rayleigh fading channels in mobile digital communication systems part ii: mitigation," *IEEE Communications Magazine*, vol. 35, pp. 102–109, July 1997.

[37] A. Oppenheim and R. Schafer, *Discrete-Time Signal Processing (2nd Edition)*. Prentice Hall, 1998.

[38] E. Ifeacher and B. Jervis, *Digital Signal Processing: A Practical Approach (2nd Edition)*. Prentice Hall, 2002.

[39] X. Wang and H. Poor, *Wireless Communication Systems: Advanced Techniques for Signal Reception*. Prentice Hall PTR, 2004.

[40] R. Schober, W. Gerstacker, and L. Lampe, "Data-aided and blind stochastic gradient algorithms for widely linear mmse mai suppression for ds-cdma," *IEEE Transactions on Signal Processing*, vol. 52, pp. 746–756, Mar. 2004.

[41] F. Verde, "Subspace-based blind multiuser detection for quasi-synchronous mc-cdma systems," *IEEE Signal Processing Letters*, vol. 11, pp. 621–624, July 2004.

[42] C. Escudero, D. Iglesia, M. Bugallo, and L. Castedo, "Analysis of a subspace channel estimation technique for multicarrier cdma systems," in *IEEE Workshop on Statistical Signal and Array Processing*, vol. 1, pp. 10–14, Aug. 2000.

[43] S. Kaiser, "Multi-carrier cdma mobile radio systems - analysis and optimization of detection, decoding and channel estimation," 1998.

[44] Z. Yang and X. Wang, "Blind adaptive multiuser detection," *IEEE Transactions on Signal Processing*, vol. 50, pp. 271–280, Feb. 2002.